NATIONAL ADVISORY COMMITTEE FOR AERONAUTICS

JUL 7 1947

TECHNICAL NOTE

No. 1352

WIND-TUNNEL INVESTIGATION OF SPLIT TRAILING-EDGE LIFT AND TRIM FLAPS ON A TAPERED WING WITH 23° SWEEPBACK

By William Letko and David Feigenbaum

Langley Memorial Aeronautical Laboratory
Langley Field, Va.

Washington
July 1947

N A C A LIBRARY
LANGLEY MEMORIAL AERONAUTICAL
LABORATORY
Langley Field, Va.

3 1176 01331 6261

NATIONAL ADVISORY COMMITTEE FOR AERONAUTICS

TECHNICAL NOTE NO. 1352

WIND-TUNNEL INVESTIGATION OF SPLIT TRAILING-EDGE LIFT AND TRIM FLAPS ON A TAPERED WING WITH 23° SWEEPBACK

By William Letko and David Feigenbaum

SUMMARY

Results of force tests and pressure-distribution measurements are presented from a wind-tunnel investigation to determine the effects of size and hinge location of lift and trim flaps on the lift and pitching-moment characteristics of a semispan tapered wing with 23° sweepback of the quarter-chord line. The flaps tested were split flaps with chords of 10, 20, 30, and 40 percent of the wing chord. The spans of the lift flaps were 20, 40, 60, 80, and 100 percent of the wing span; the spans of the trim flaps were 10, 20, 40, and 60 percent of the wing span. The flaps were tested with the hinge axes at several different chordwise locations.

The static longitudinal stability of the swept-back wing, as indicated by the slope of the curves of pitching-moment coefficient against lift coefficient, was increased when the lift flaps were deflected, especially for the larger flaps.

Increments in maximum lift coefficient of the order of 0.4 were produced in some configurations by self-trimming lift flaps, that is, lift flaps that produced no increment in pitching moment about the aerodynamic center. By the use of trim flaps to counteract the pitching moments produced by the lift flaps, increments in maximum lift coefficient of the order of 0.5 might be attained. The chord of the trim flap used had a negligible effect on the net lift coefficients attainable, although use of a large-chord trim flap meant that a smaller span was required. Using a trim flap with the hinge axis moved back to the trailing edge, however, allowed slightly greater lift increments to be attained. The increments in trimmed lift coefficient produced by the lift flap increased with flap chord and reached a maximum value for all flap chords at a flap span of about 50 percent of the wing span. Moving the hinge axis of the lift flaps forward increased the lift-coefficient increment attainable at a 10° angle of attack with self-trimming flaps. The greatest increment in maximum lift coefficient attainable

with self-trimming flaps occurred, however, when the flap hinge axis was on the 70-percent-chord line. A comparison of the results with analytical results showed, in general, reasonably good agreement.

INTRODUCTION

In order to apply high-lift flaps to "all-wing" airplanes, a flap arrangement that produces small pitching moments about the center of gravity is necessary, since the longitudinal-control device generally used is not well adapted to trimming out large pitching moments. The analysis of reference 1 indicates that trim flaps (upward deflected flaps) near the wing tips of a swept-back wing may be used to trim-out the pitching moment of the lift flap or that lift flaps might be designed to be self trimming if the wing has enough sweepback. A means of reducing the pitching moment of the lift flap is to move the center of pressure of the flap forward by moving the flap hinge line forward of its normal position. In order to obtain experimental data for checking and comparing these means of obtaining high lift coefficients on all-wing airplanes and for checking the analysis of reference 1, tests were conducted in the Langley stability tunnel on a semispan, swept-back wing equipped with various sizes and configurations of split flaps.

SYMBOLS

C_L lift coefficient $\left(\frac{L}{qS}\right)$

$\left(\Delta C_L\right)_f$ increment of lift coefficient produced by flap

Δc_{n_f} increment of section normal-force coefficient produced by flap

C_D drag coefficient $\left(\frac{D}{qS}\right)$

C_m pitching-moment coefficient $\left(\frac{M}{qS\bar{c}}\right)$

ΔC_{m_f} increment of pitching-moment coefficient produced by flap

L lift

n section normal force

D	drag
M'	pitching moment about quarter chord of mean geometric wing chord
ΔP_R	increment of resultant pressure coefficient
S	wing area
b	model span normal to plane of symmetry (semispan of wing)
b_f	flap span
c	local wing chord parallel to plane of symmetry
$\bar{c}$	mean geometric wing chord
c_f	local flap chord
q	dynamic pressure
α	angle of attack measured at root section
α_u	uncorrected angle of attack
δ_f	flap deflection measured with respect to airfoil surface in plane normal to hinge axis (lift-flap deflection positive downward; trim-flap deflection positive upward)
R	Reynolds number
A	aspect ratio $\left(\frac{b}{S}^2\right)$
λ	taper ratio; ratio of tip chord of wing to root chord of wing
Λ	angle of sweepback of quarter-chord line

Subscripts:

L	lift
T	trim
max	maximum

MODEL AND APPARATUS

The semispan tapered-wing model used for these tests had the quarter-chord line swept back 23°. The geometric constants of the model are as follows:

Area of full-span wing, square feet	13.55
Wing span (full span), feet	10.10
Mean geometric chord, feet	1.51
Aspect ratio	7.51
Taper ratio	0.243
Sweepback of quarter-chord line, degrees	23
Geometric twist (washout), degrees	-4
Root airfoil section	NACA 4418
Tip airfoil section	NACA 4418

The model was constructed of laminated mahogany and had 25 pressure orifices spaced at constant percentages of the local chord for each of nine spanwise stations. (See fig. 1.) The wing is the same wing which was used in the tests reported in reference 2 except that the row of orifices one inch from the tunnel wall was not utilized in the present tests.

The model was mounted horizontally (with zero dihedral) in the Langley stability tunnel on the side support of the tunnel balance frame, free from the tunnel wall except for a flexible seal used to prevent flow through the gap between the tunnel wall and the wing-root block. The wing-root section was larger than the diameter of the opening in the tunnel wall through which the model was mounted and, consequently, forward of the 17-percent-chord point of the root section there was an unsealed gap of about 1/8 inch between the tunnel wall and the root section (fig. 2).

The lift and trim flaps were made of $\frac{3}{8}$-inch plywood in sections covering 20 percent of the wing span and were supported by wooden blocks fastened to the back of the flaps. The blocks were made with an angle of approximately 60° so that, when the flaps were mounted, each section was shimmed separately to obtain 60° deflection. Flaps with chords 0.10, 0.20, 0.30, and 0.40 wing chord were tested. The locations of these flaps are shown in figure 3.

TESTS

In this investigation, force, moment, and pressure-distribution tests were run at a dynamic pressure of 39.7 pounds per square foot;

this pressure corresponds to an airspeed of 124.6 miles per hour at standard sea-level conditions. The Reynolds number based on the mean geometric chord of the model was 1.78×10^6.

For the tests reported herein, the flaps were set at 60° with respect to airfoil surface in a plane perpendicular to the flap at the middle of each flap section; the trim flaps were deflected upward, and the lift flaps were deflected downward. Lift-flap spans of 0.20, 0.40, 0.60, 0.80, and 1.00 wing span and trim-flap spans of 0.10, 0.20, 0.40, and 0.60 wing span were tested. The lift and trim flaps were tested separately on the model, but some tests were made with both lift and trim flaps to determine whether the data from the separate tests could be superposed with sufficient accuracy for design purposes. Tests were also made at several flap hinge locations to determine the effects of hinge location, and the 0.20c, 0.40b lift flap was tested with the hinge axis skewed to be perpendicular to the free-stream direction. The tests were run for angles of attack from -8° to the angle of attack at which stall occurred in 2° increments. Pressure distributions were made for angles of attack of 0° and 10° for some of the lift- and trim-flap arrangements.

CORRECTIONS

Corrections for the effect of the jet boundaries were applied to the force and pitching-moment coefficients. These corrections do not account for the effects of the tunnel-wall boundary layer or for the clearance gap between the wing section and the tunnel wall. A weighted mean value for the correction to the angle of attack was used, although the correction should vary along the span. The wing twisted under the air loads, especially the tip when full-span lift flap or large-span trim flaps were used. The corrections for the twist, however, were not applied. The order of magnitude of this correction for twist would be approximately 2° at the tip for some of the extreme conditions.

For the pressure distributions on the wing the pressures were corrected for streamline curvature with an average correction factor of 0.991; this correction factor was applied to the increment of the resultant pressure. The angles of attack of each section were not corrected because each flap arrangement would necessitate a different set of corrections, which would involve an impractical amount of work.

PRESENTATION OF DATA

The results of the tests are presented in figures 4 to 21. In figures 4 to 7 are presented the force data in the form of plots of pitching-moment coefficient, drag coefficient, and angle of attack against lift coefficient for lift flaps of different chords and spans at various hinge locations. Figures 8 to 11 give the characteristics of various trim flaps. In figure 12, the force and pitching-moment data for one flap configuration with its hinge axis on a constant percentage chord line is compared with that of the same flap with its hinge axis skewed to be perpendicular to the plane of symmetry. Figures 13 to 16 give the chordwise distribution of the increment of resultant pressure coefficient ΔP_R caused by the flaps at several spanwise stations, and figures 17 to 19 give the spanwise distribution of the incremental loading $\Delta c_{n_f} c$ caused by the flaps for the 20- and 40-percent-chord flaps. Figures 20 and 21 compare the results obtained by superposition of the lift-flap data and the trim-flap data with the data obtained by testing several configurations of lift and trim flaps together.

DISCUSSION OF RESULTS

Lift Flaps

Lift.- Characteristics of the 23° swept-back wing with various lift flaps can be seen in figures 4 to 7 and 13 to 18. The lift of the wing increases with flap chord and span in a manner similar to that of an unswept wing with comparable taper. The lift decreases as the flap hinge is moved forward, since the flaps produced no increment in chordwise load beyond their trailing edges. (See fig. 16.) Although the maximum lift coefficient increased with flap span, the angle of attack for maximum lift decreased with flap span up to spans of 0.80b and then increased for the full-span flap; the increase was probably caused by the reduction in the discontinuity of the flow near the tip. Both the maximum lift coefficient and angle of attack for maximum lift decrease as the hinge line of the flap is moved forward. The slope of the lift curve is usually greater for the wing with the flaps deflected than for the plain wing, but the slope decreases as the hinge line is moved forward and is the same for the plain wing as for the wing with the flap at the most forward location tested.

Pitching moment.- With small-span flaps in the center section of a swept-back wing the center of pressure of the wing with the flap is ahead of the center of pressure of the plain wing and causes a

positive increment of pitching moment. As the flap span is increased, however, the sweep of the wing moves the flap back and the resulting shift in center of pressure makes the pitching-moment increment negative. (See fig. 22.) At some intermediate flap span, the increment of pitching moment produced by the flap will be zero, and this flap will thus be self trimming. Moving the hinge line of the flap forward increases the flap pitching moment in a positive sense and tends to make the self-trimming flaps have larger spans. For a given flap span and chord, however, moving the hinge line forward causes the lift increment to decrease (fig. 23). Skewing the hinge axis of a 0.20c, 0.40b flap caused a slight decrease in the pitching moment and a decrease in lift at high lift coefficients. (See fig. 12.)

The slope of the curves of pitching-moment coefficient against lift coefficient is more negative for the wing with the flaps deflected than for the plain wing. This result is probably caused by the fact that the drag of the flap acts below the chord line and the effect is accentuated, especially for the large-span flaps, by the sweepback. The increase in the negative slope of the curve of pitching-moment coefficient against lift coefficient indicates an increase of stability with the flaps deflected.

Trim Flaps

Lift.- The trim flaps cause a decrement in lift, the magnitude of which increases with flap span and chord. The magnitude of the decrement in lift for a given increment in span increases as the span increases since the aerodynamic load ordinarily increases toward the center of the wing, and this effect is magnified by the wing taper. (See fig. 22.) At low values of lift coefficient, the lift is about the same for all hinge locations, but the slope of the lift curve increases as the hinge line moves farther back, which decreases the decrement in lift at high angles of attack for the flaps with the more rearward hinge locations. This effect is mainly due to the increase in chord of the wing as the hinge line moves back and the flap projects beyond the trailing edge.

No decrease in maximum lift coefficient is noted with the trim flaps deflected (figs. 8 to 11). At angles of attack near maximum lift the flow starts separating from the wing and, with the flow separated near the trailing edge, the flaps on the upper surface of the wing have no effect. Although the tests were not run up to maximum lift coefficient, it is probable that the maximum lift coefficients for the large-chord flaps at the more rearward hinge locations are higher than those for the plain wing. This increase in maximum lift coefficient is shown in figures 8 and 9. Such an increase in maximum lift coefficient may be attributed, again, to the effective

increase in the wing chord.

Pitching moment.- The increment in pitching-moment coefficient caused by the trim flaps increases almost rectilinearly with flap span (figs. 22 and 23). Although the lift decrement produced by a given increment in flap span increases as the flap span increases, the pitching-moment increment does not increase since, because of the wing sweep, the center of pressure of the flap moves closer to the quarter-chord point of the mean geometric chord. Near maximum lift the pitching moments for the wing with any of the trim flaps are nearly the same and are about equal to the pitching moment of the plain wing, since the flaps on the upper surface of the wing lose their effectiveness at high angles of attack. The larger-span flaps, which give a more positive increment in pitching moment at low lift coefficients, therefore, will have to give a more negative slope to the pitching-moment curve. This increase in negative slope makes the wing more stable. As the chord increases and as the hinge line moves backward, the increase in stability becomes greater.

Superposition of Lift- and Trim-Flap Data

If the flap data are to be applied to an all-wing airplane, the wing must always be in trim since those airplanes have no tail to trim out any unbalanced pitching moments on the wing. Unless the lift flap used is self trimming, therefore, a trim flap will have to be used in conjunction with the lift flap to bring the pitching moment down to the value for which the plain wing is trimmed. Tests were made with several configurations of lift and trim flaps combined, and the results were compared with those obtained from superposition of the data from the tests already discussed. Figures 20 and 21 show the comparison between the results of the tests of the combinations and the results obtained by superposition. This comparison shows good agreement.

Trimmed Lift-Coefficient Increments

Figures 22 and 23 were prepared to show the increments in lift coefficient and pitching-moment coefficient for various configurations of lift or trim flaps. In these figures some of the variations in lift and pitching moments already discussed can be seen. From these plots, the trim flap required to trim out the pitching moment caused by the lift flap, the net increment in lift coefficient, and the maximum trimmed lift coefficients may be obtained.

Lift increment at $\alpha = 10^{\circ}$.- The increment in trimmed lift coefficient at a constant angle of attack is an indication of the

relative effectiveness of the various flaps in increasing the lift coefficient of a wing if stalling does not occur. The lift increments at an angle of attack of 10° are shown graphically in figures 24 and 25. With the lift flaps hinged at the normal locations, the greatest lift increment occurs for flap spans between 0.40 and 0.60 of the wing span. As the hinge line is moved forward, the flap span at which this greatest increment occurs is generally increased; whereas, at a constant hinge location this span decreases with increasing flap chord. The lift increment increases with increasing chord and seems to be a maximum when the hinge axis of the lift flap is located at about the 0.70 chord line. As the hinge line is moved forward or backward of this hinge location, the lift increment decreases. With all the lift flaps except the 0.10c flap at the normal hinge location, there is some flap span at which the lift flap produces no increment in pitching moment and thus is self trimming. In figures 24 and 25 this condition is indicated where the trim-flap span required goes to zero. The self-trimming lift-flap configurations and the lift increment produced thereby are listed in table I. The data in this table show that the increments in lift produced by self-trimming flaps increase with flap chord and with forward movement of the hinge axis.

The effect of trim-flap chord on the lift-coefficient increments is small. In figure 26 is plotted the variation of pitching-moment-coefficient increment with lift-coefficient increment produced by various trim-flap configurations. This figure indicates that, in order to trim out a given pitching moment, almost the same decrease in lift coefficient is encountered regardless of the chord of the trim flap used, except when the pitching moment is of such magnitude as to require a trim-flap span of more than about 0.50 wing span, in which case a larger-chord flap is advantageous. Using a larger-chord trim flap reduces somewhat the flap span required; however, no increase in trimmed lift results. Using a trim flap hinged at the wing trailing edge, however, results in some slight increase in trimmed-lift coefficient. In the best case, using a trim flap hinged at the trailing edge results in an increase in lift coefficient of about 0.1 over the lift coefficient obtained by using a normally hinged trim flap at an angle of attack of 10°.

Maximum lift coefficient.- In figure 27 is shown the maximum lift coefficients attainable with the different lift-flap configurations and the flap span required for trim. With the lift flaps hinged at their normal locations, the maximum lift coefficient occurs for flap spans of 0.50 wing span. Also, the increments in maximum lift coefficient of the wing may be increased by about 0.5 as indicated in figure 27. As the flap hinge axis is moved forward, the span at which the greatest maximum lift coefficient occurs is increased, and at a constant hinge location, this span decreases with increasing chord. The maximum lift coefficient increases with increasing chord and is

greatest with the flaps hinged at their normal locations. With all the lift flaps except the 0.10c flap at the normal hinge location, there is some flap span at which the lift flap is self trimming. The self-trimming lift-flap configurations and the maximum lift coefficients attained thereby are listed in table I. In this table, it can be seen that the maximum lift coefficient increases with flap chord and seems to be a maximum when the hinge axis is located at about the 70-percent-chord line. The table also shows that self-trimming flaps may increase the lift coefficient of the wing by about 0.4.

The most convenient way of obtaining high maximum lift coefficients would probably be to use a large-chord self-trimming flap. The maximum lift coefficient obtained with a self-trimming 0.40c flap is only about 0.08 less than the greatest maximum lift coefficient attainable with the same-chord flap in combination with a trim flap. With a self-trimming flap, no trim flap is required and, therefore, the entire outer part of the wing is left free for control surfaces.

Comparison of Experimental Results with Results Based on Analytical Methods

The results of the present tests are similar to the results obtained by analytical methods in reference 1. The data of reference 1 are presented for a wing similar to the wing used in the present tests; the physical characteristics are compared as follows:

	Sweepback, Λ (deg)	Aspect ratio, A	Taper ratio, λ	δ_f (deg)
Present tests	23	7.51	0.243	60
Reference 1	20	7.35	.25	60

A comparison of the analytical results with the experimental results shows good agreement in that the trends are similar, although the magnitudes of the net lift-coefficient increments are about 0.1 lower than the increments predicted for a 0.30c flap. Figure 28 shows a comparison between the experimental and analytical predictions (reference 1) of net lift increments and trim-flap spans required for 0.30c flaps, with the analytical results corrected to an angle of sweep of 23°. The experimental results (fig. 26) verify the contention in

reference 1 that the trim-flap chord has a negligible effect on the net lift increments.

The adoption of 0.9 in reference 1 as the ratio between the increment in $C_{L_{max}}$ and the increment in C_L at $\alpha = 10^\circ$ produced by the lift flaps is based on data for unswept wings or for wings with very little sweepback. The results of the present tests (fig. 29) indicate that the aforementioned ratio is considerably less than 0.9 for the wing of 23° sweepback, the ratio indicated herein being about 0.75 for normally hinged flaps and averaging about 0.70 for all the flaps tested.

CONCLUSIONS

From the results of the force and pressure distribution tests of the 23° swept-back tapered wing having lift and trim flaps of various size and hinge location, the following conclusions were drawn:

1. The maximum lift coefficient of the wing may be increased by about 0.5 without changing the pitching moment about the aerodynamic center by the use of split trailing-edge lift and trim flaps.

2. Certain lift-flap configurations were self trimming (that is, lift flaps that produced no increment in pitching moment about the aerodynamic center), and with some of these configurations the maximum lift coefficient of the wing might be increased by about 0.4. Also, increments in maximum lift coefficient of the order of 0.5 might be attained by use of trim flaps.

3. The wing had greater static longitudinal stability with the flaps deflected (especially for larger flaps) as indicated by the slope of the curves of pitching-moment coefficient against lift coefficient.

4. The chord of the trim flap used had a negligible effect on the net lift coefficients attainable, although use of a large-chord trim flap meant that a smaller span was required. Using a trim flap with the hinge axis moved back to the trailing edge, however, allowed slightly greater lift increments to be attained.

5. The increment in trimmed lift coefficient produced by the lift flap increased with flap chord and reached a maximum value for all flap chords at a flap span of about 50 percent of the wing span.

6. Moving the hinge axis of the lift flaps forward increased the lift-coefficient increment attainable at a 10° angle of attack with self-trimming flaps; however, the greatest increment in maximum lift coefficient attainable with self-trimming lift flaps occurred when the flaps were hinged at about the 70-percent-chord line.

7. In general the experimental results agreed reasonably well with those predicted by analysis.

Langley Memorial Aeronautical Laboratory
National Advisory Committee for Aeronautics
Langley Field, Va., February 24, 1947

REFERENCES

1. Pitkin, Marvin, and Maggin, Bernard: Analysis of Factors Affecting Net Lift Increment Attainable with Trailing-Edge Split Flaps on Tailless Airplanes. NACA ARR No. L4I18, 1944.

2. Mendelsohn, Robert A., and Brewer, Jack D.: Comparison between the Measured and Theoretical Span Loadings on a Moderately Swept-Forward and a Moderately Swept-Back Semispan Wing. NACA TN No. 1351, 1947.

TABLE I.- SELF-TRIMMING LIFT-FLAP CONFIGURATIONS

$\frac{c_{f_L}}{c}$	Hinge location	At $\alpha = 10^\circ$		At $C_{L_{max}}$	
		$\frac{b_{f_L}}{b}$	$\left(\Delta C_L\right)_{f_L}$	$\frac{b_{f_L}}{b}$	$C_{L_{max}}$
0.10	0.90c	0	0	0	1.29
.10	.70c	.32	.29	.35	1.47
.10	.50c	.61	.33	.68	1.36
.20	.80c	.10	.19	.21	1.53
.20	.70c	.27	.38	.36	1.63
.20	.50c	.52	.52	.52	1.53
.30	.70c	.18	.33	.27	1.62
.30	.50c	.44	.58	.43	1.60
.40	.60c	.25	.48	.34	1.70
.40	.50c	.35	.58	.42	1.68

NATIONAL ADVISORY
COMMITTEE FOR AERONAUTICS

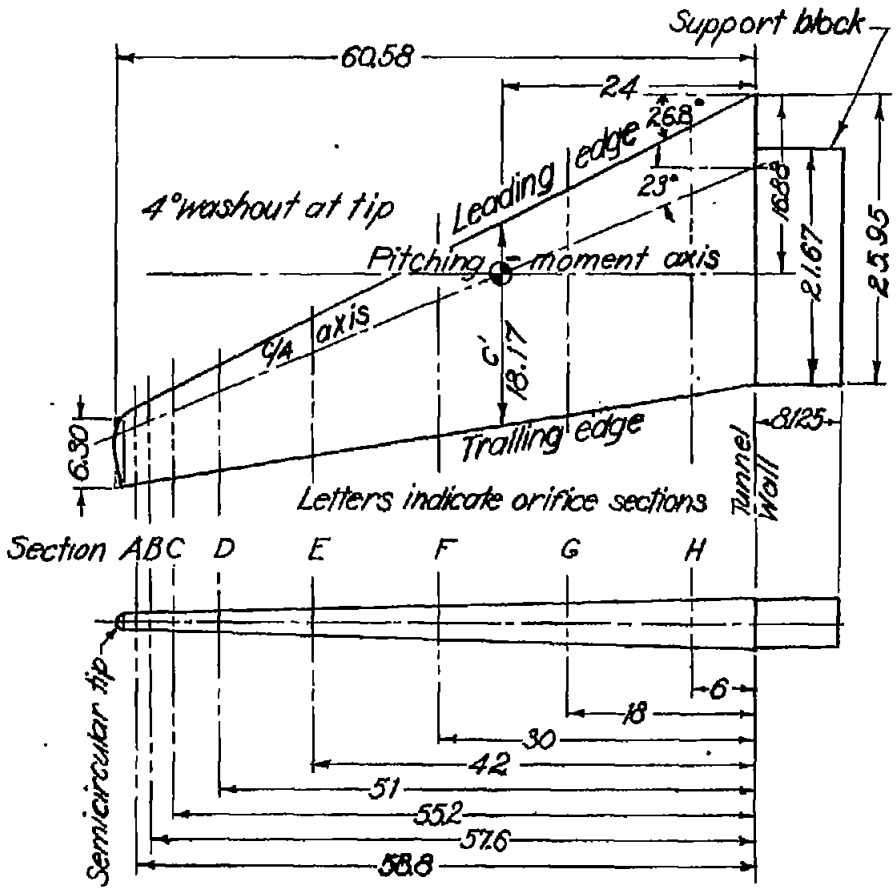

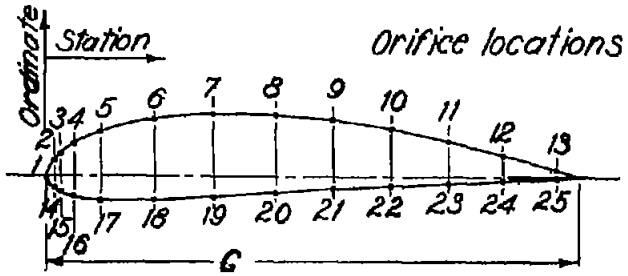

Orifice	Station (percent c)
1	0
2-14	1.0
3-15	2.5
4-16	5.0
5-17	10.0
6-18	18.125
7-19	28.50
8-20	39.50
9-21	50.50
10-22	61.50
11-23	72.50
12-24	83.50
13-25	94.50

NATIONAL ADVISORY COMMITTEE FOR AERONAUTICS

Airfoil NACA 4418		
Station (percent c)	Upper (percent c)	Lower (percent c)
0	-	0
1.25	3.76	-2.11
2.50	5.00	-2.99
5.00	6.75	-4.06
7.50	8.06	-4.67
10.00	9.11	-5.06
15.00	10.66	-5.49
20.00	11.72	-5.56
25.00	12.40	-5.49
30.00	12.76	-5.26
40.00	12.70	-4.70
50.00	11.85	-4.02
60.00	10.44	-3.24
70.00	8.55	-2.45
80.00	6.22	-1.67
90.00	3.46	-0.93
95.00	1.89	-0.55
100.00	(0.19)	(-0.19)

L.E. radius 3.56 percent c
Slope of radius through end of chord: 4/20

Figure 1.-Details of the swept-back wing model. Area (complete wing) 13.550 square feet; aspect ratio 7.51; taper ratio 0.243. All dimensions are in inches.

(a) Top view of swept-back wing.

Figure 2.- Views of swept-back-wing model in the 6- by 6-foot section of the Langley stability tunnel.

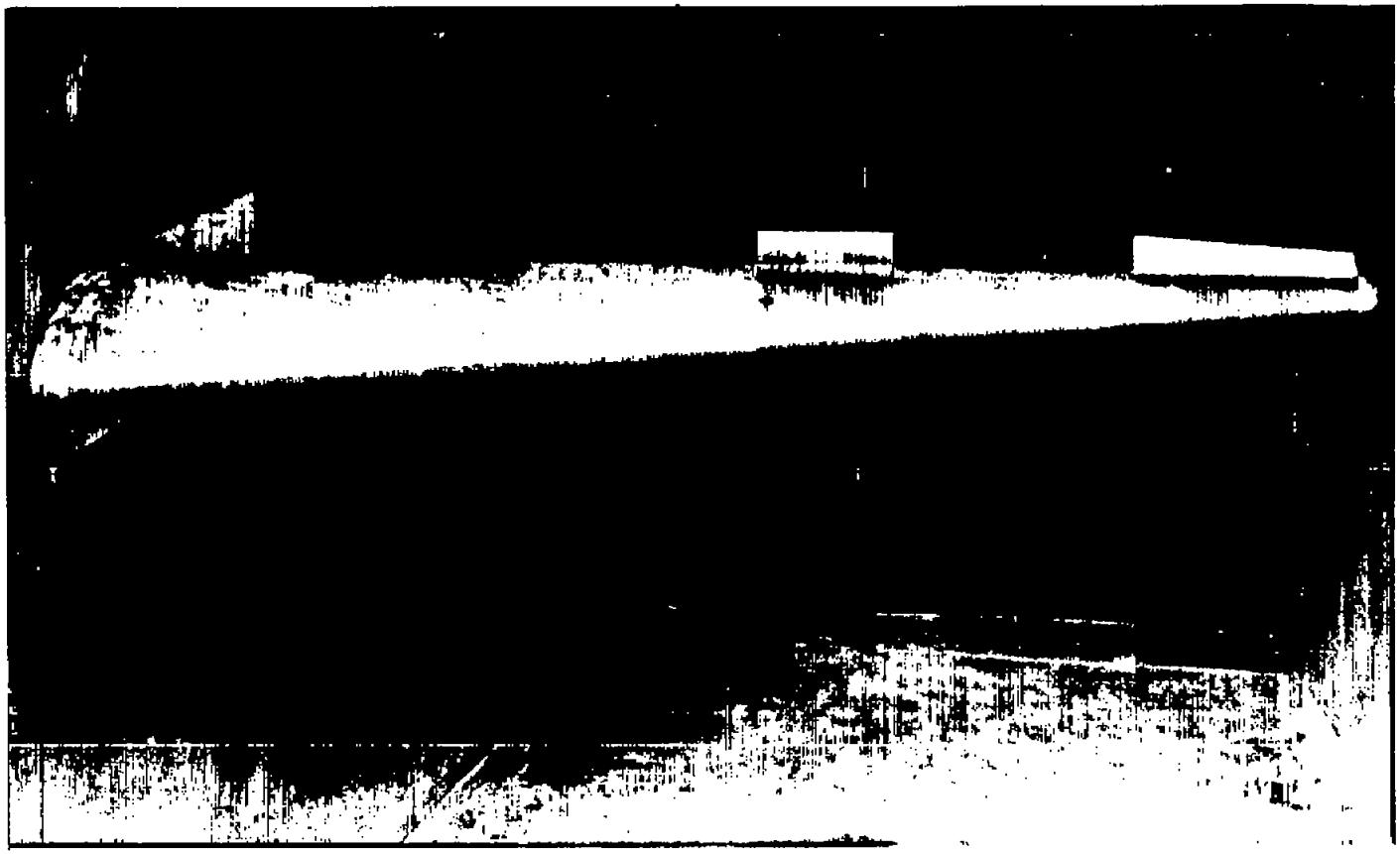

(b) Front view of swept-back wing with a 0.20c-chord 0.20b-span trim flap.

Figure 2.- Continued.

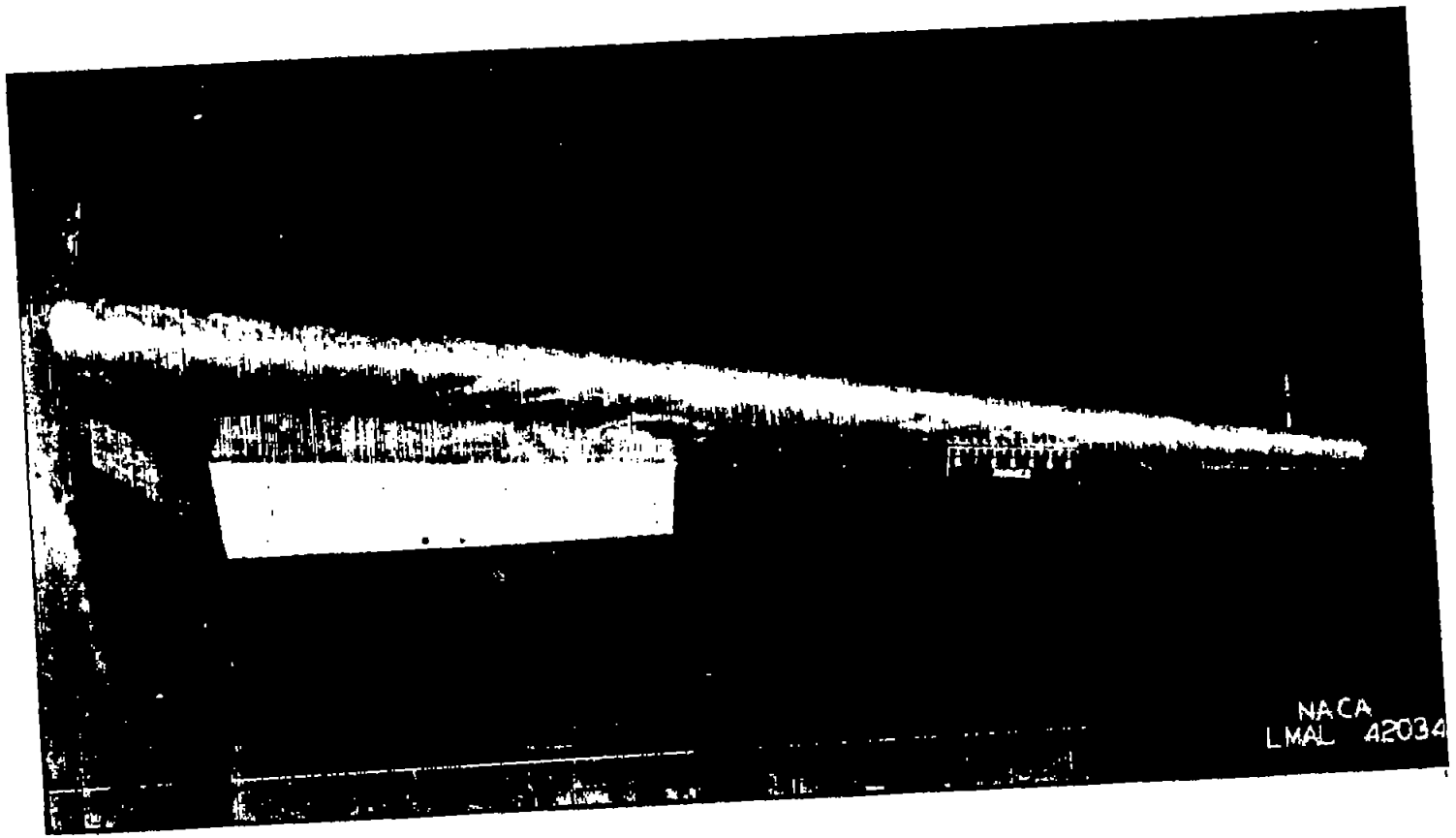

(c) Front view of swept-back wing with a 0.20c-chord 0.40b-span lift flap.

Figure 2.- Concluded.

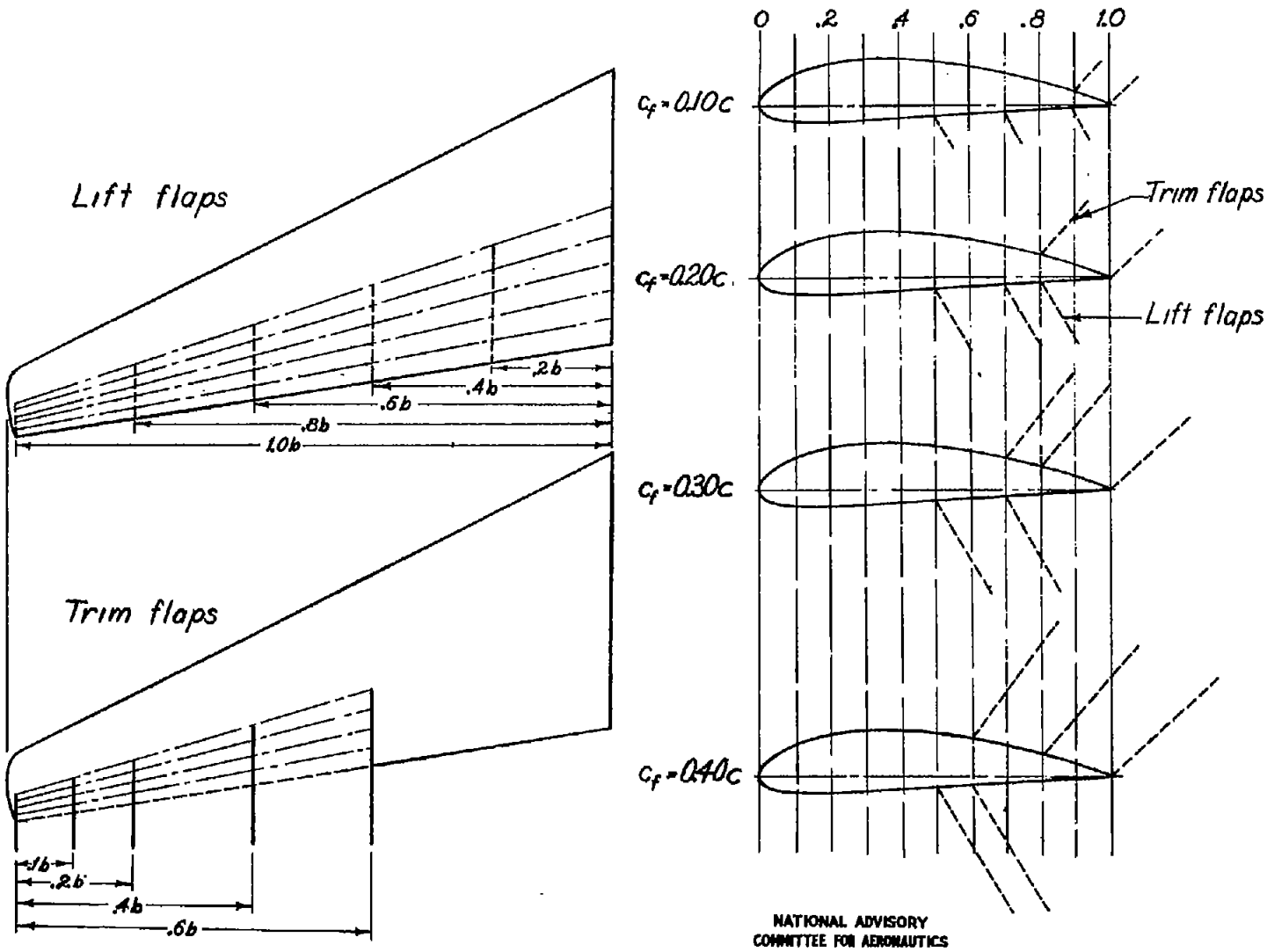

Figure 3.-Lift- and trim-flap configurations.

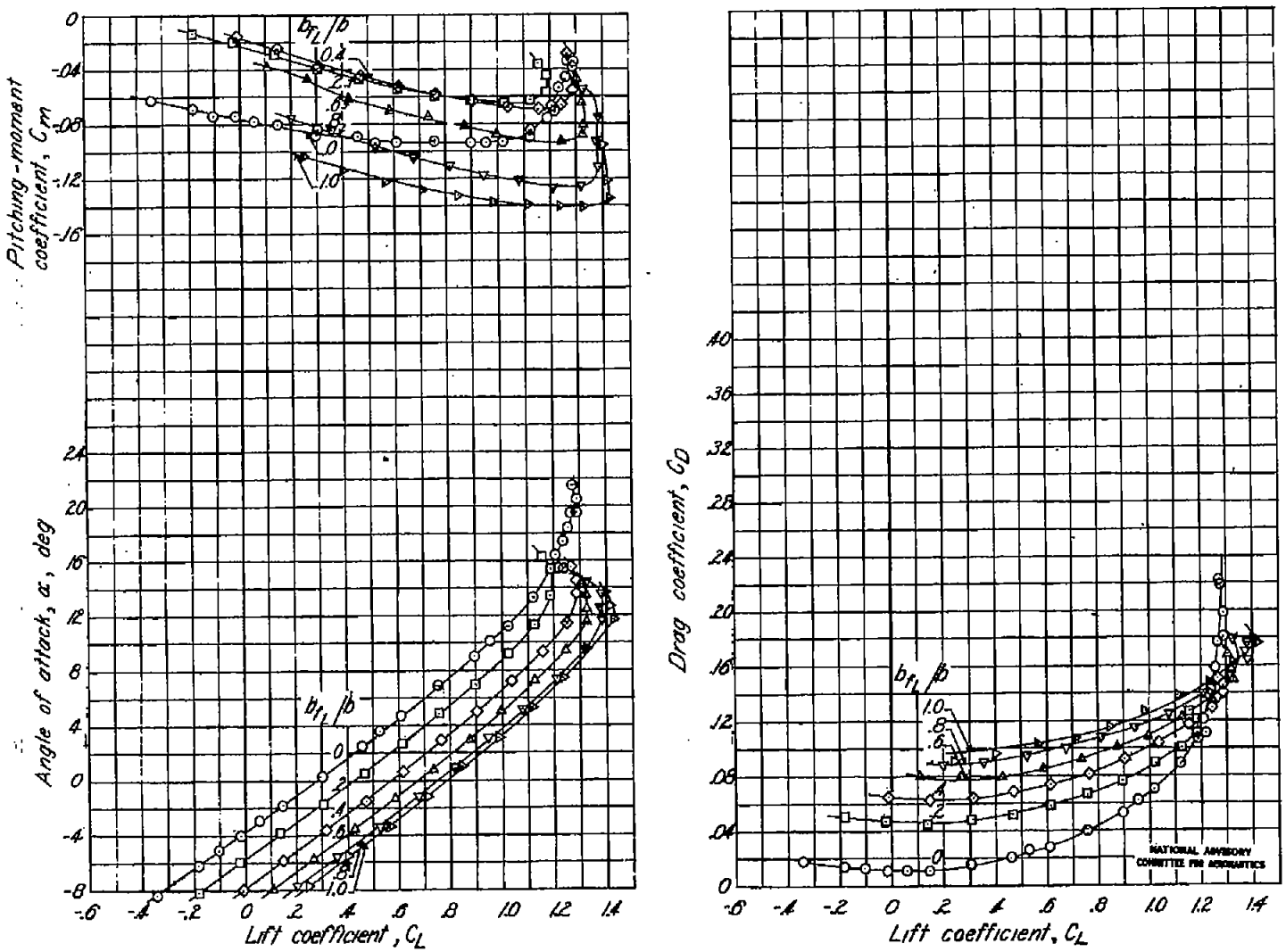

(a) Lift-flap hinge, 0.60c.

Figure 4.-Lift, drag, and pitching-moment coefficients of wing with 0.10c-chord lift flap for various flap spans. $\delta_{f_L} = 60°$; $R = 1.78 \times 10^6$.

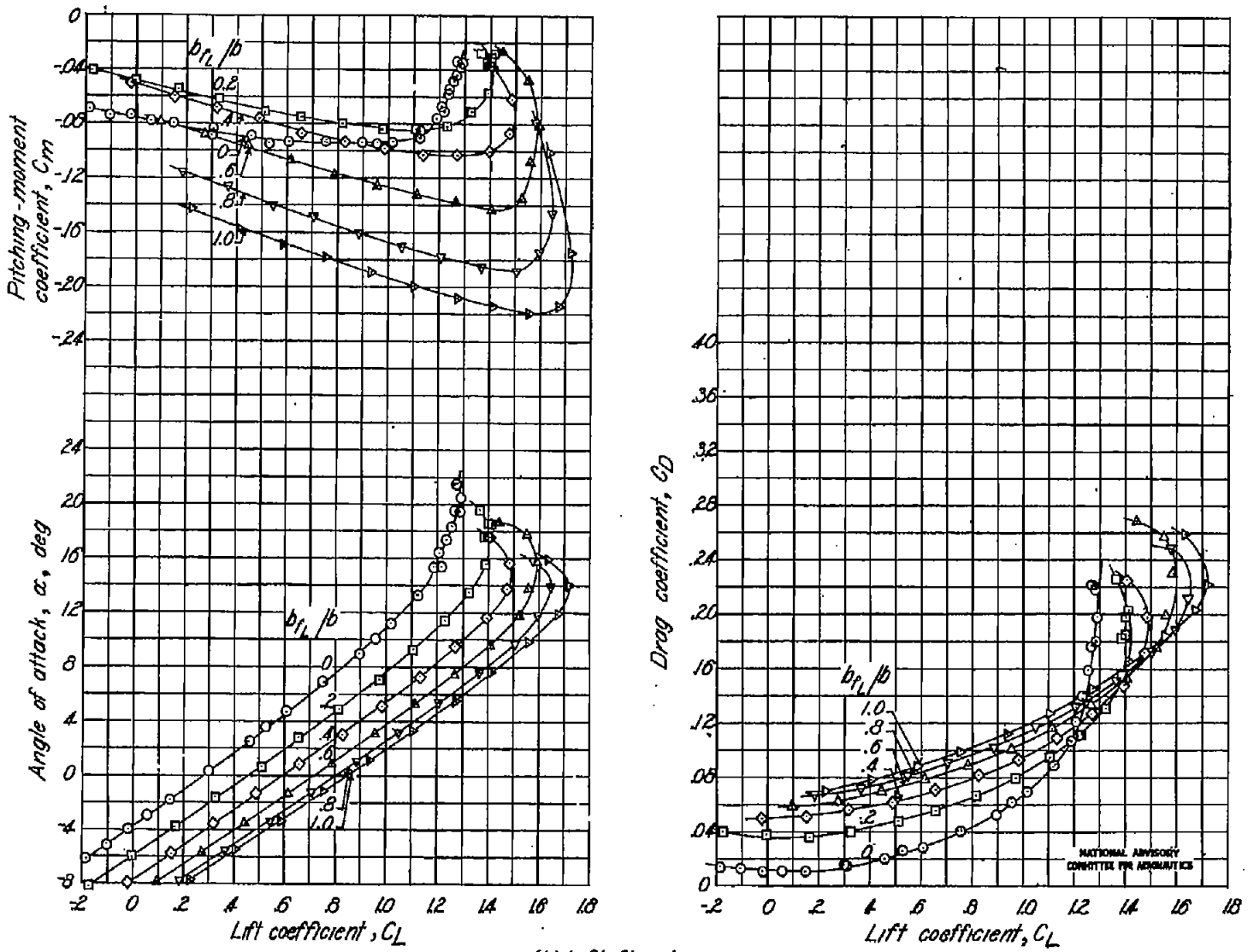

(b) Lift-flap hinge, 0.70c.

Figure 4.—Continued.

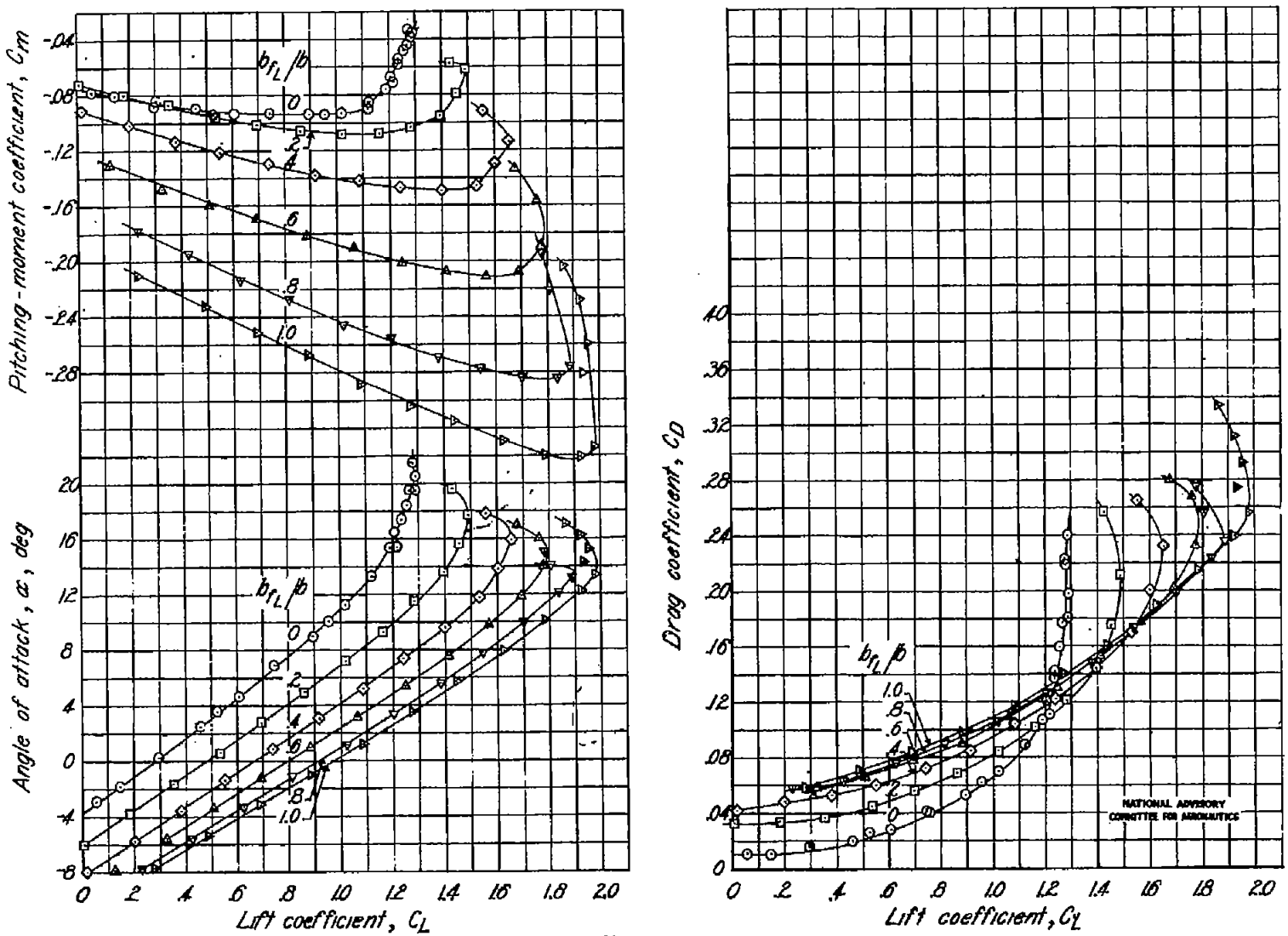

(c) Lift-flap hinge, 0.40c.

Figure 4.– Concluded.

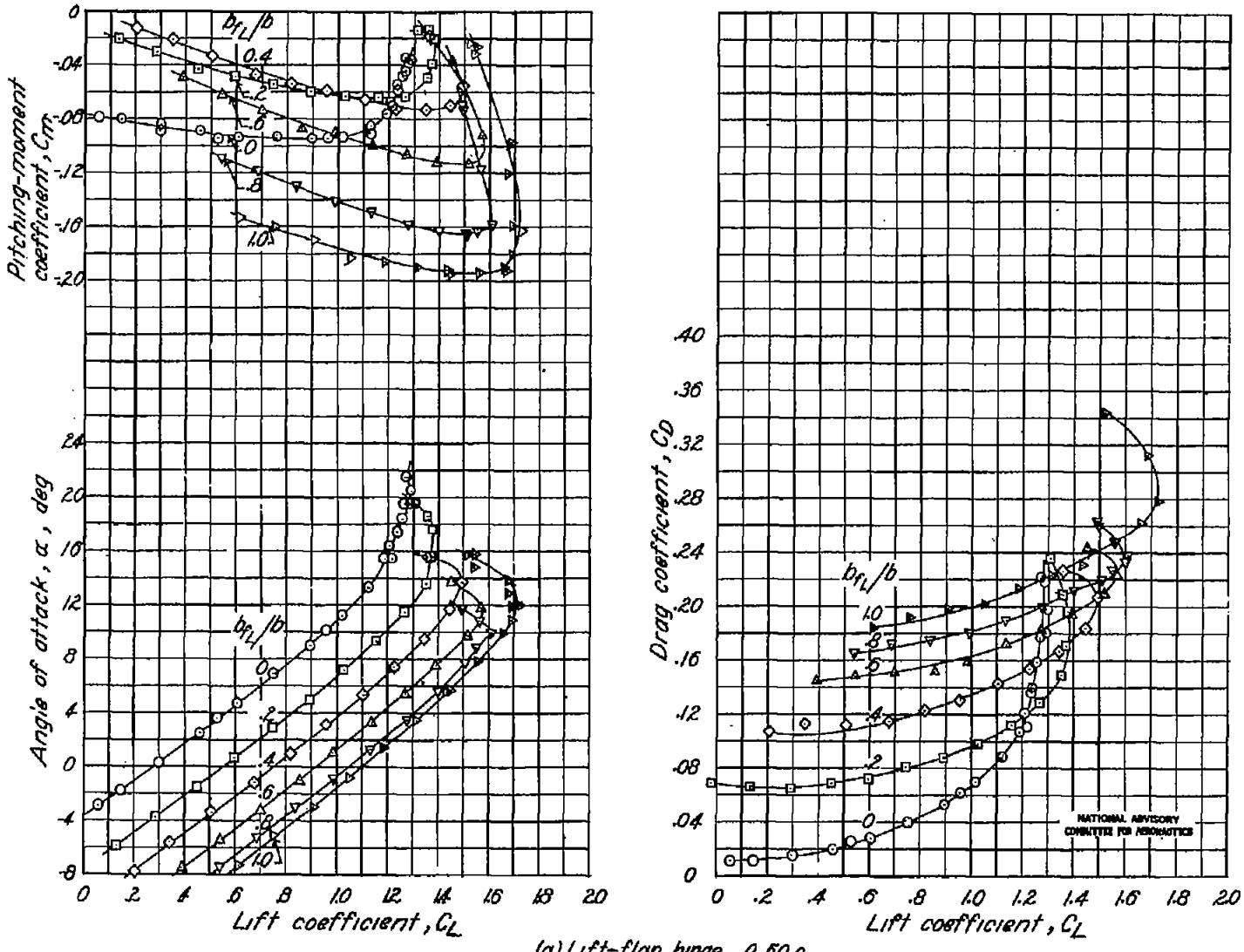

(a) Lift-flap hinge, 0.50c.

Figure 5.- Lift, drag, and pitching-moment coefficients of wing with 0.20c-chord lift flap for various flap spans. $\delta_{f_L} = 60°$, $R = 1.78 \times 10^6$.

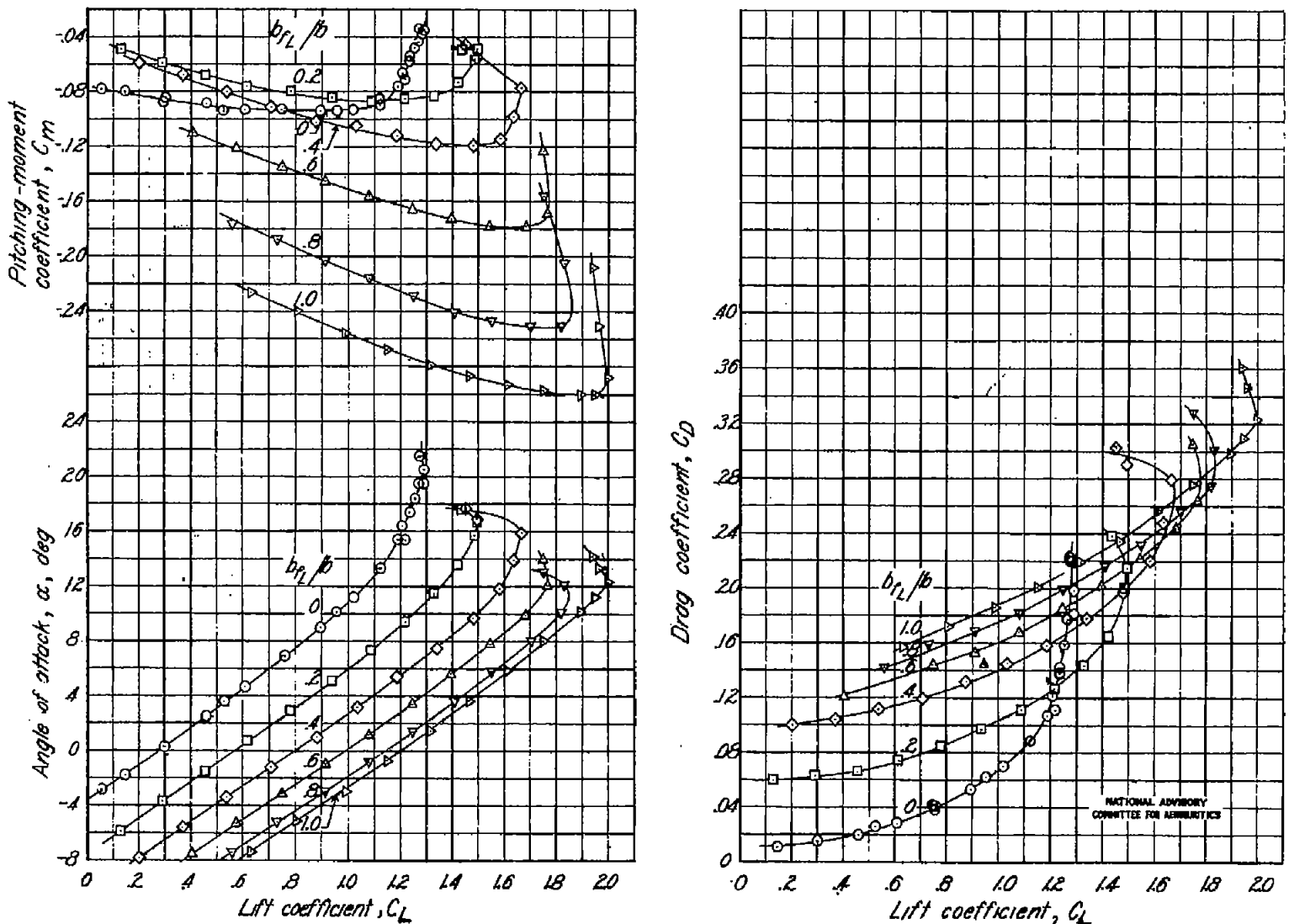

(b) Lift-flap hinge, 0.70c.

Figure 5.- Continued.

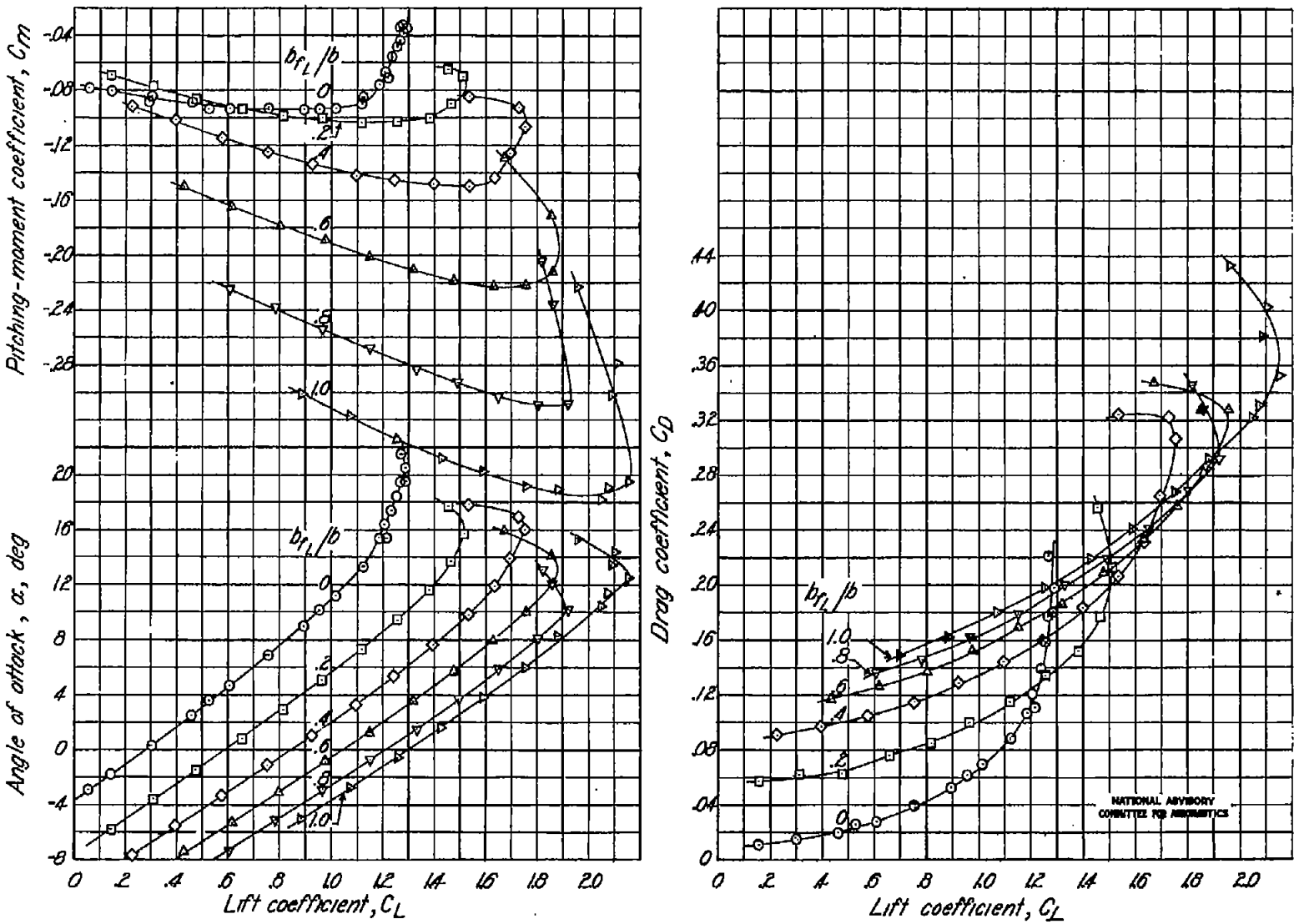

(c) Lift-flap hinge, 0.80c.

Figure 5.- Concluded.

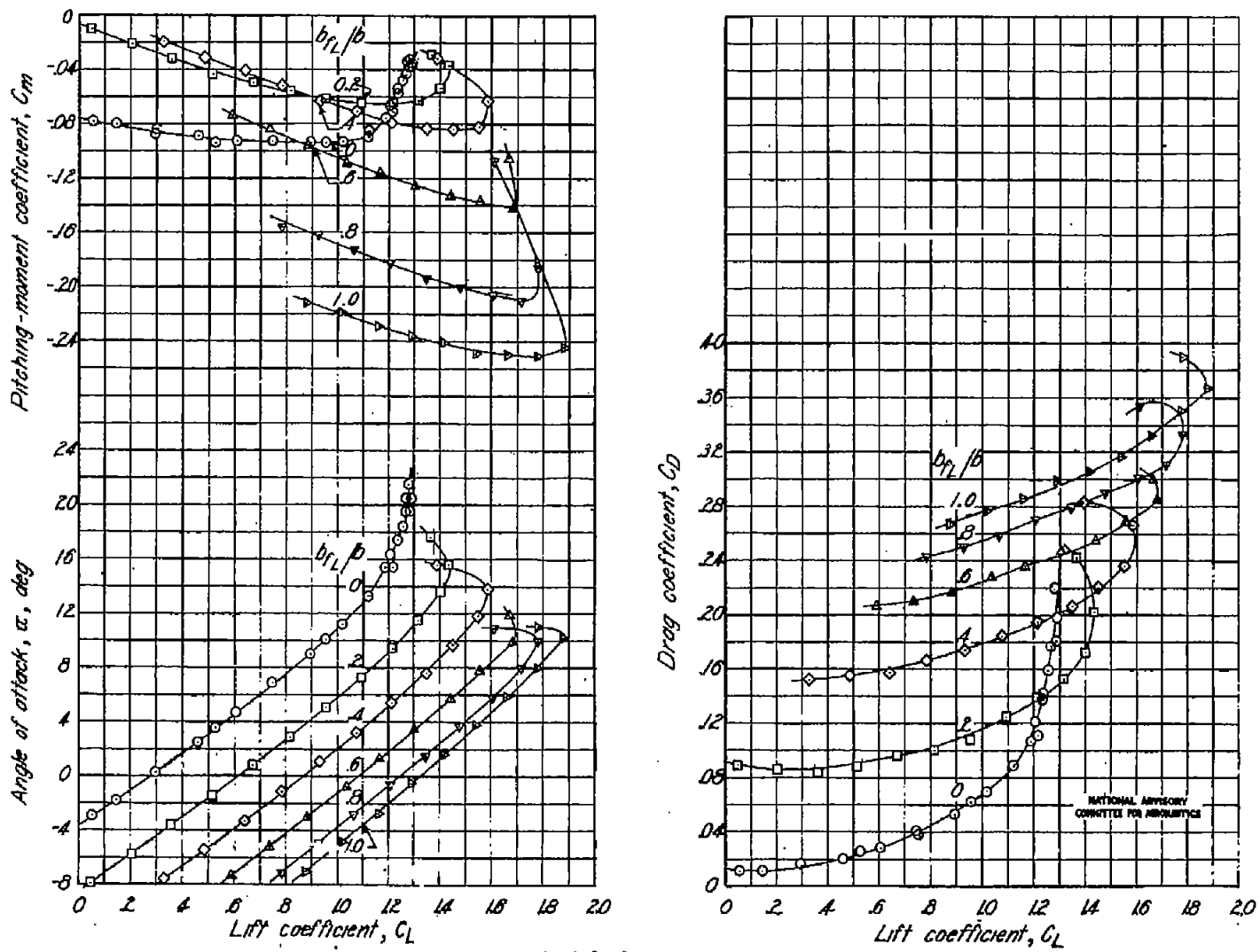

(a) Lift-flap hinge, 0.50c.

Figure 6.-Lift, drag, and pitching-moment coefficients of wing with 0.30c-chord lift flap for various flap spans. $\delta_{f_L} = 60°$; $R = 1.78 \times 10^6$.

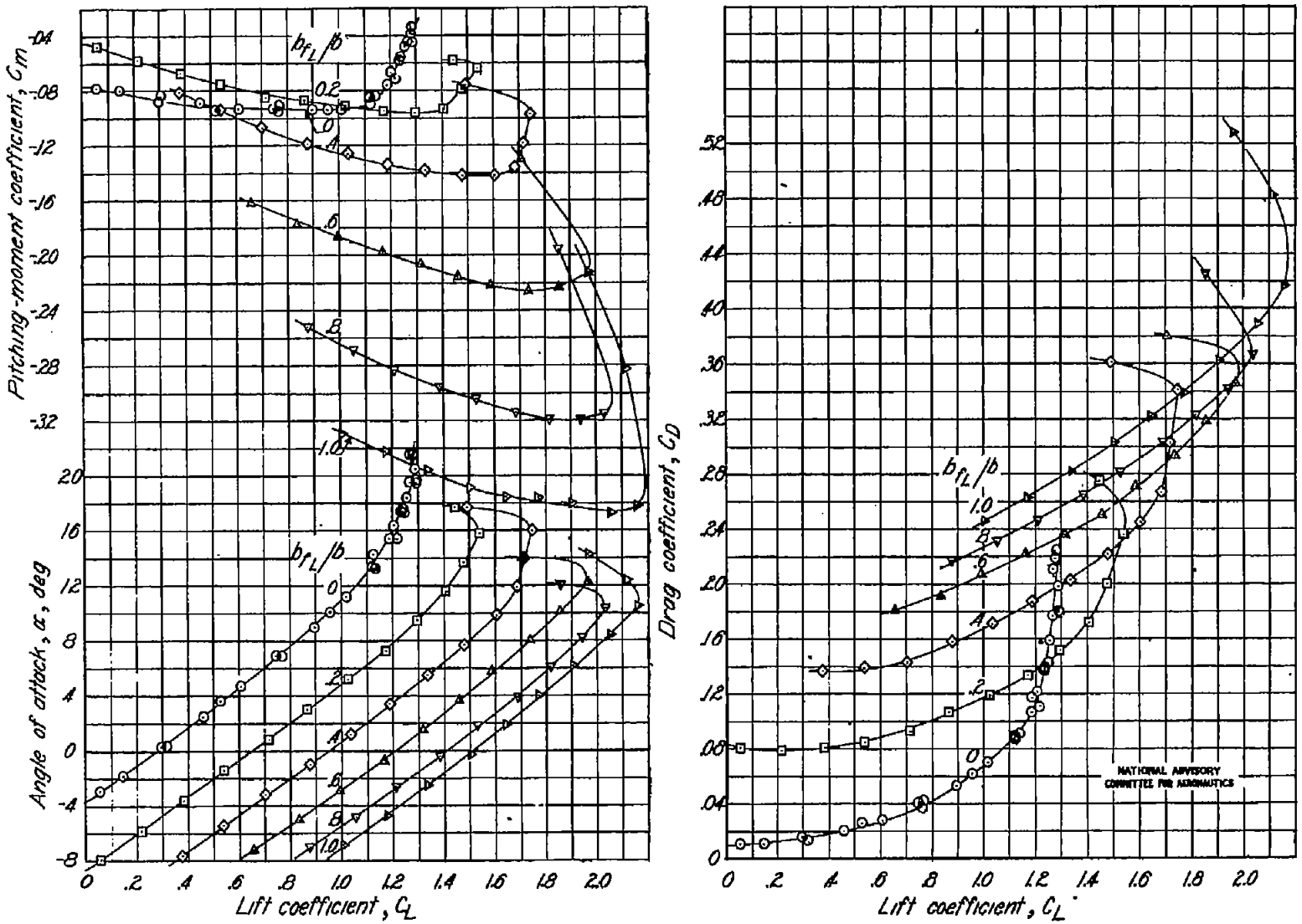

(b) Lift-flap hinge, 0.70c.

Figure 6.– Concluded.

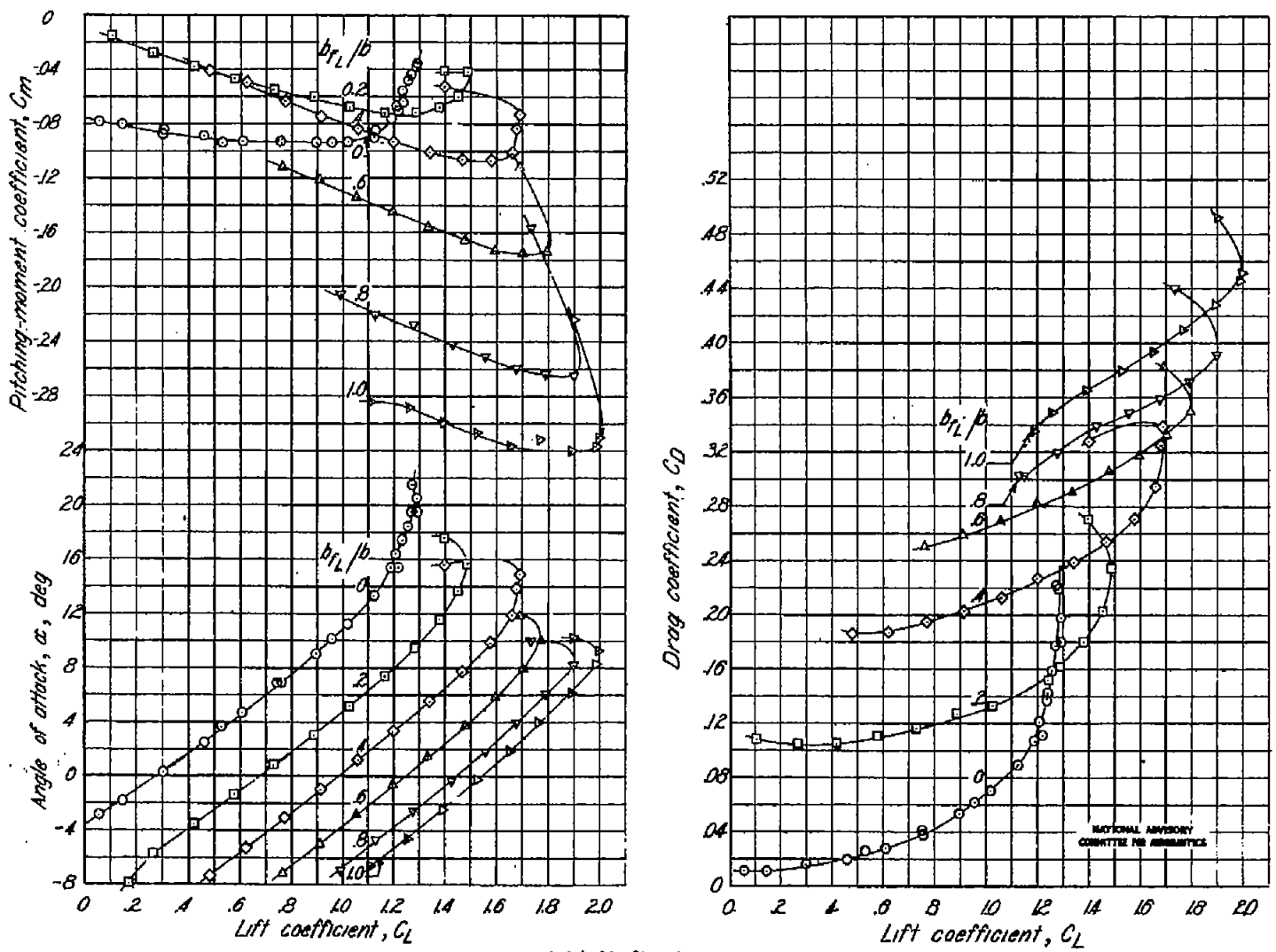

(a) Lift-flap hinge, 0.50c.

Figure 7.-Lift, drag, and pitching-moment coefficients of wing with 0.40c-chord lift flap for various flap spans. $\delta_{f_L} = 60°$; $R = 1.78 \times 10^6$.

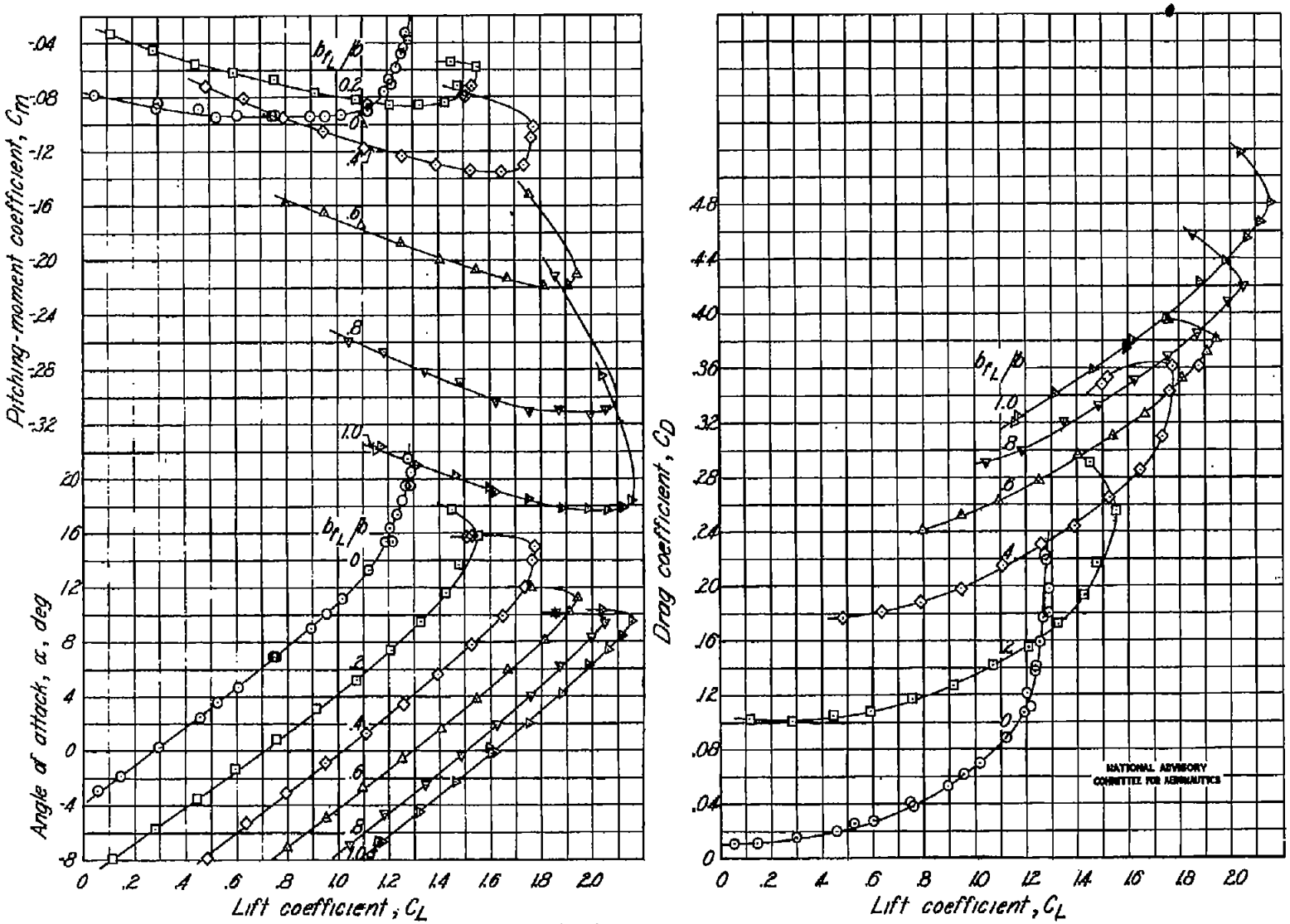

(b) Lift-flap hinge, 0.60c.

Figure 7. - Concluded.

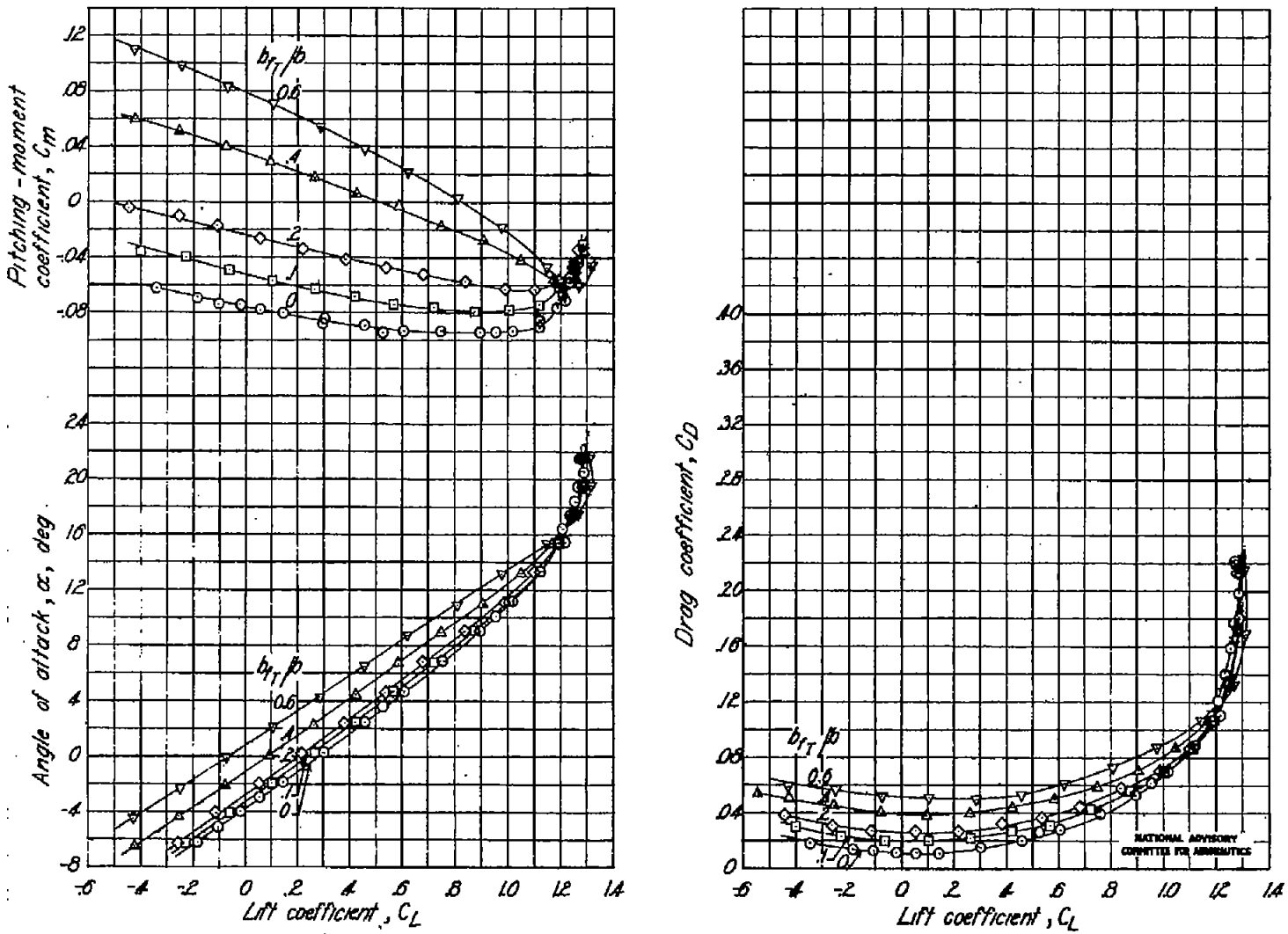

(a) Trim-flap hinge, 0.90c.

Figure 8.- Lift, drag, and pitching-moment coefficients of wing with 0.10c-chord trim flap for various flap spans. $\delta_{f_T} = 60°$; $R = 1.78 \times 10^6$.

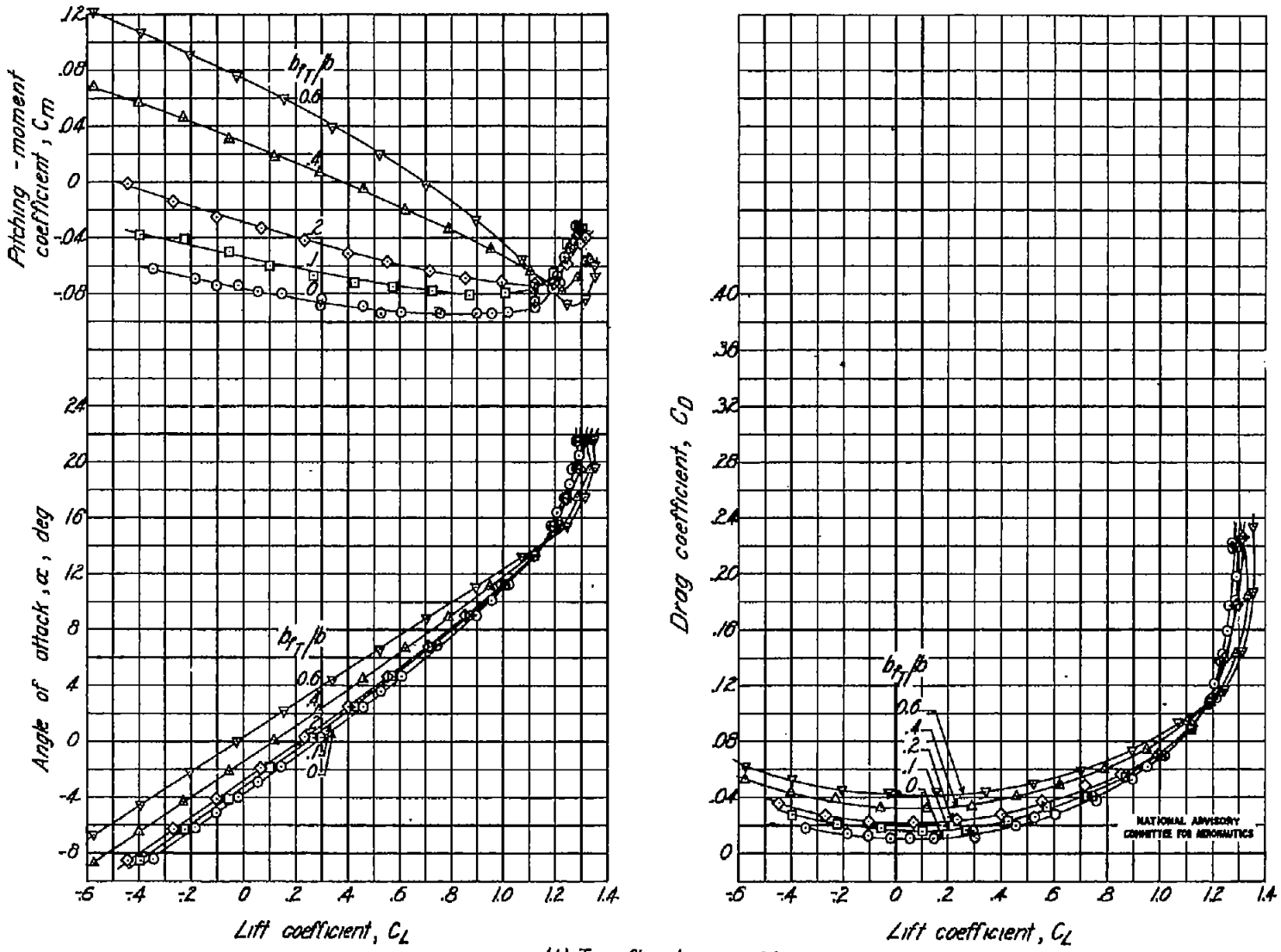

(b) Trim-flap hinge, 1.00c.

Figure 8.- Concluded.

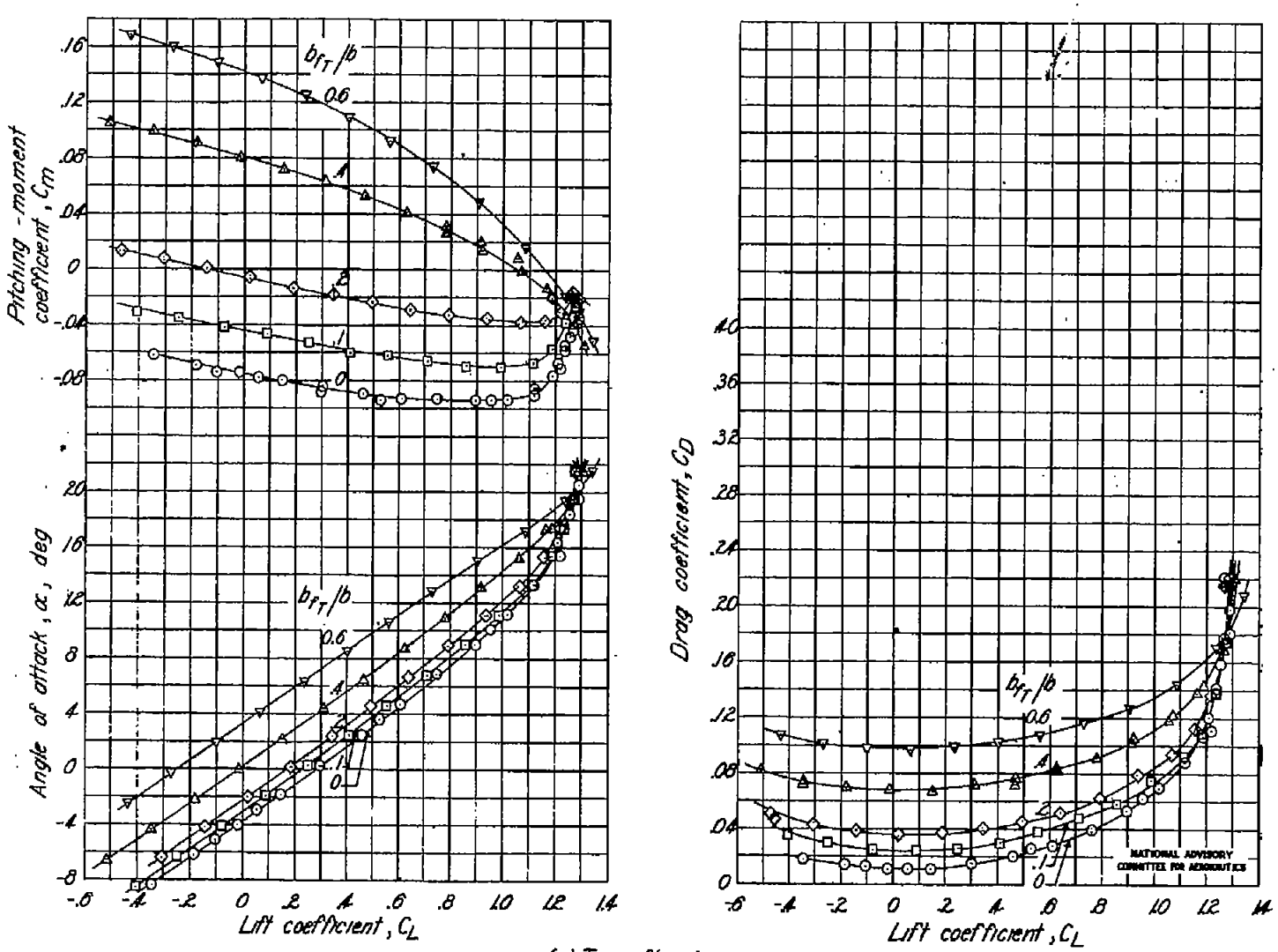

(a) Trim-flap hinge, 0.80c.

Figure 9.- Lift, drag, and pitching-moment coefficients of wing with 0.20c-chord trim flap for various flap spans. $\delta_{f_T} = 60°$, $R = 1.78 \times 10^6$.

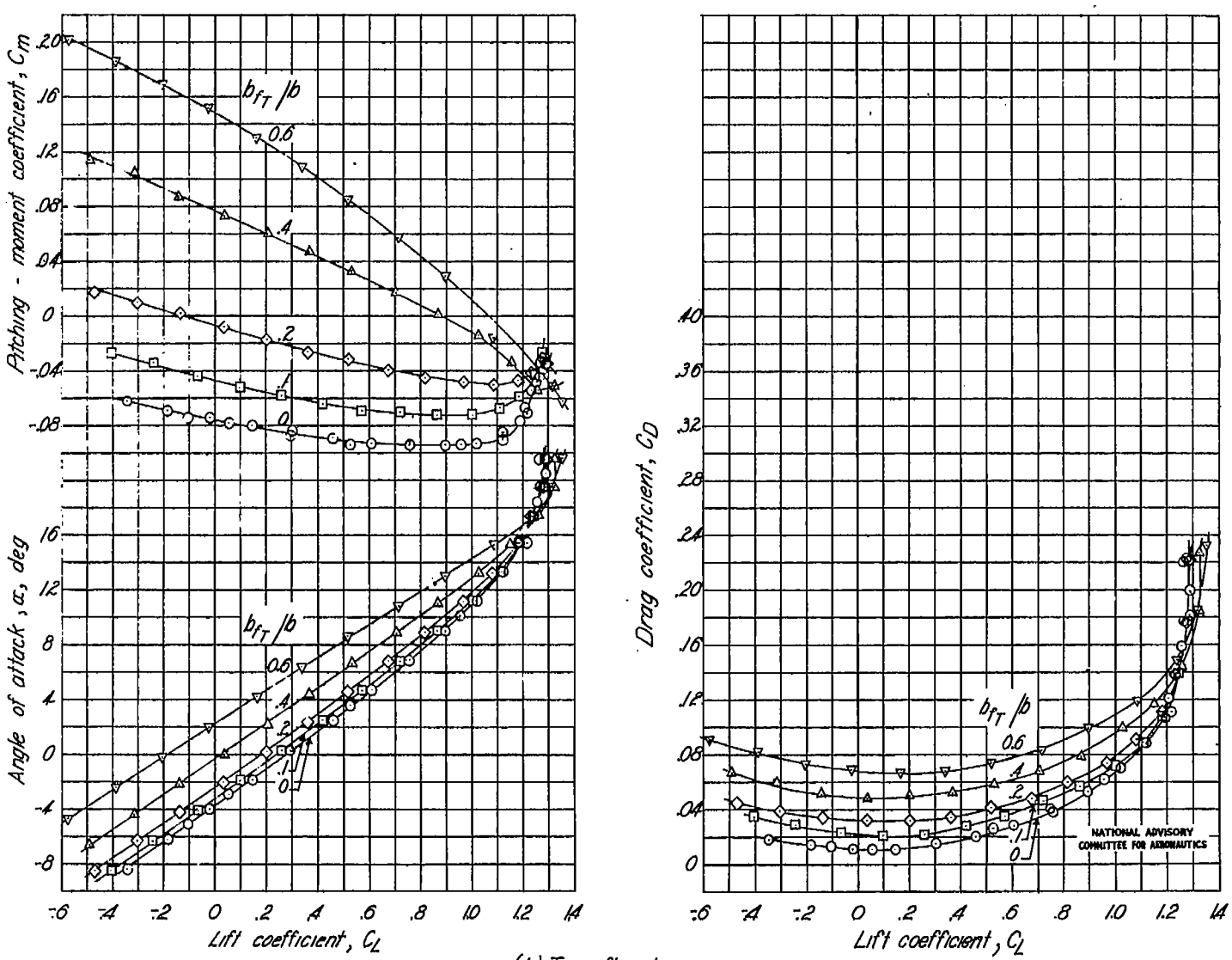

(b) Trim-flap hinge, 1.00c.

Figure 9.- Concluded.

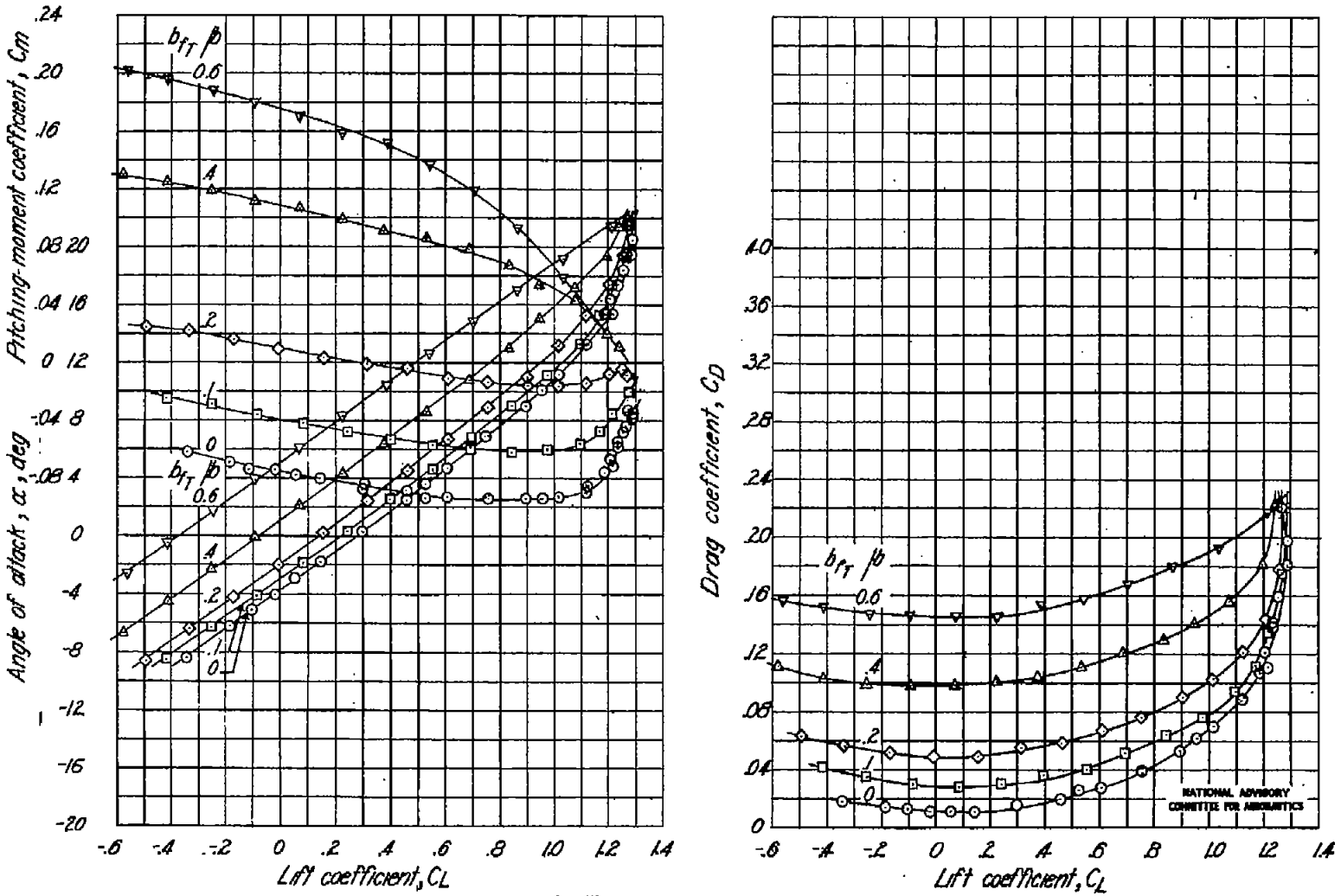

(a) Trim-flap hinge, 0.70c.

Figure 10.– Lift, drag, and pitching-moment coefficients of wing with 0.30c-chord trim flap for various flap spans. $\delta_{f_T} = 60°$; $R = 1.78 \times 10^6$.

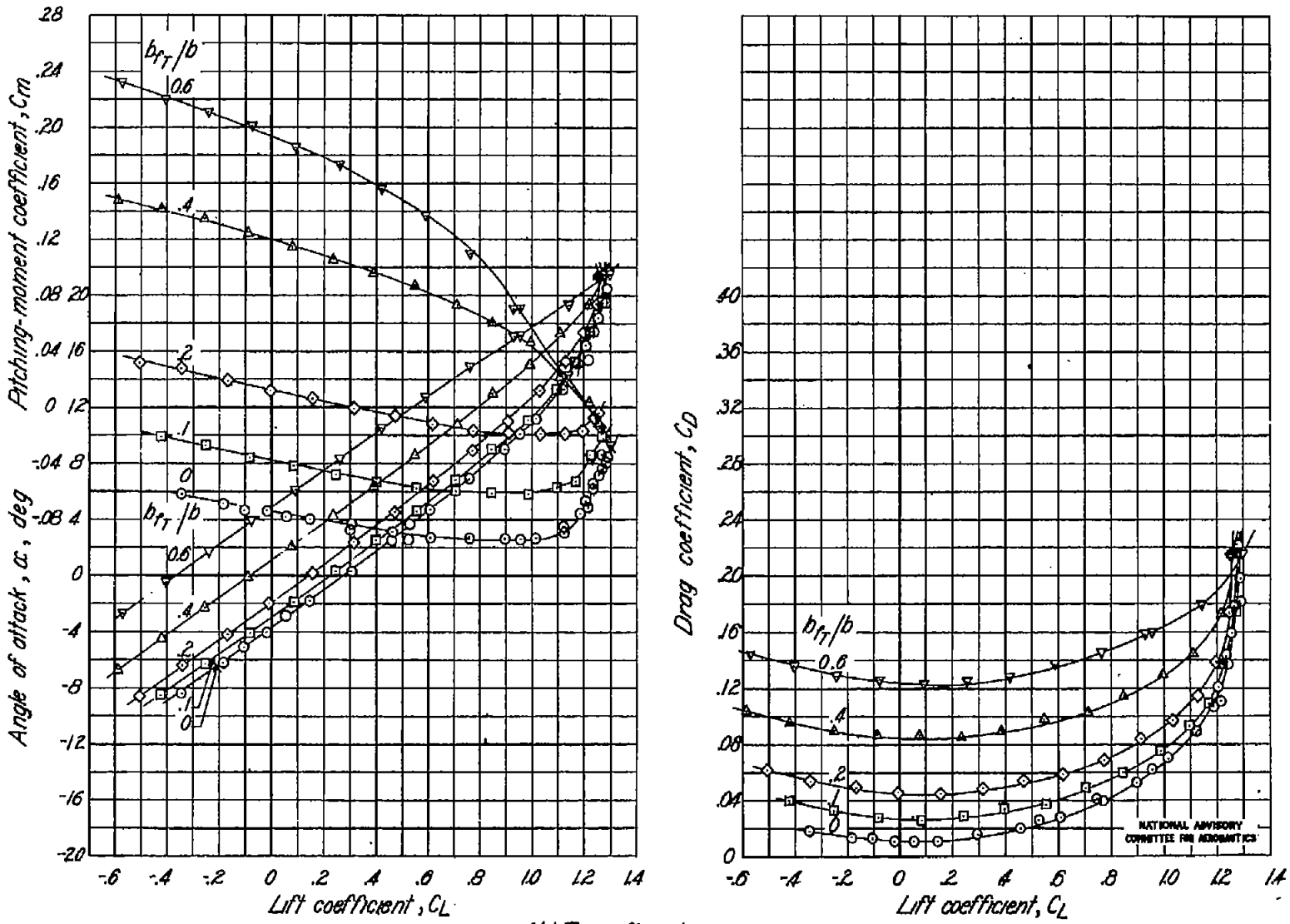

(b) Trim-flap hinge, 0.80c.

Figure 10.– Continued.

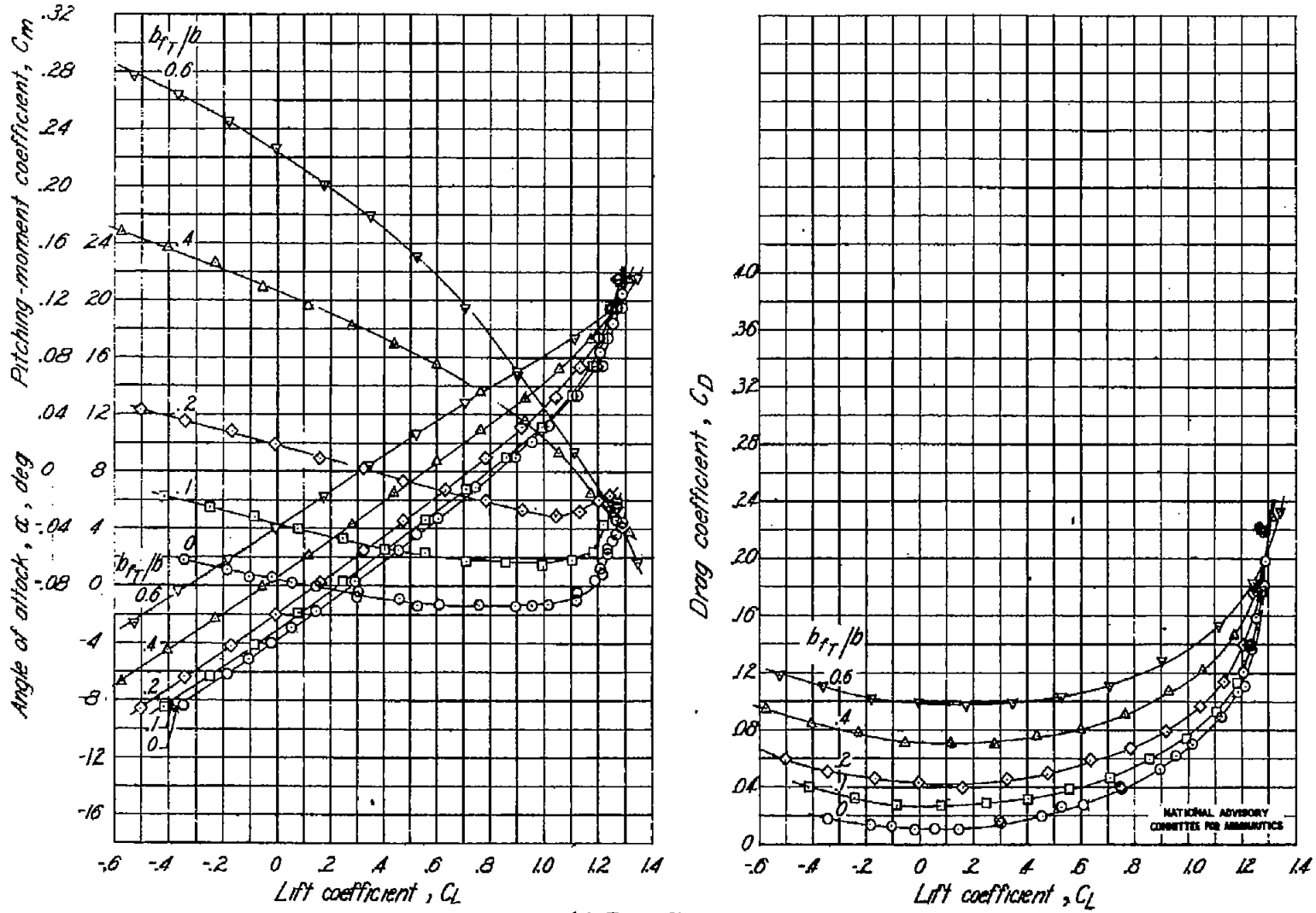

(c) Trim-flap hinge, 1.00c.

Figure 10.– Concluded.

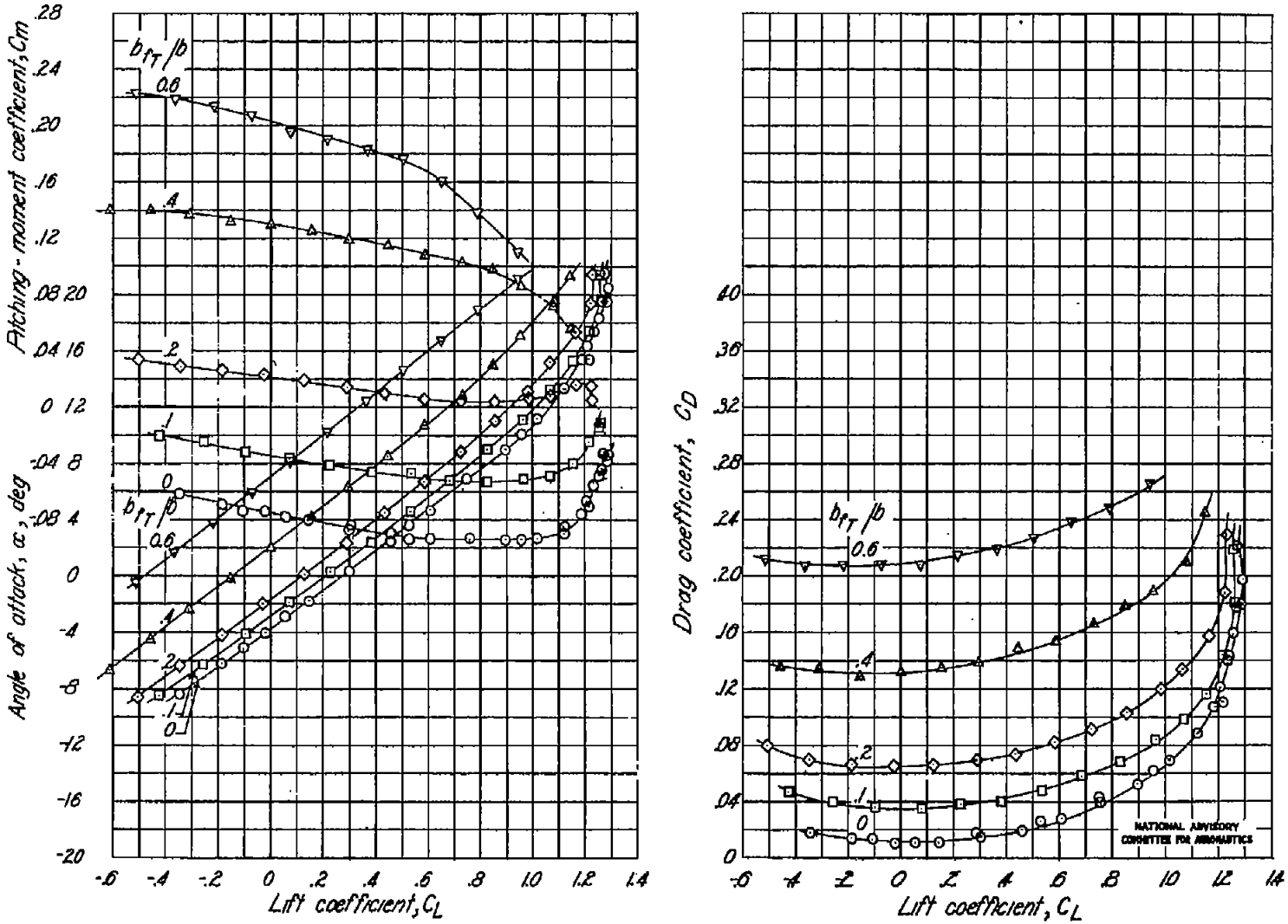

(a) Trim-flap hinge, 0.60c.

Figure 11.- Lift, drag, and pitching-moment coefficients of wing with 0.40c-chord trim flap for various flap spans. $\delta_{f_T} = 60°$, $R = 1.78 \times 10^6$.

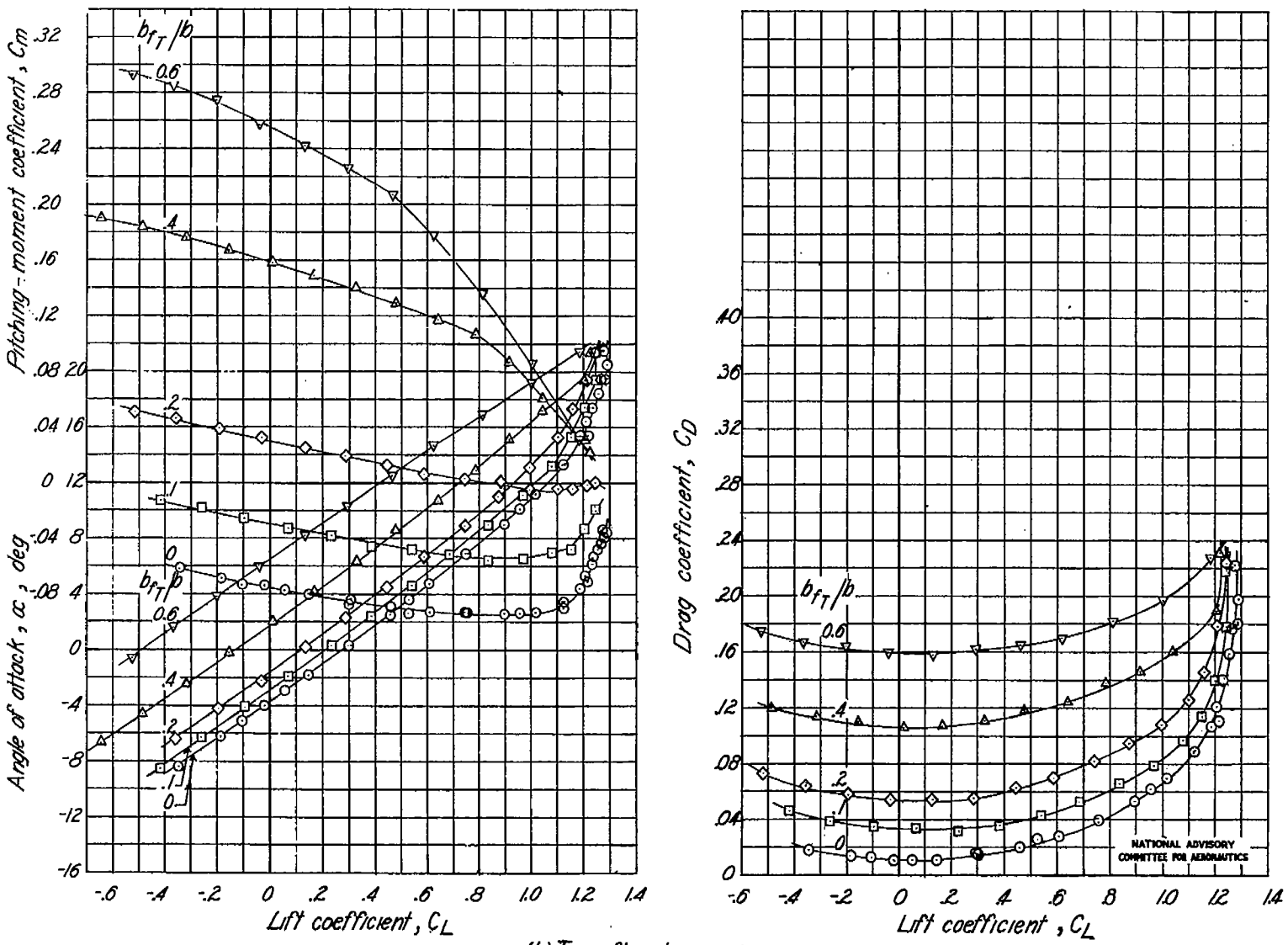

(b) Trim-flap hinge, 0.80c.

Figure 11.– Continued.

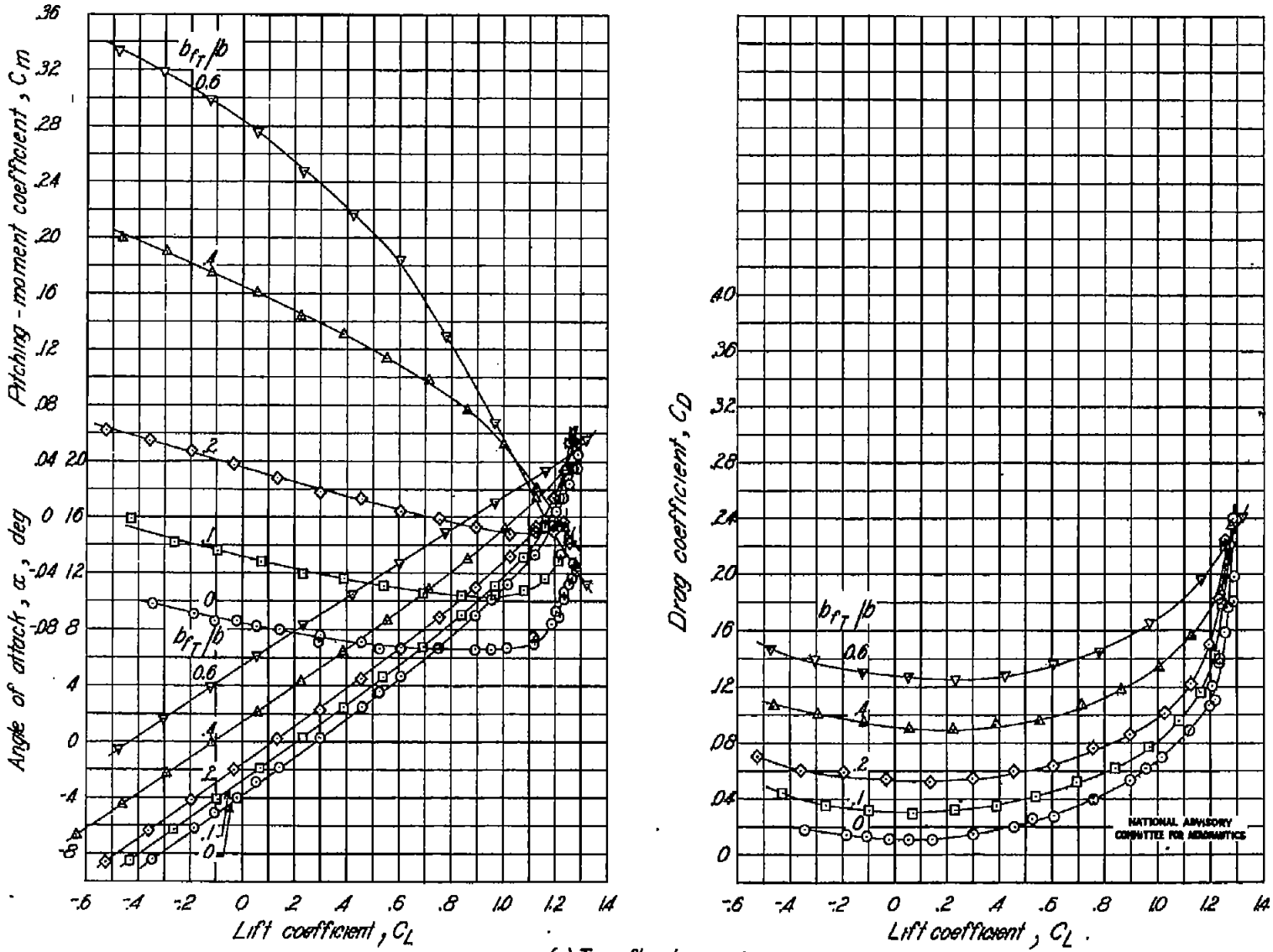

(c) Trim-flap hinge, 1.00c.

Figure 11. - Concluded.

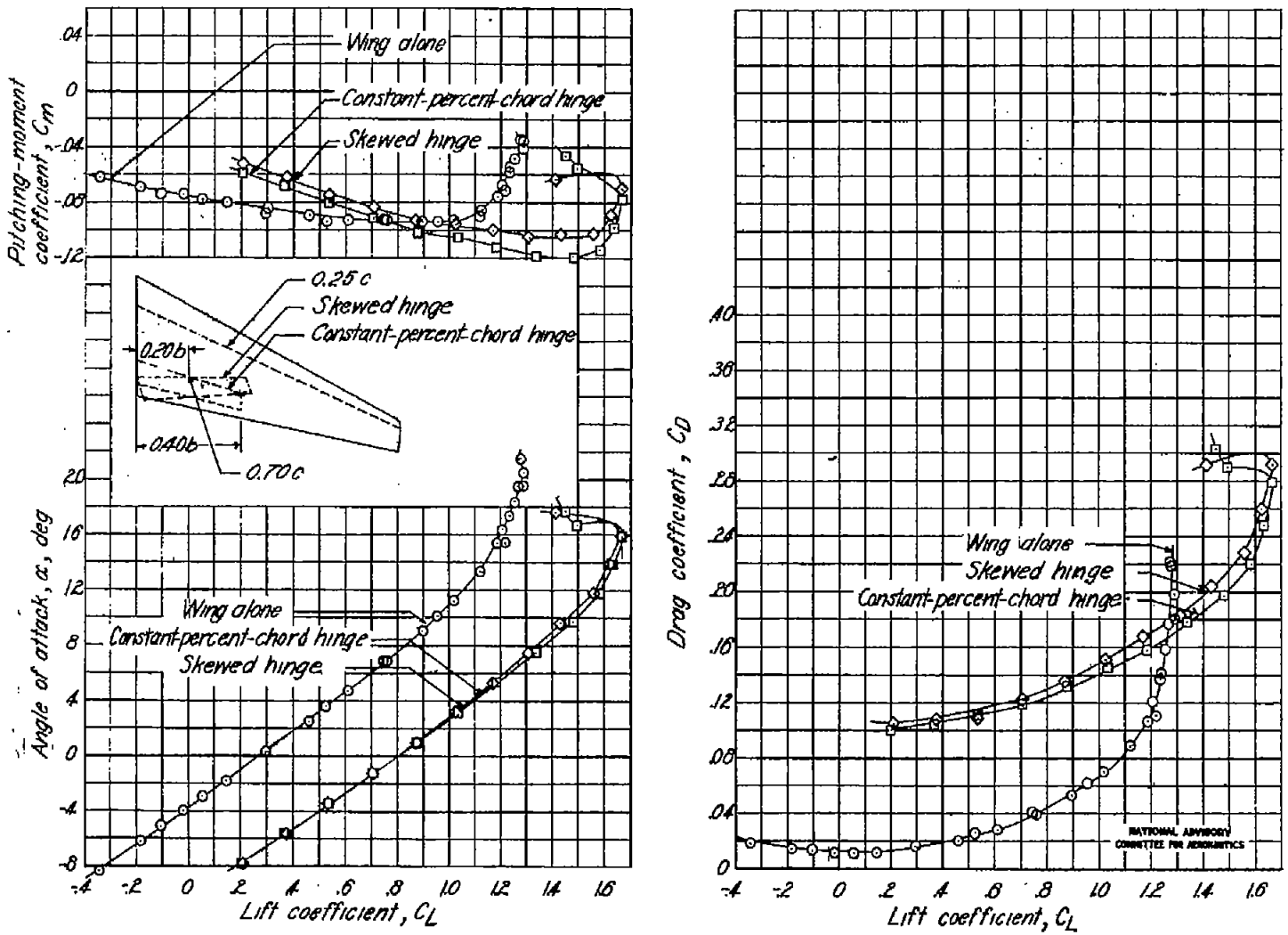

Figure 12. - Lift, drag, and pitching-moment coefficients of wing with 0.20c-chord lift flap with the hinge line coinciding with and skewed relative to 0.70c of wing. Lift-flap span, 0.40 b; $\delta_{f_L} = 60°$; $R = 1.78 \times 10^6$.

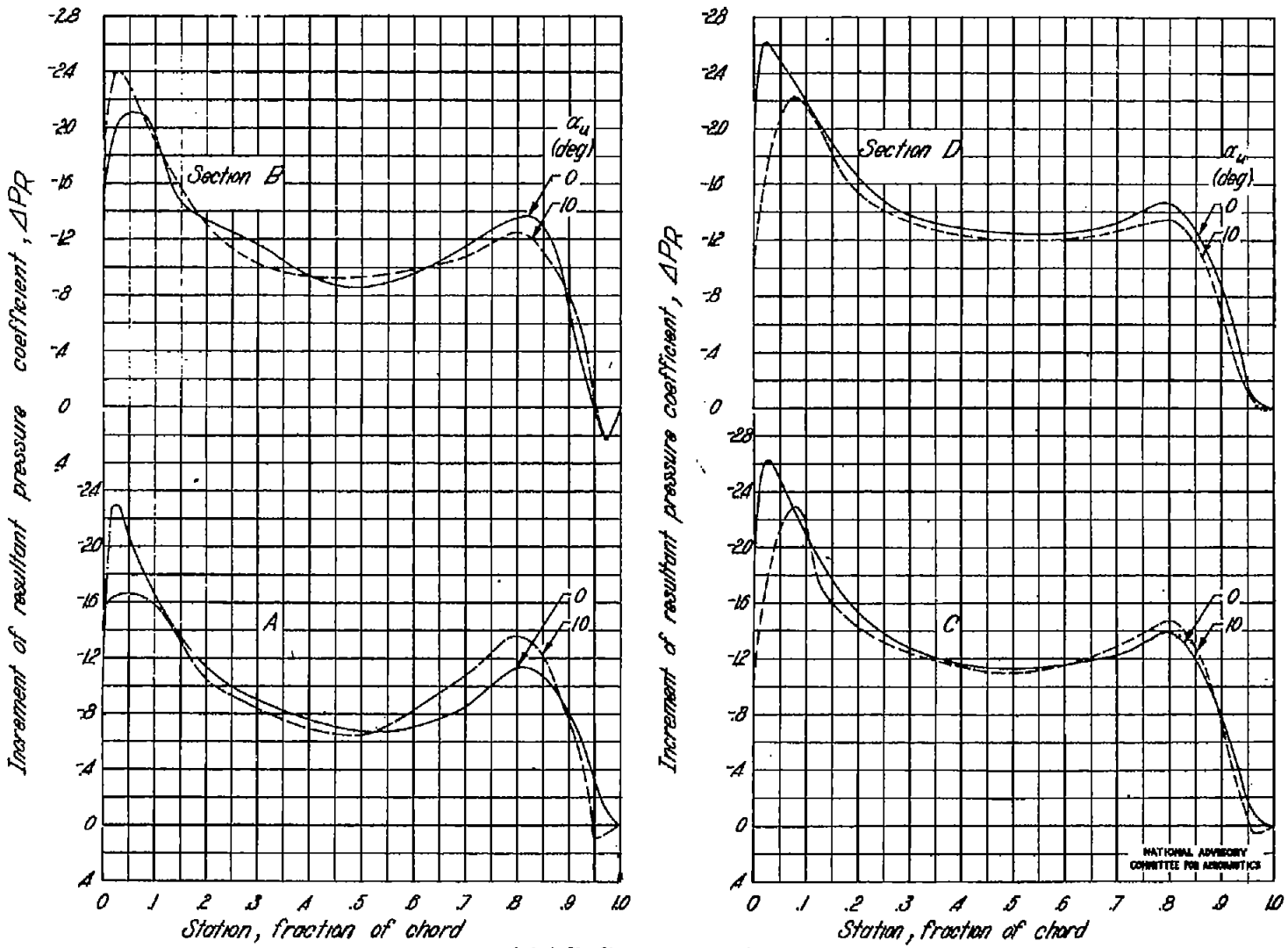

(a) Lift-flap span, 1.0 b.

Figure 13.-Increment of resultant pressure coefficient at different spanwise sections caused by a 0.20c-chord lift flap hinged at 0.80c. $\delta_{f_L}=60°$; $R=178\times10^6$.
(Section locations are shown in fig. 1.)

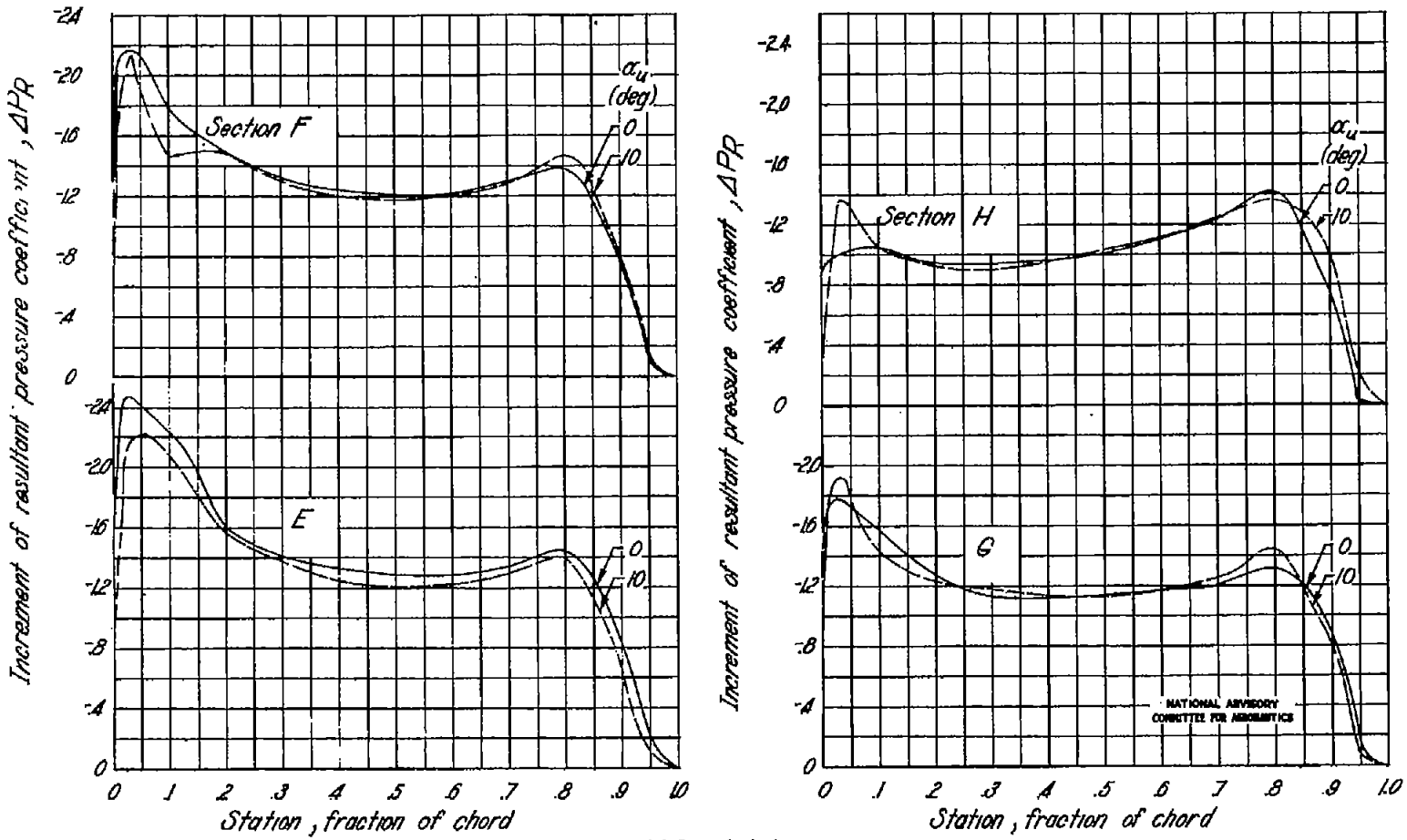

(a) Concluded.

Figure 13.– Continued.

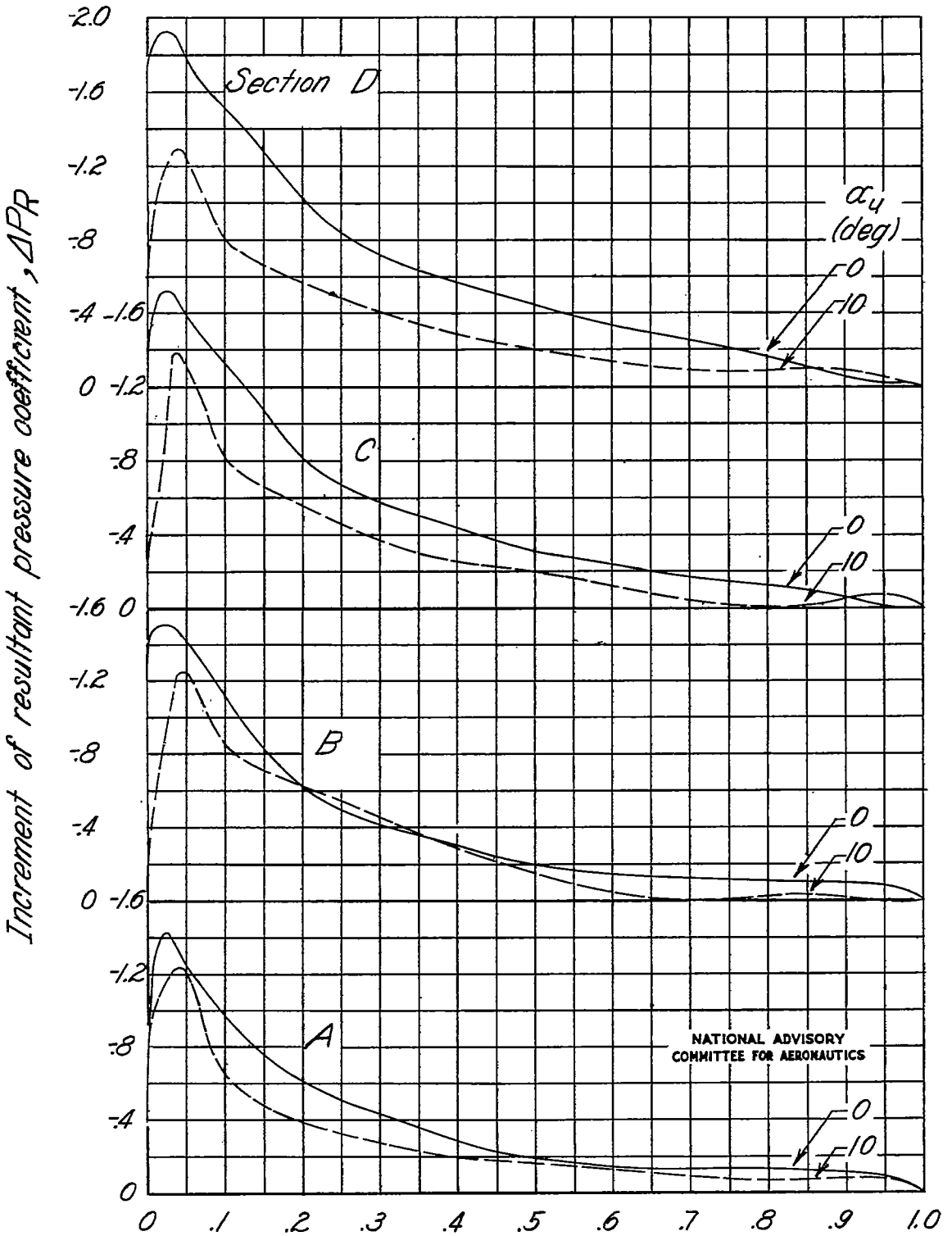

(b) Lift-flap span, 0.6b.

Figure 13. – Continued.

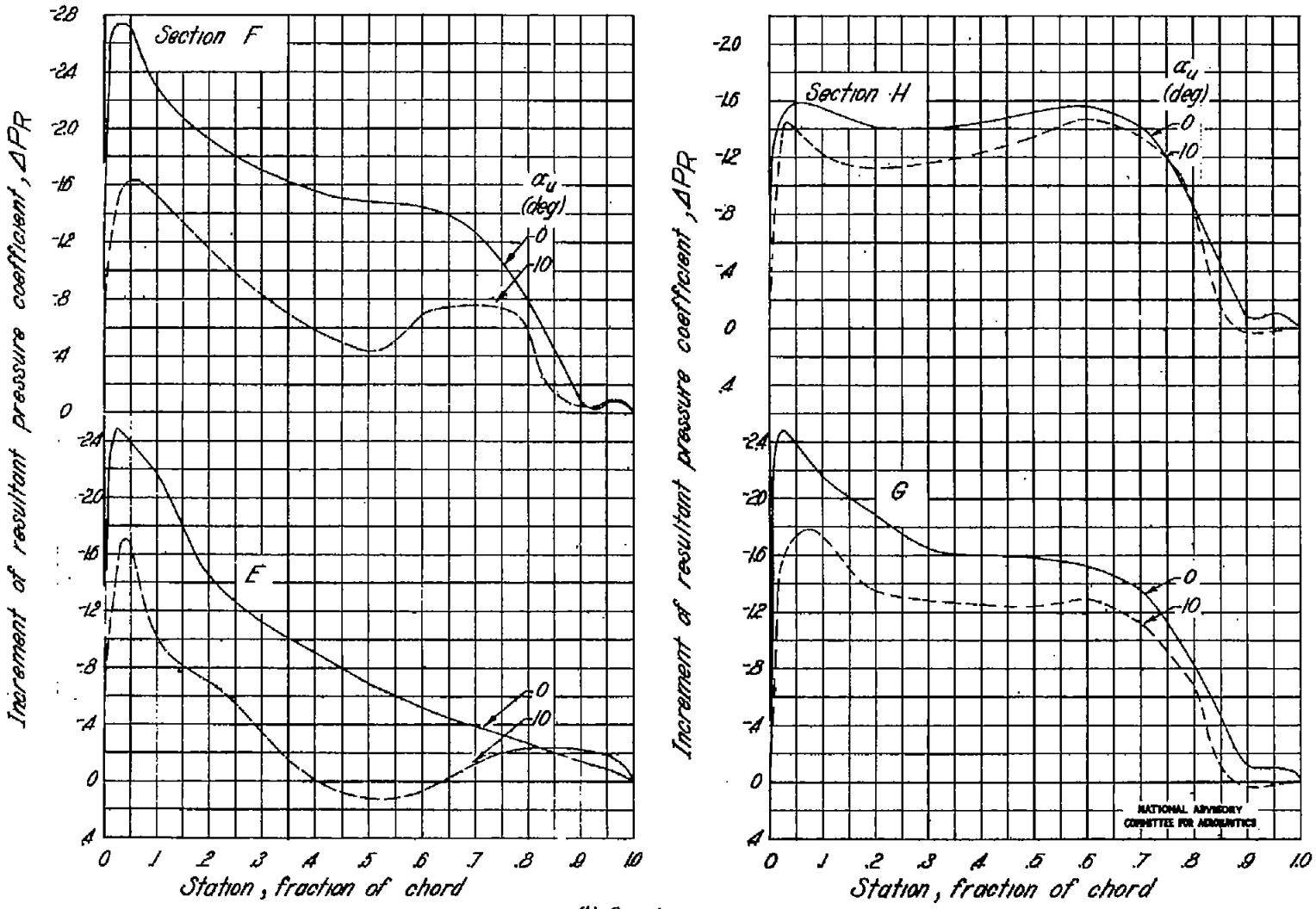

(b) Concluded.

Figure 13. – Continued.

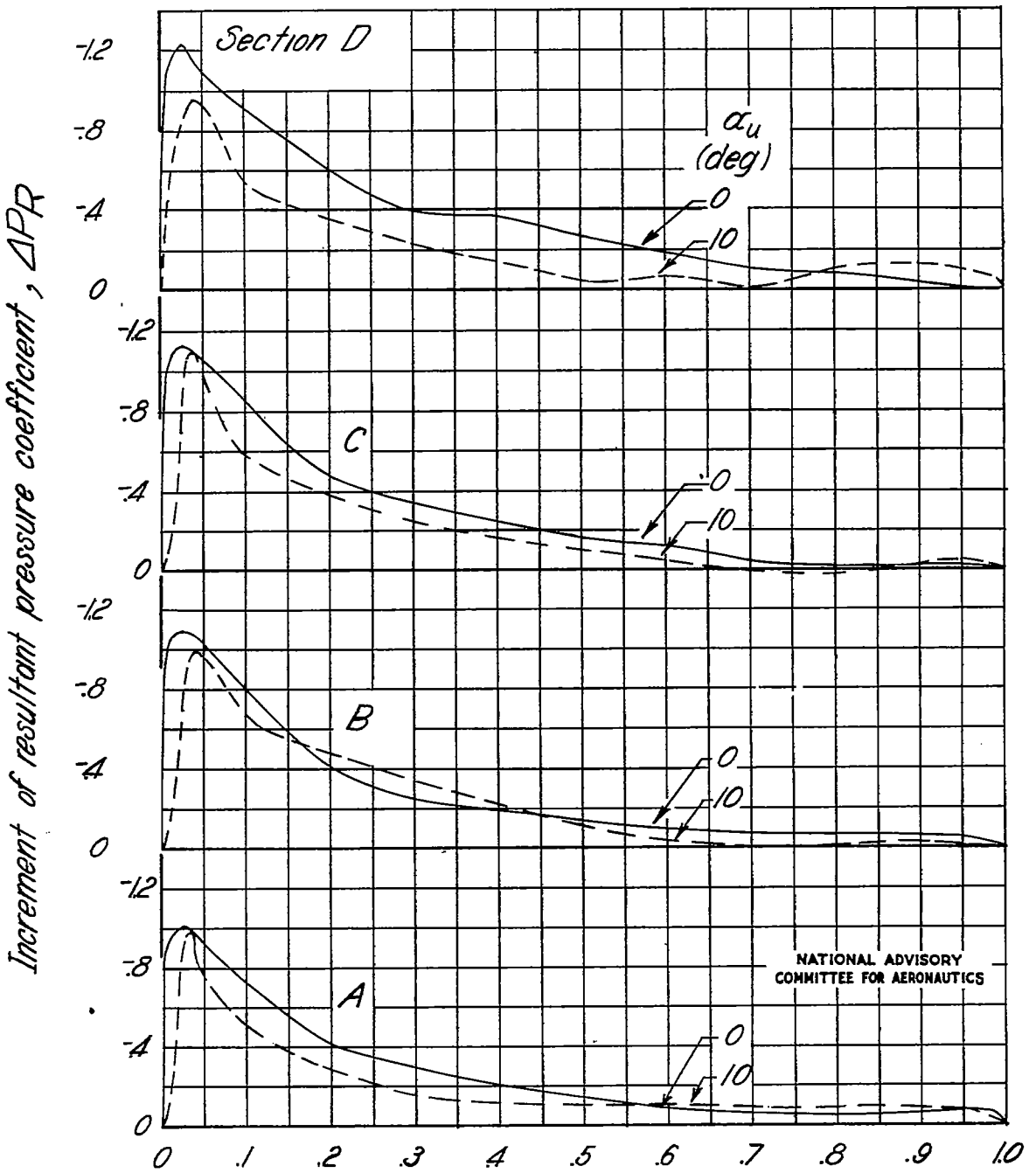

(c) Lift-flap span, 0.4b.

Figure 13.- Continued.

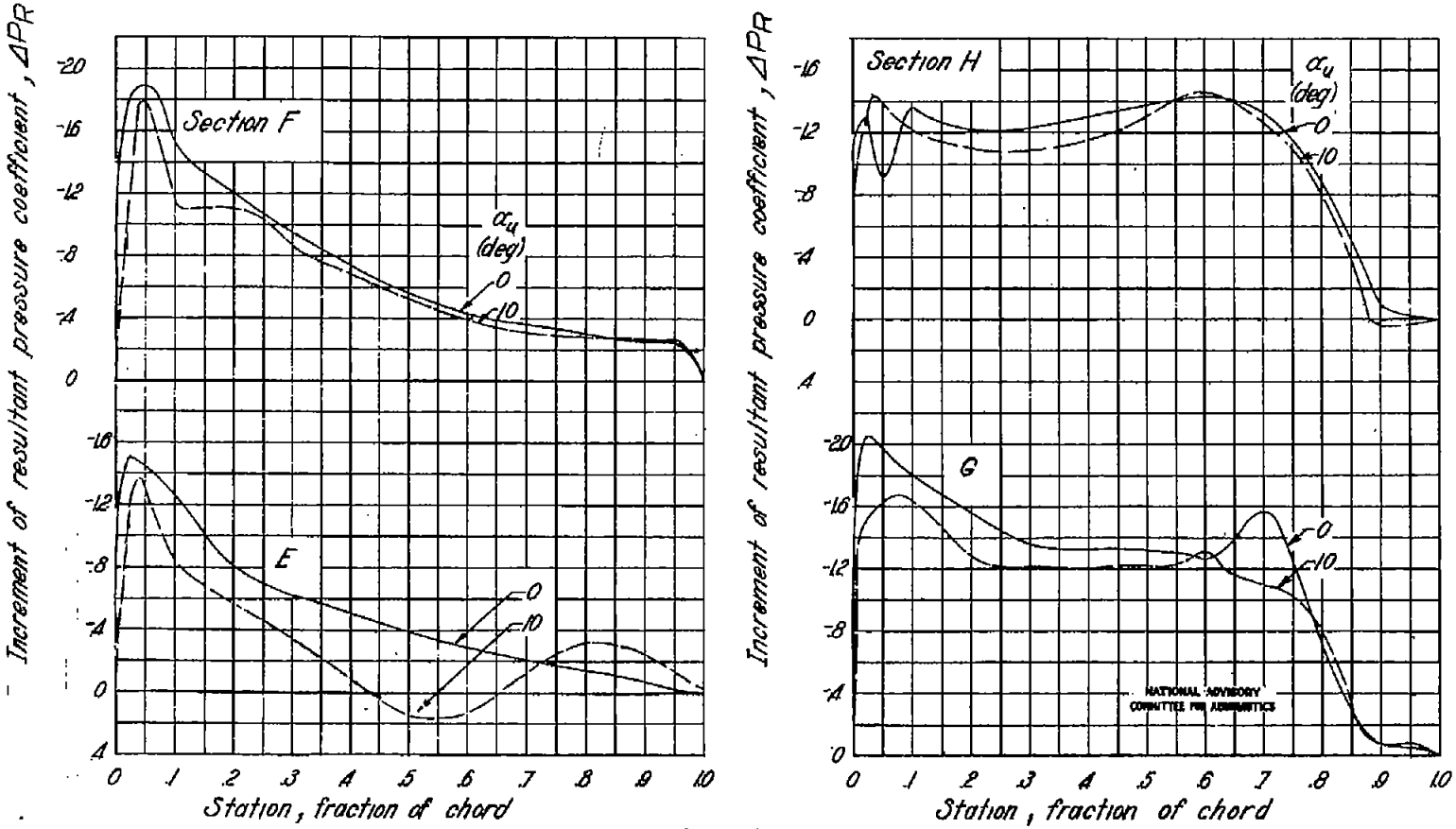

(c) Concluded.

Figure 13.--Concluded.

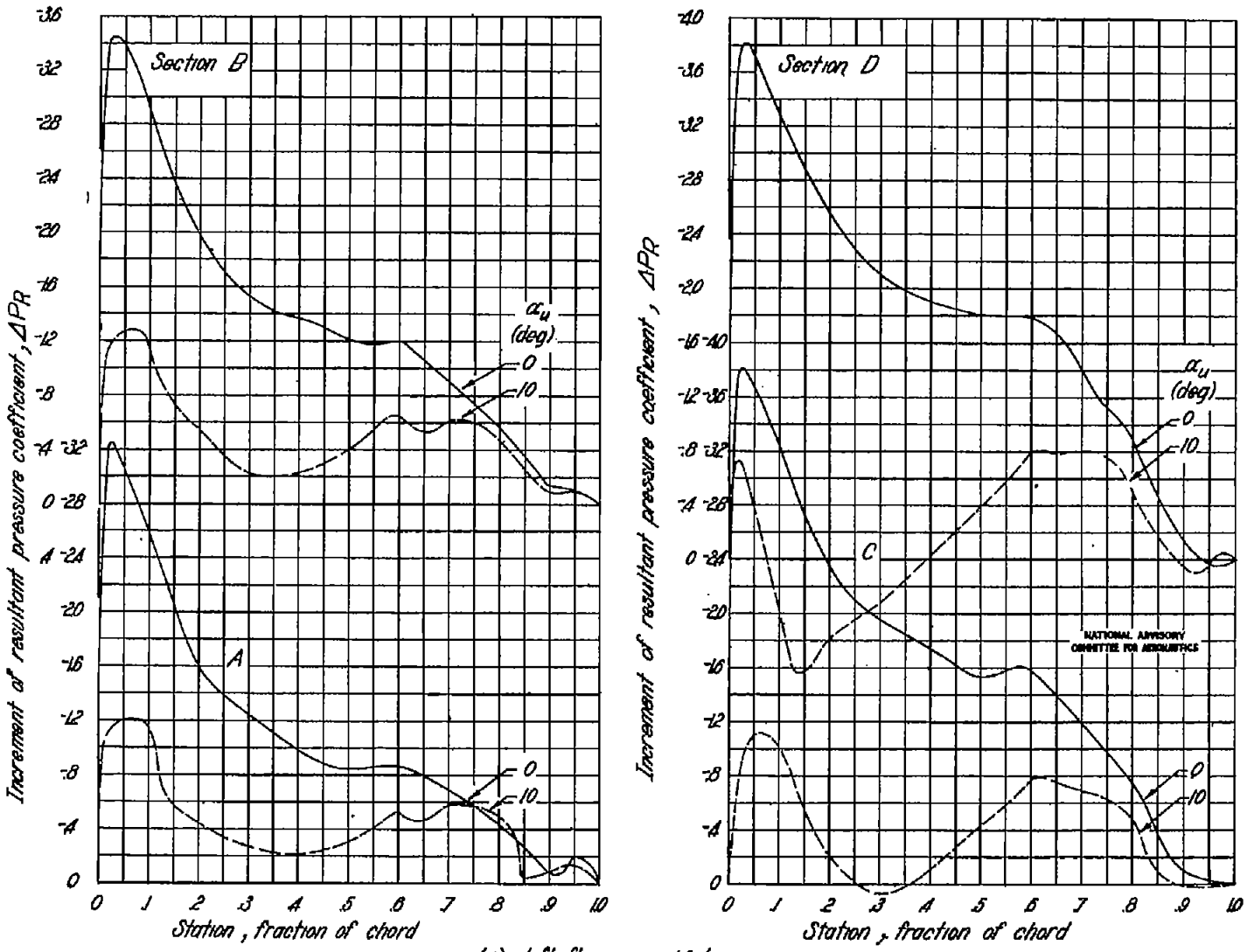

(a) Lift-flap span, 1.0 b.

Figure 14.-Increment of resultant pressure coefficient at different spanwise sections caused by a 0.40c-chord lift flap hinged at 0.80c. $\delta_{fL}=60°$; $R=1.78\times10^6$. (Section locations are shown in fig. 1.)

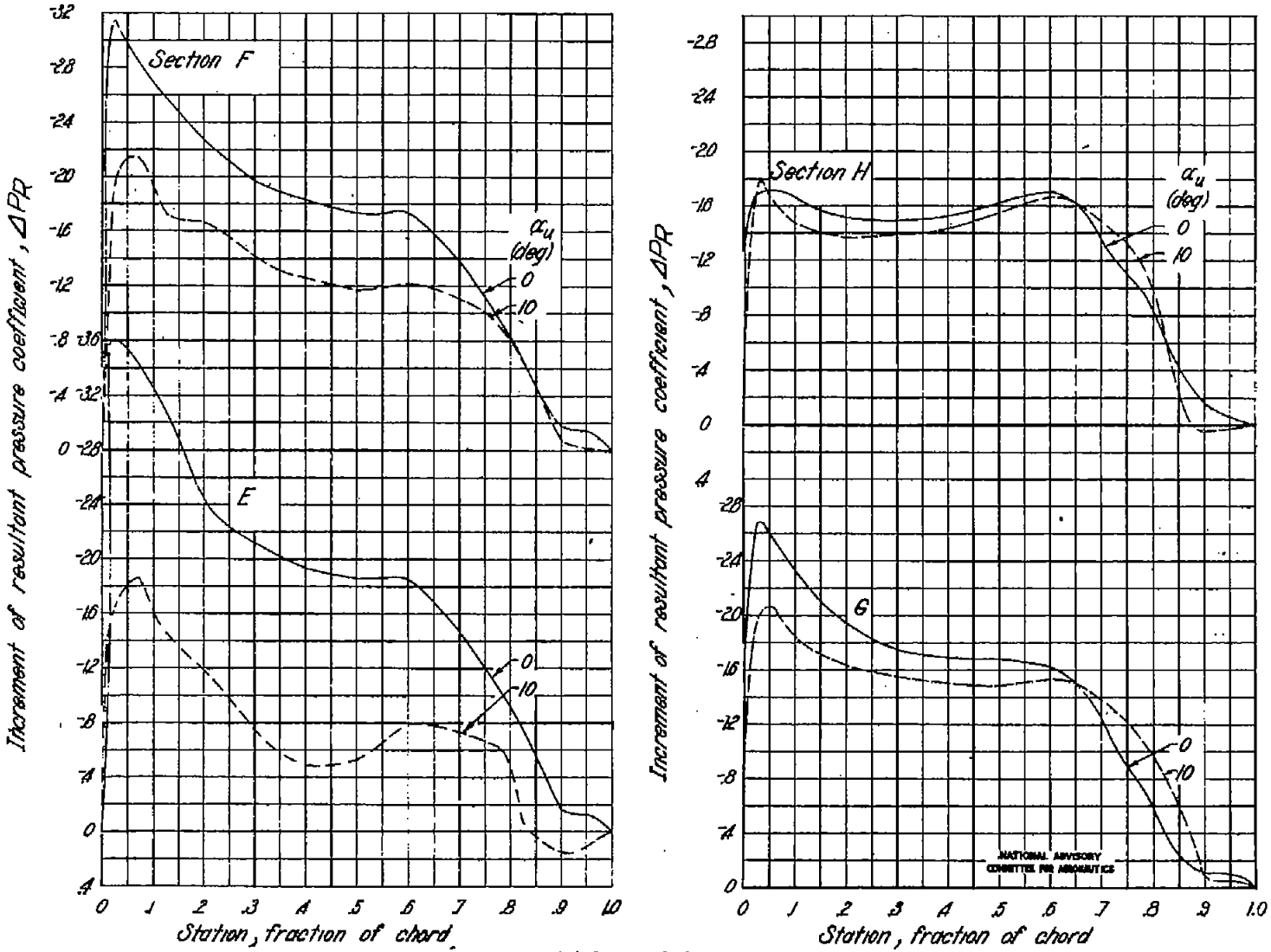

(a) Concluded.

Figure 14.-Continued.

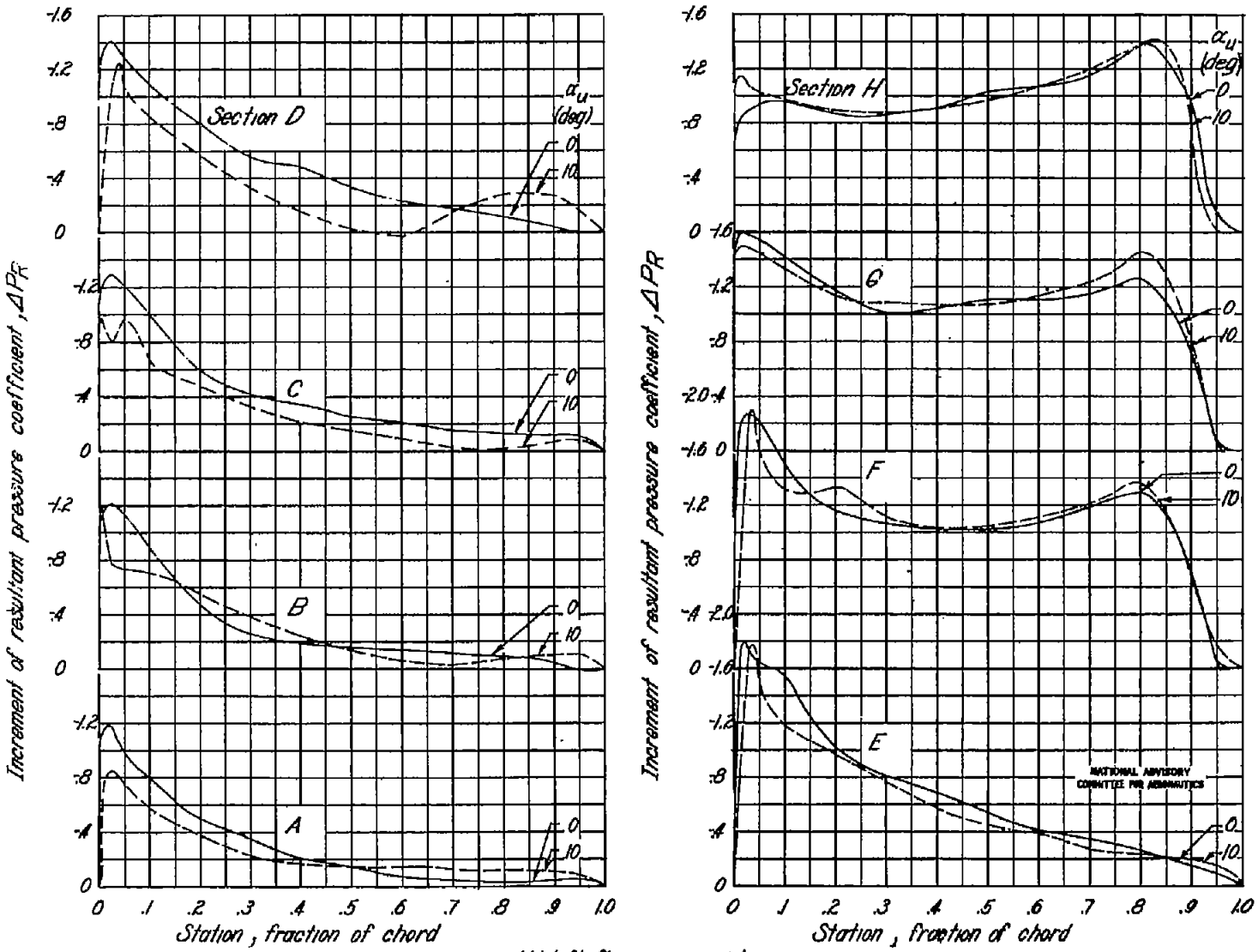

(b) Lift-flap span, 0.6b.

Figure 14.- Continued.

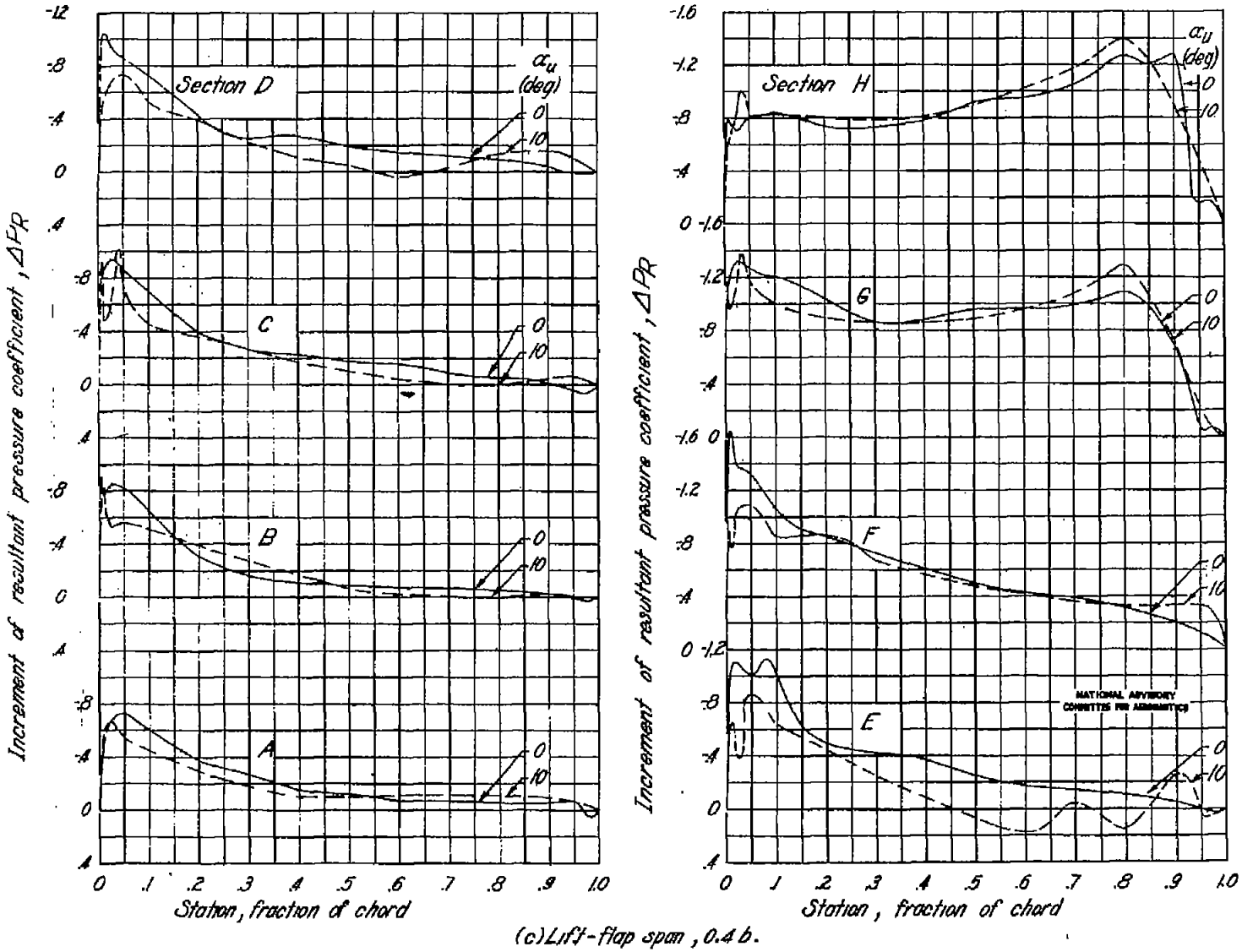

(c) Lift-flap span, 0.4 b.

Figure 14.- Concluded.

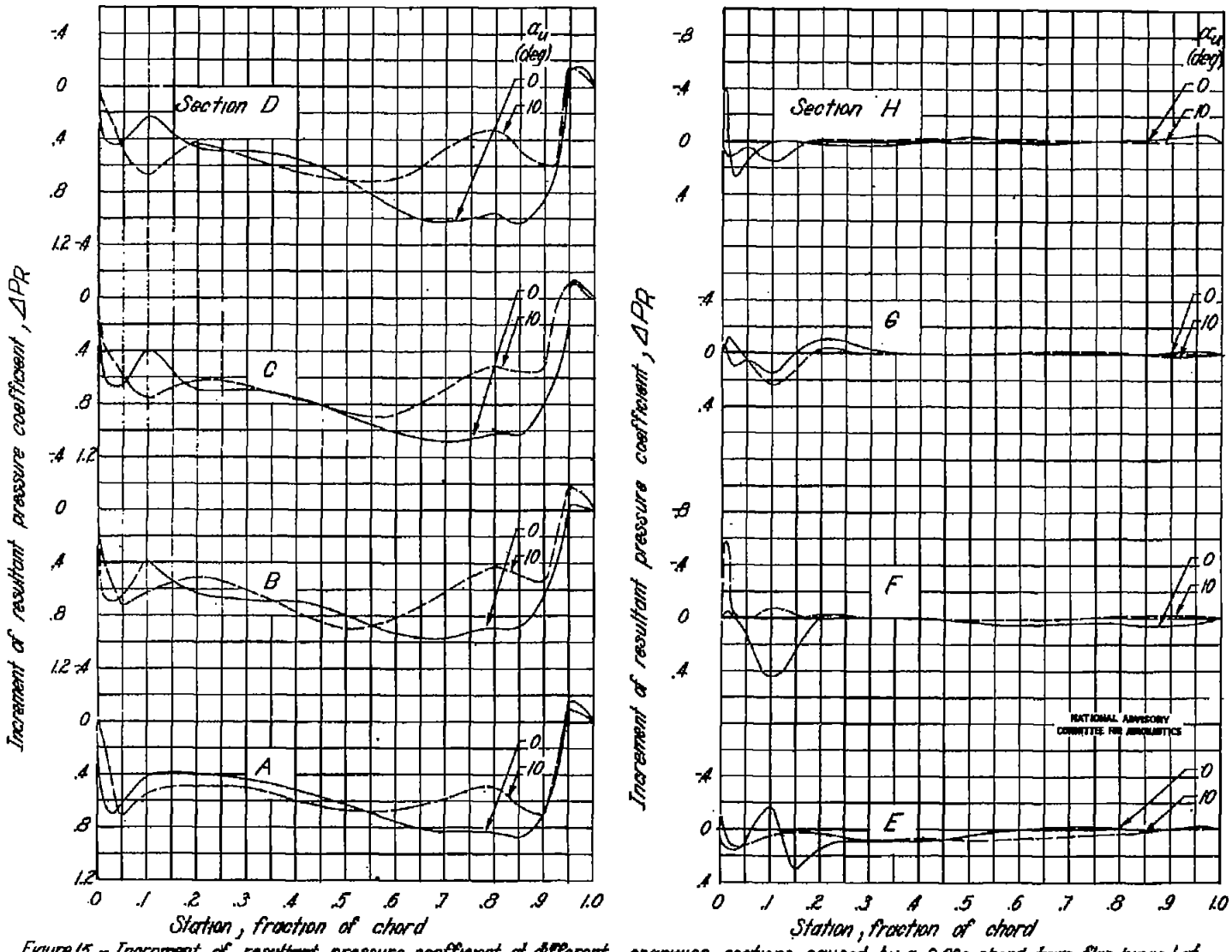

Figure 15.- Increment of resultant pressure coefficient at different spanwise sections caused by a 0.20c-chord trim flap hinged at 0.80c. Flap span, 0.20b; $\delta_f = 60°$; $R = 1.78 \times 10^6$. (Section locations are shown in fig. 1.)

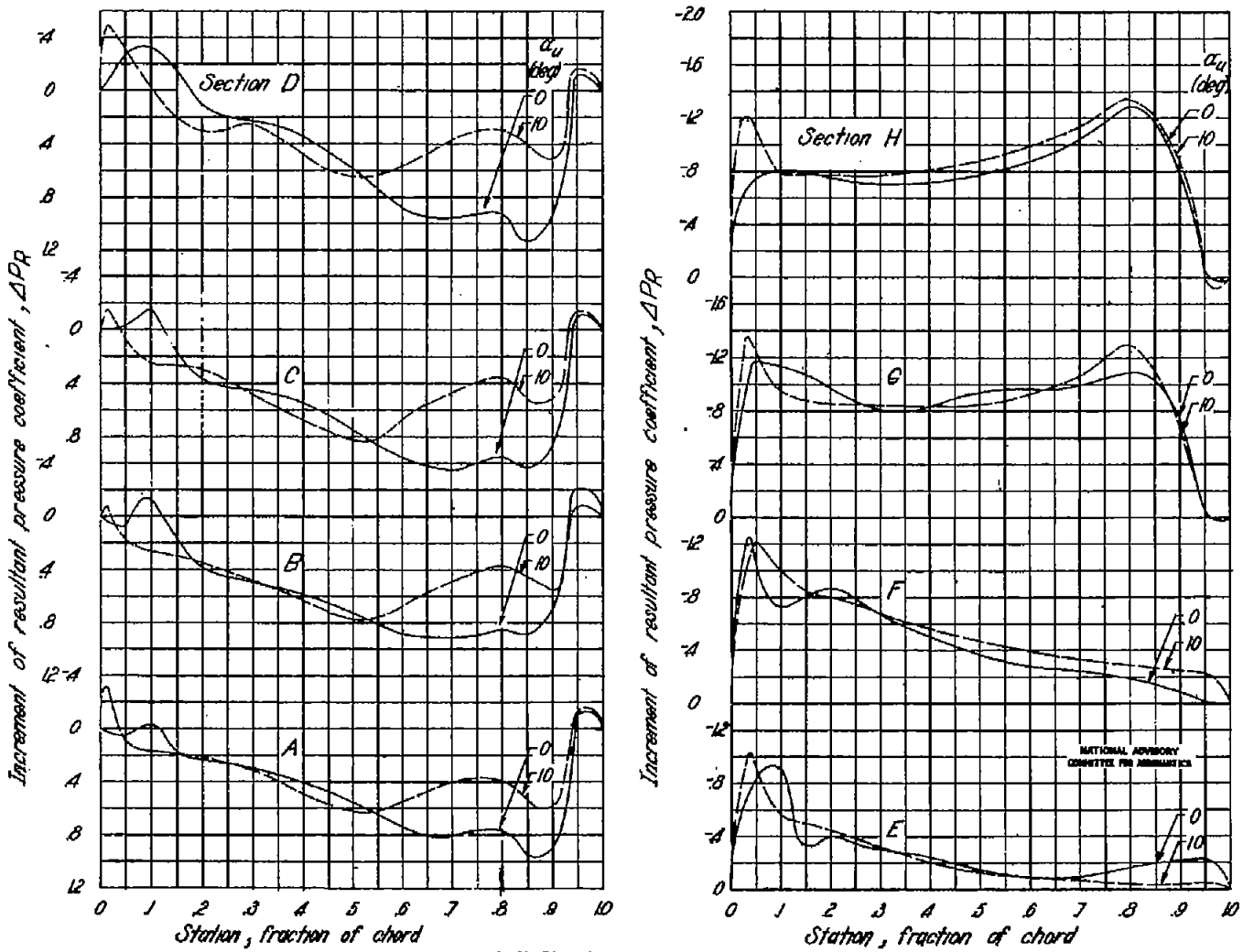

(a) Lift-flap hinge, 0.80c.

Figure 16.- Increment of resultant pressure coefficient at different spanwise sections caused by 0.20c-chord lift and trim flaps. Trim flap hinged at 0.80c. Lift-flap span, 0.40 b; trim-flap span, 0.20 b; $\delta_L = 60°$; $\delta_T = 60°$; $R = 1.78 \times 10^6$.
(Section locations are shown in fig. 1.)

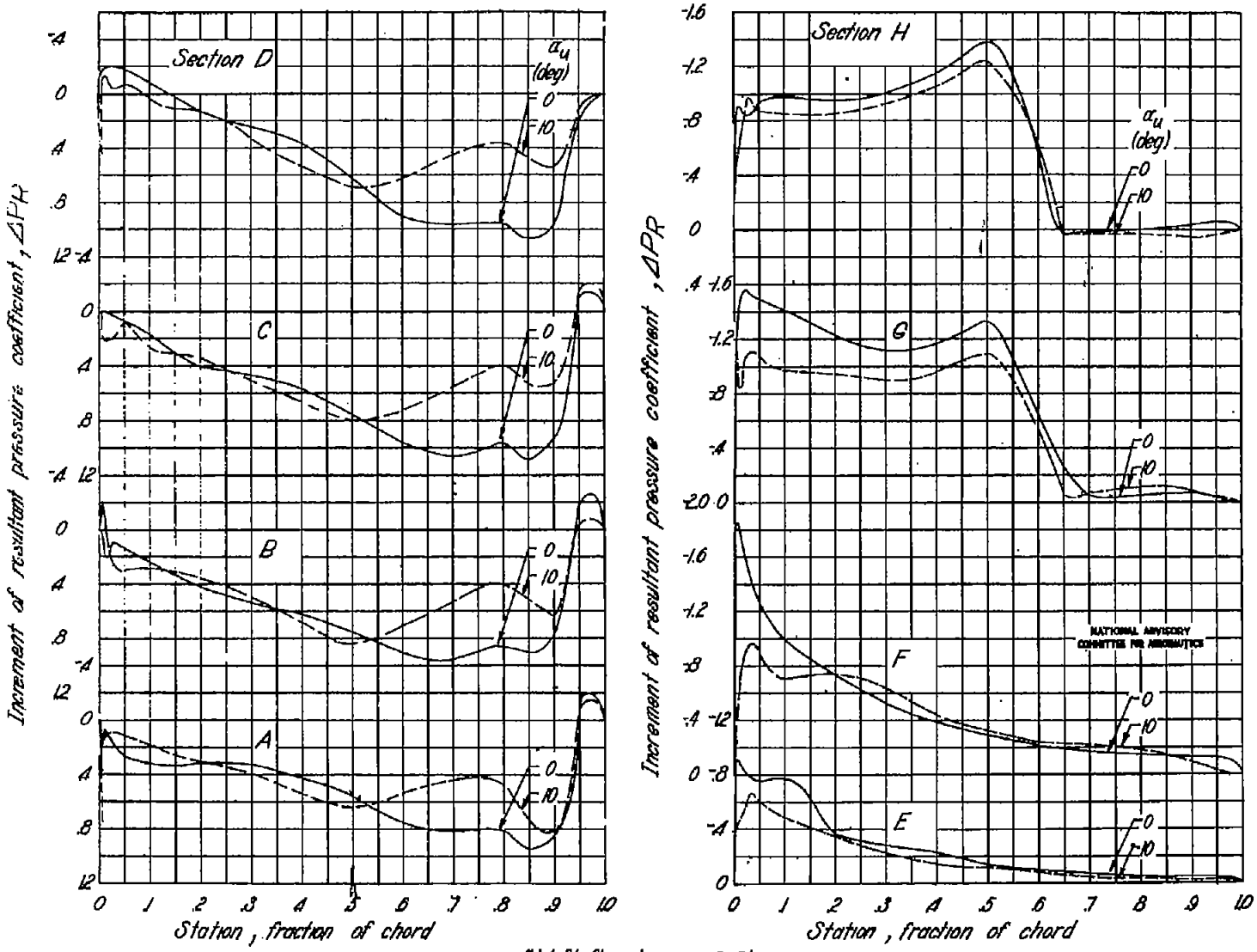

(b) Lift-flap hinge, 0.50c.

Figure 16.- Continued.

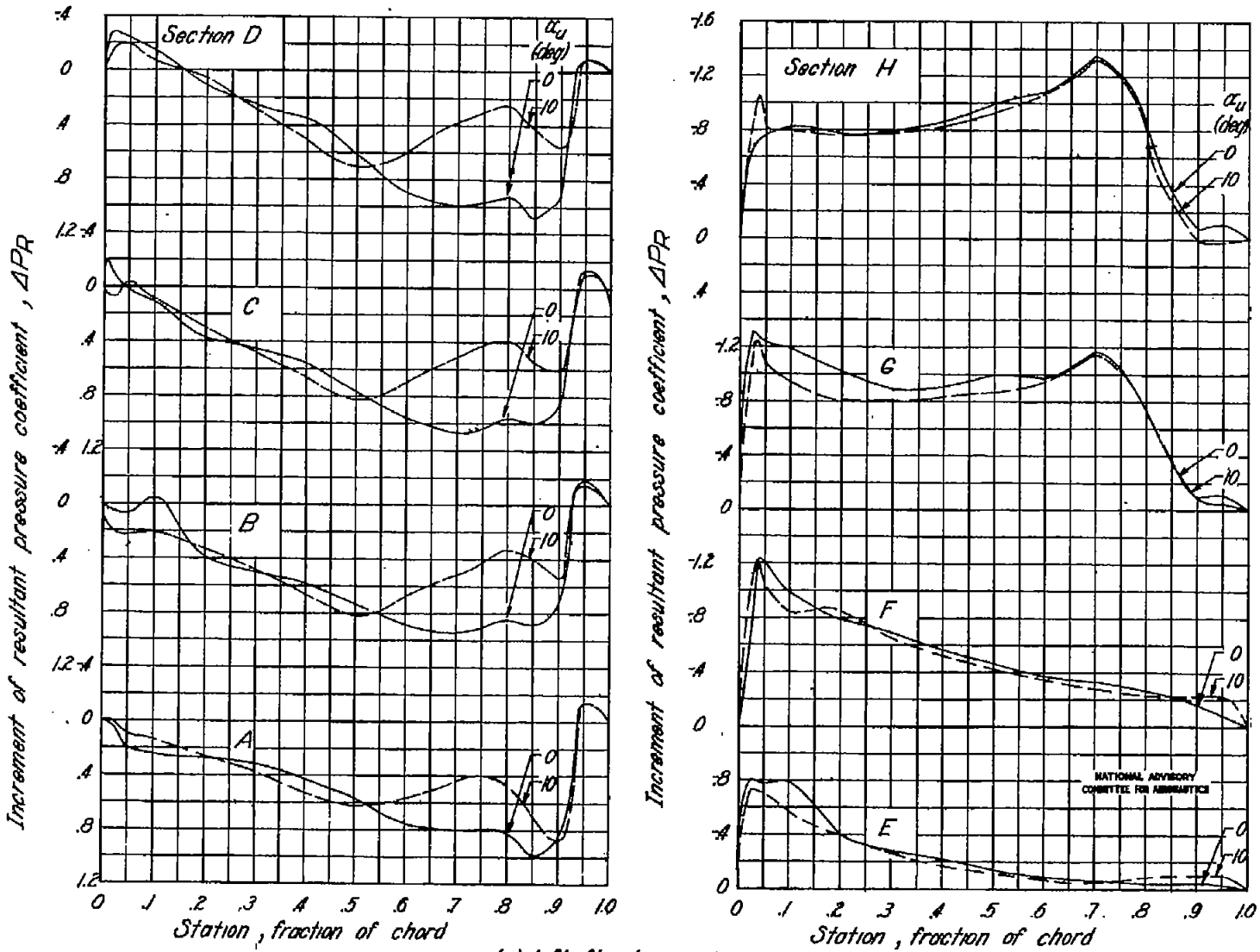

(c) Lift-flap hinge, 0.70c.

Figure 16. – Concluded.

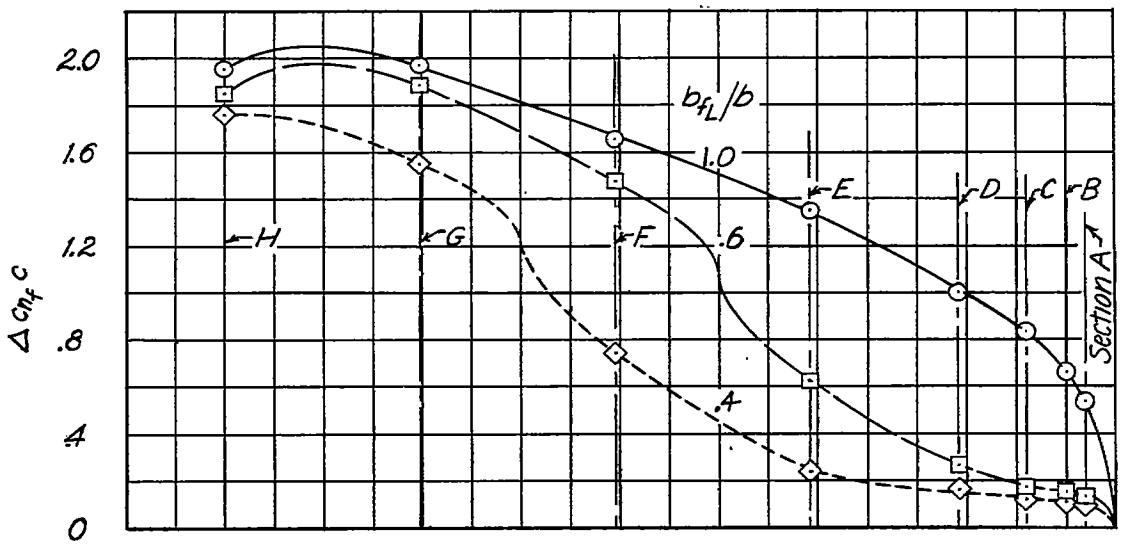

(b) $\alpha_u = 10°$.

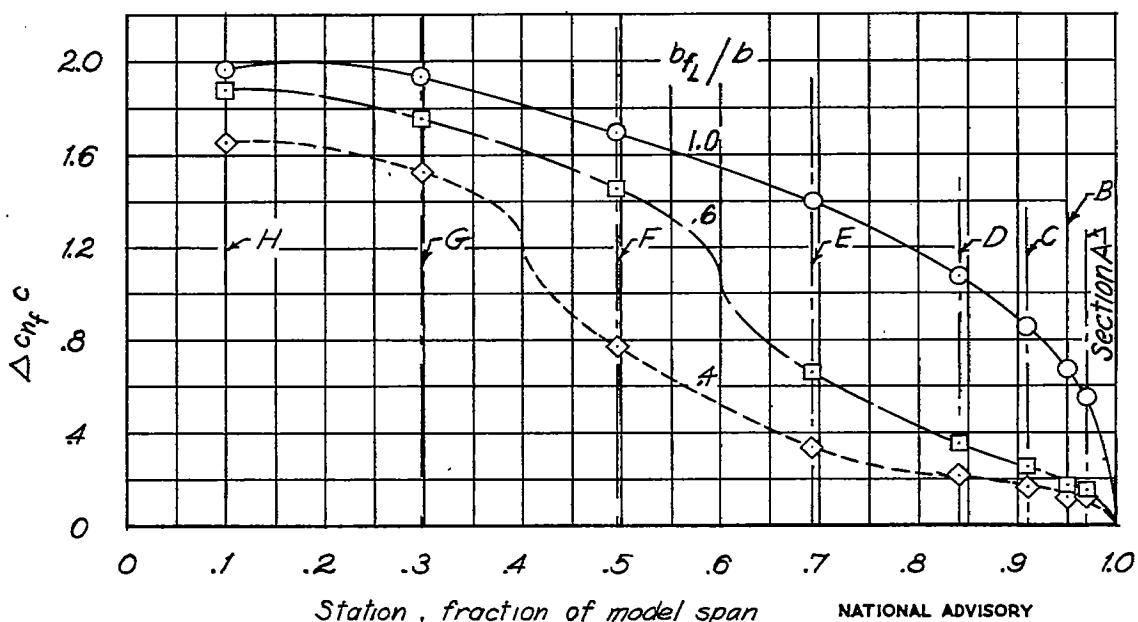

NATIONAL ADVISORY COMMITTEE FOR AERONAUTICS

(a) $\alpha_u = 0°$.

Figure 17. – Variation of the incremental spanwise loading caused by a 0.20c-chord lift flap of various spans. $\delta_{f_L} = 60°$.

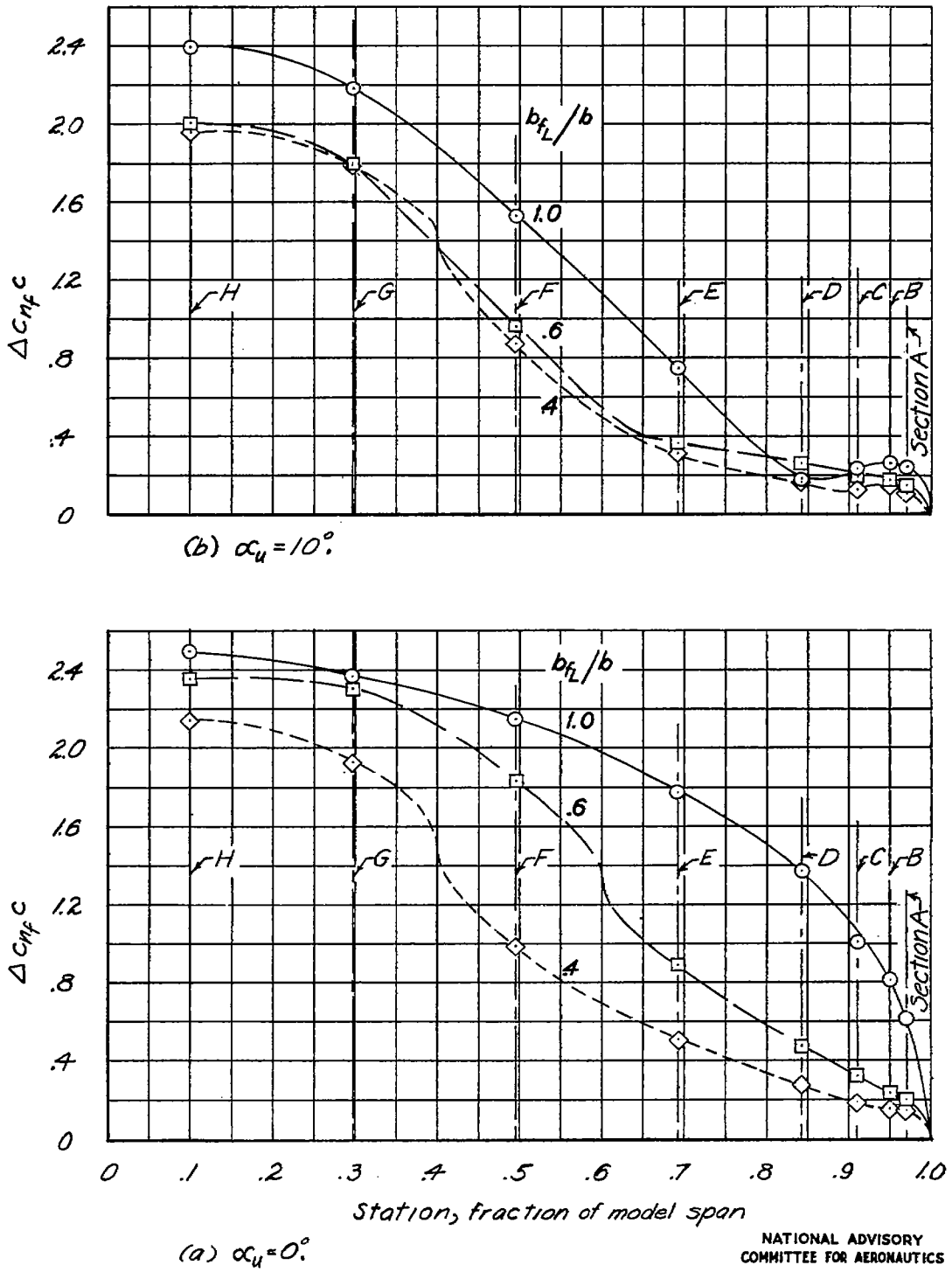

NATIONAL ADVISORY COMMITTEE FOR AERONAUTICS

Figure 18. - Variation of the incremental spanwise loading caused by a 0.40c-chord lift flap of various spans. $\delta_{f_L} = 60°$.

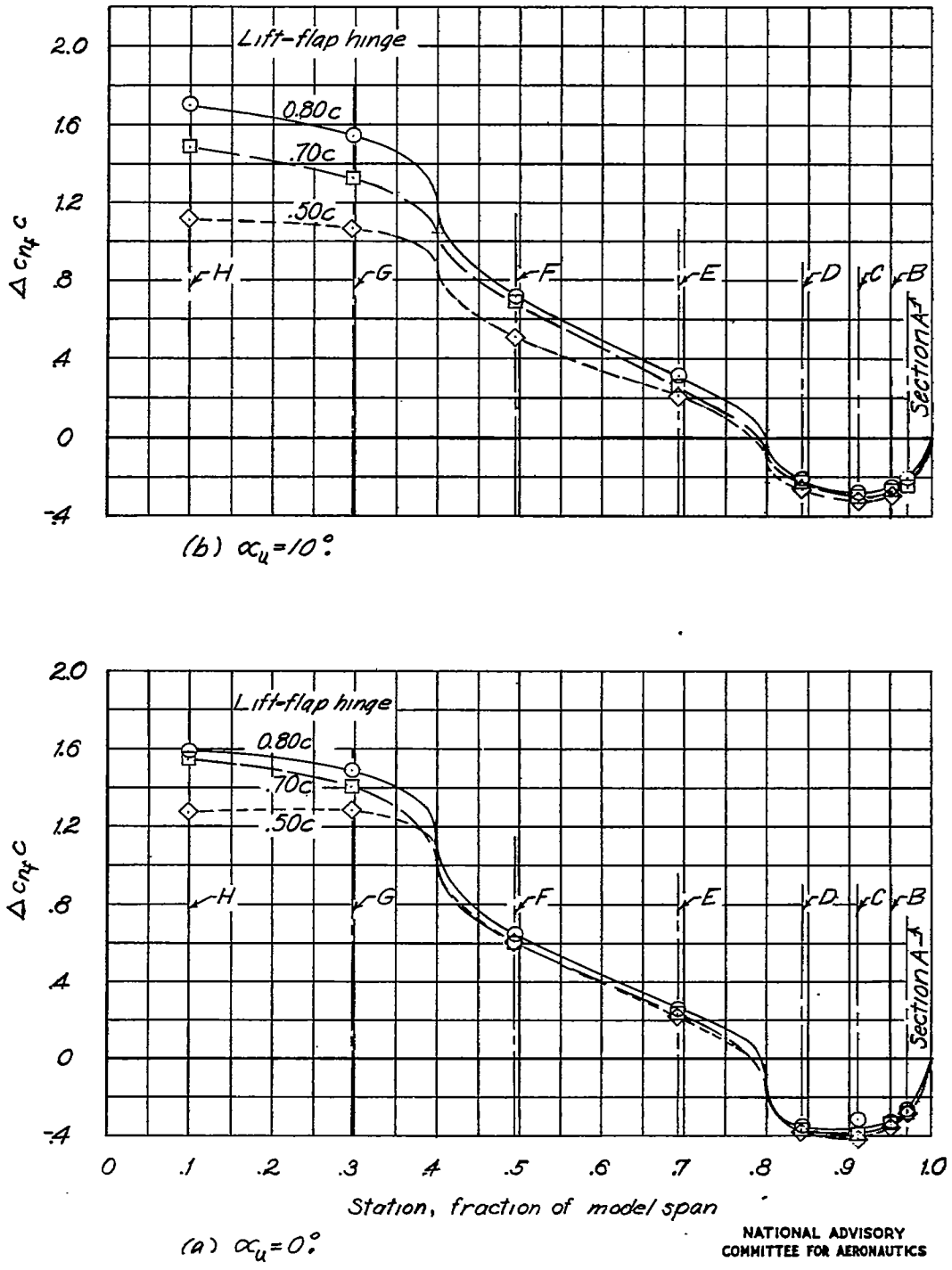

NATIONAL ADVISORY COMMITTEE FOR AERONAUTICS

Figure 19. – Variation of the incremental spanwise loading caused by varying the hinge location of a 0.20c-chord lift flap with a 0.20c-chord trim flap hinged in the normal position. $b_{f_L} = 0.40\ b$; $b_{f_T} = 0.20\ b$; $\delta_{f_L} = 60°$; $\delta_{f_T} = 60°$.

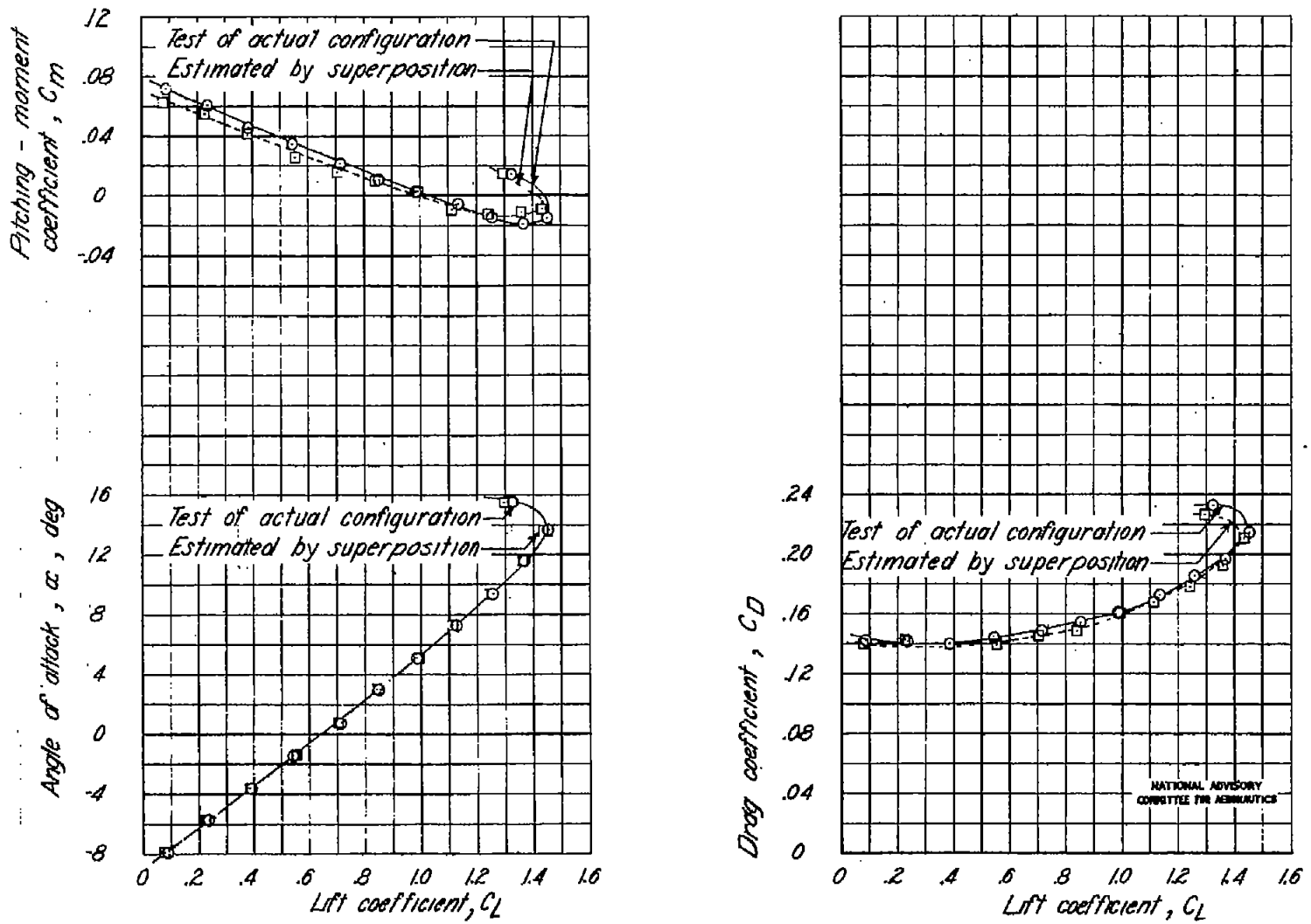

(a) Lift-flap hinge, 0.50c; trim-flap hinge, 0.80c.

Figure 20.- Lift, drag, and pitching-moment coefficients of wing with 0.20c-chord lift and trim flaps. Lift-flap span, 0.40 b; trim-flap span, 0.20 b; $\delta_{f_L} = 60°$; $\delta_{f_T} = 60°$; $R = 1.78 \times 10^6$.

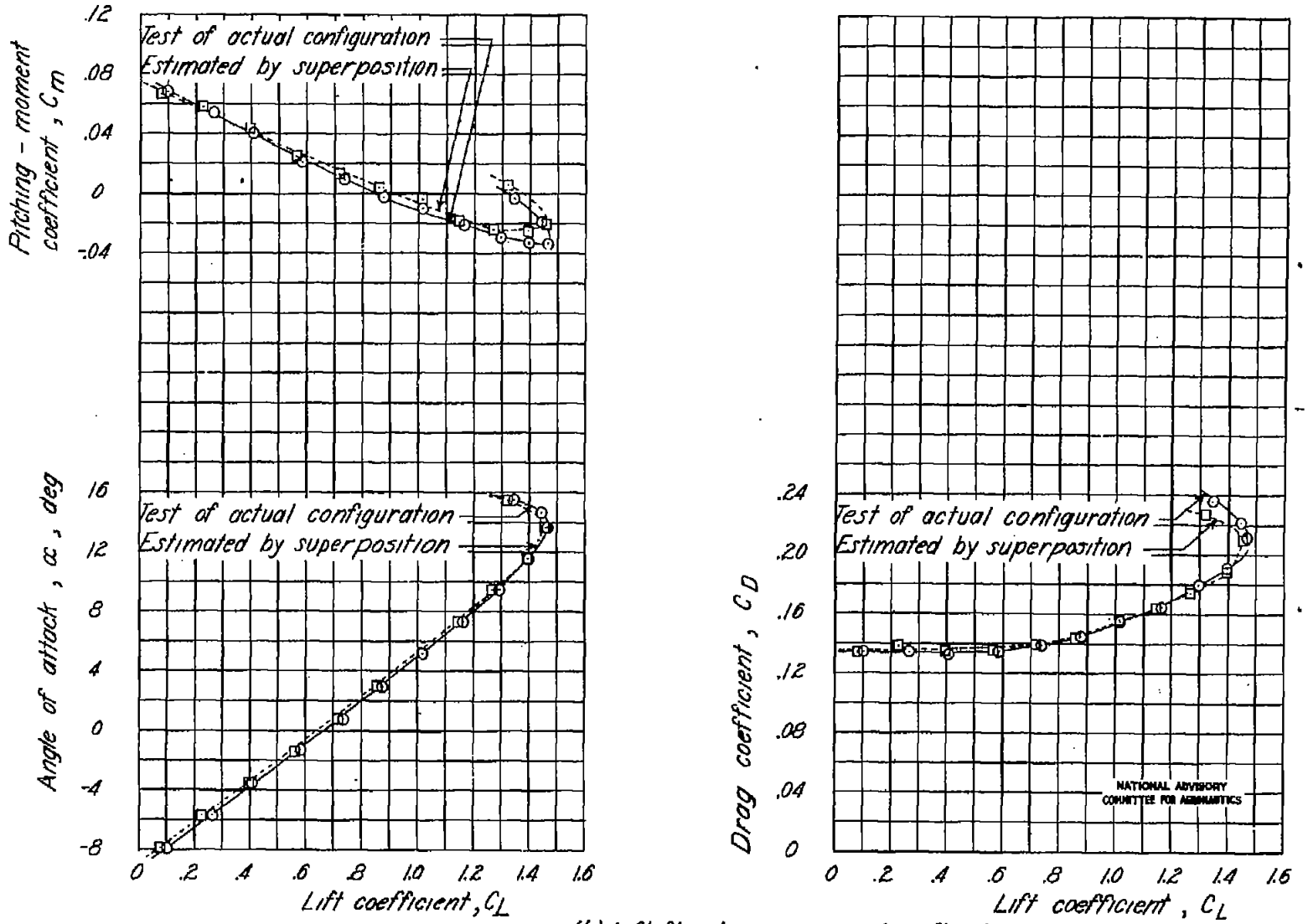

(b) Lift-flap hinge, 0.50c ; trim-flap hinge, 1.00c.

Figure 20. – Continued.

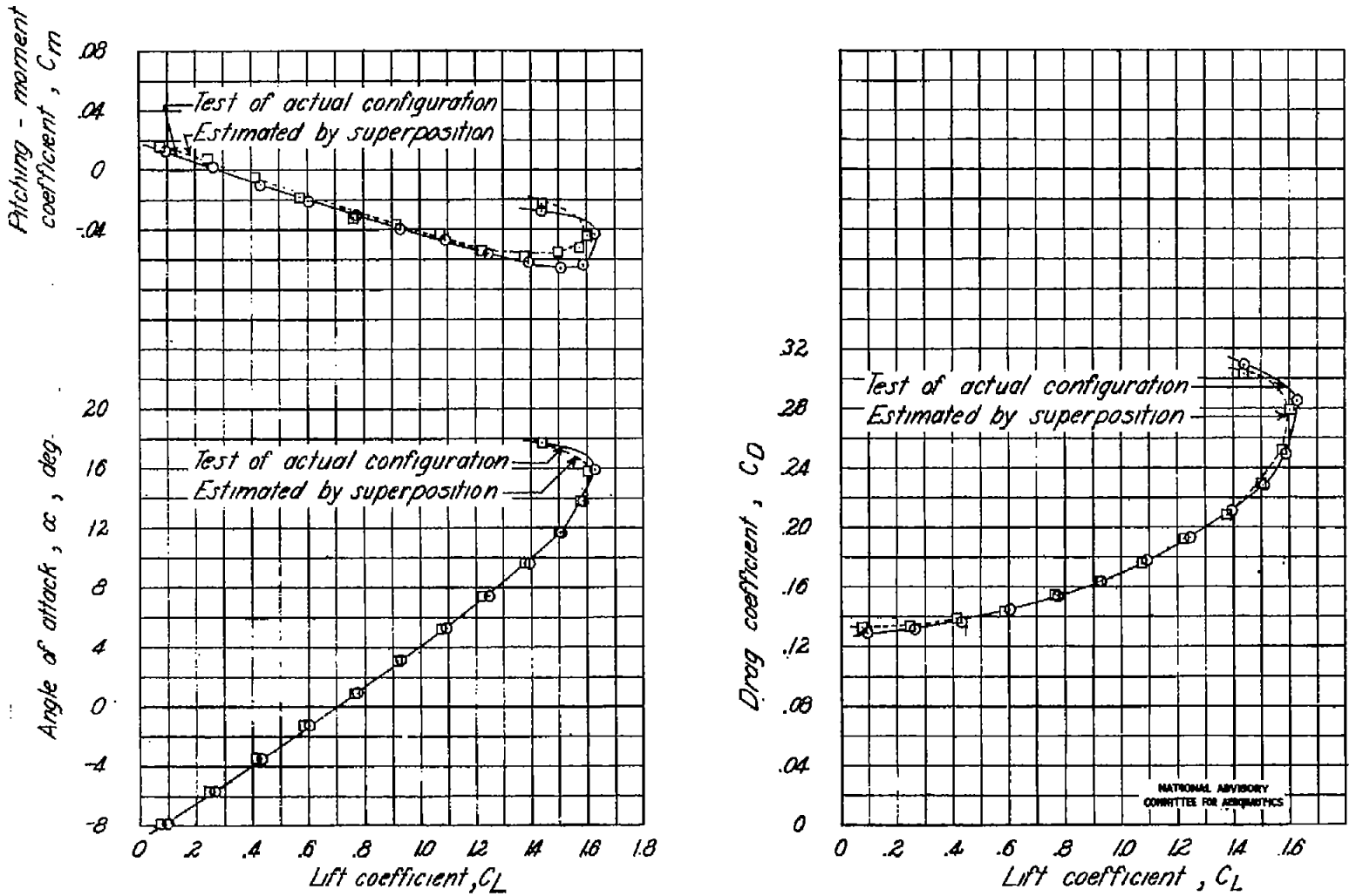

(c) Lift-flap hinge, 0.70c; trim-flap hinge, 0.80c.

Figure 20.-Concluded.

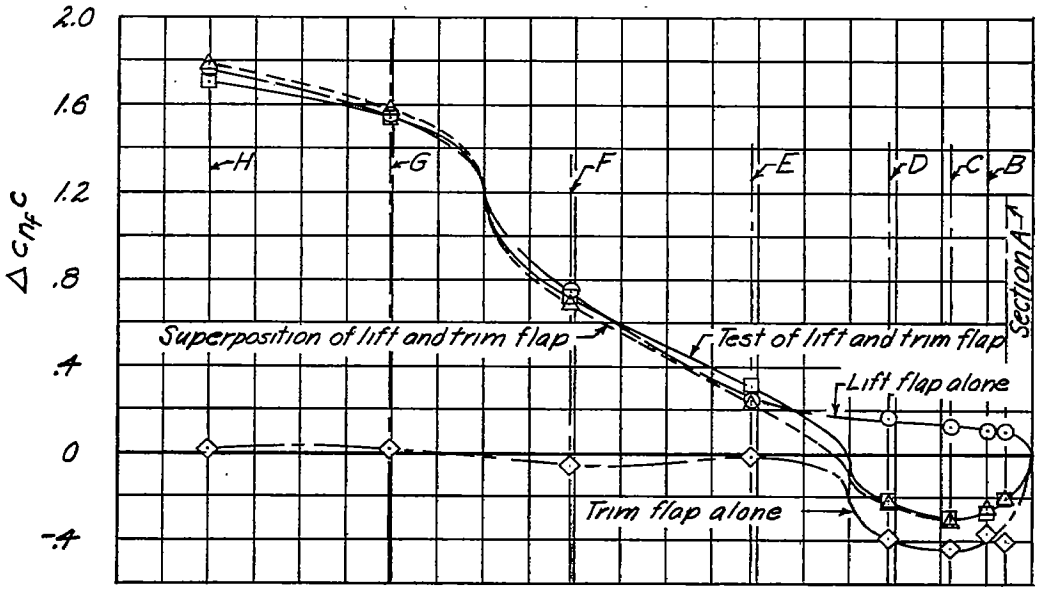

(b) $\alpha_u = 10°$.

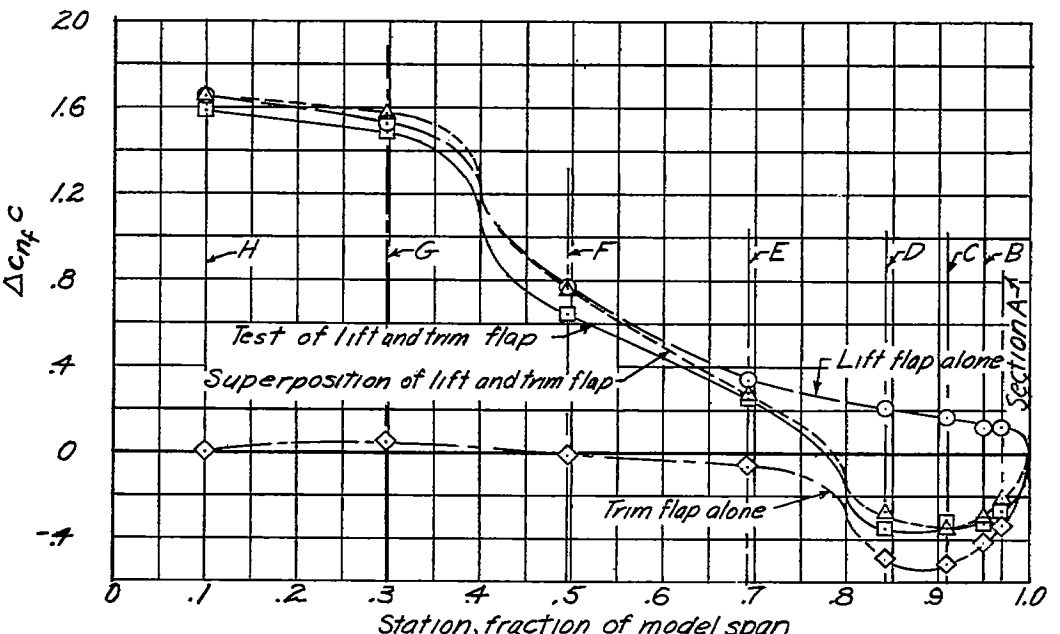

(a) $\alpha_u = 0°$.

NATIONAL ADVISORY COMMITTEE FOR AERONAUTICS

Figure 21. - Comparison of the incremental spanwise loading obtained from tests of a lift flap and a trim flap with that obtained by a superposition of the loadings obtained with each flap tested separately. Hinge location normal; $c_{f_L} = 0.20c$; $c_{f_T} = 0.20c$; $b_{f_L} = 0.40\ b$; $b_{f_T} = 0.20\ b$; $\delta_{f_L} = 60°$; $\delta_{f_T} = 60°$.

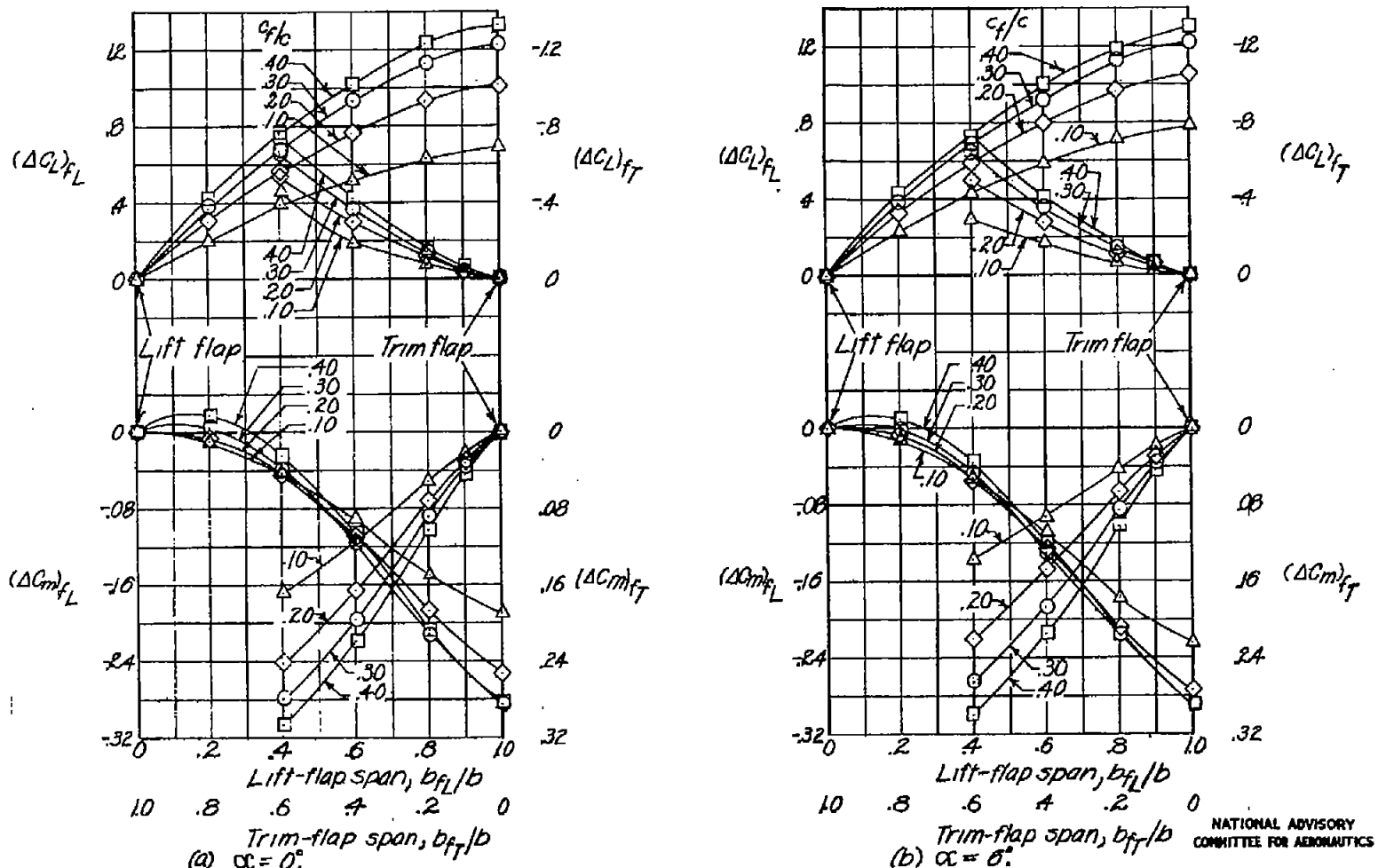

(a) $\alpha = 0°$.

(b) $\alpha = 6°$.

Figure 22.- Effect of lift-flap span and trim-flap span on the increment of lift coefficient and increment of pitching-moment coefficient of various-chord lift and trim flaps. $\delta_{f_L} = 60°$; $\delta_{f_T} = 60°$.

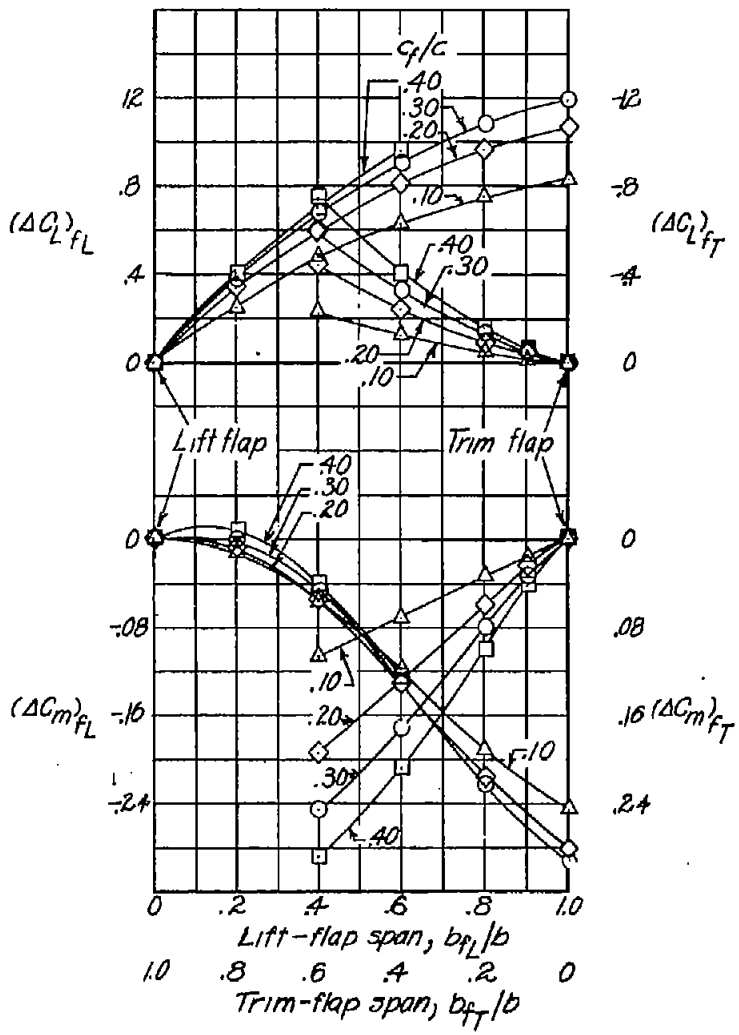

(c) $\alpha = 10°$.

Figure 22.- Continued.

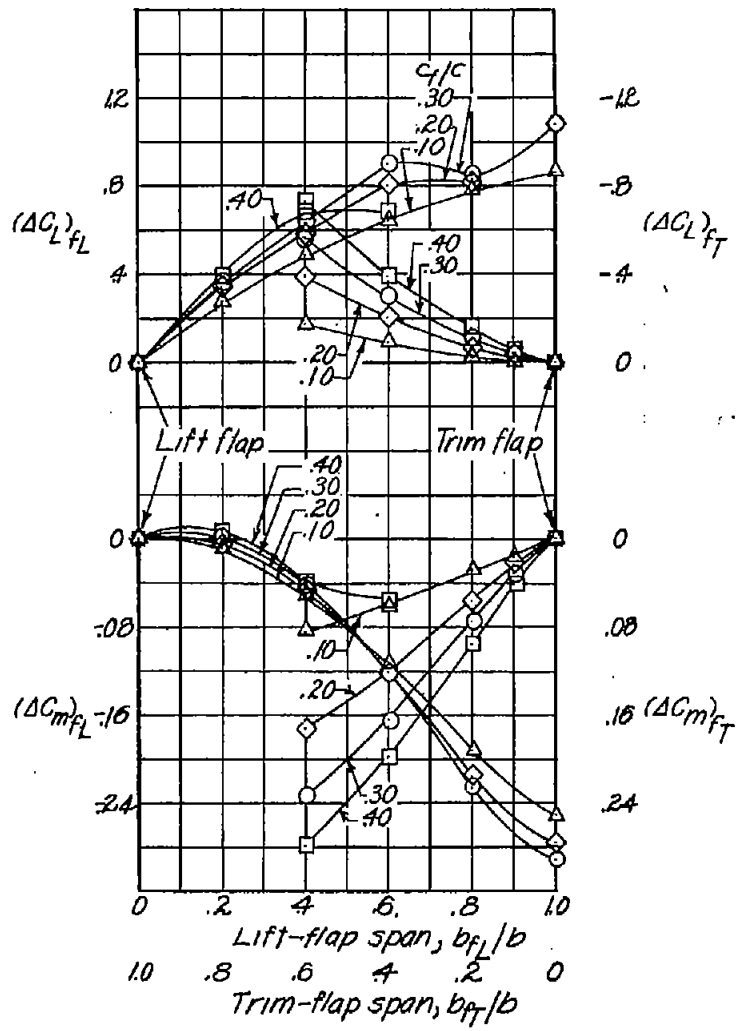

(d) $\alpha = 12°$.

NATIONAL ADVISORY COMMITTEE FOR AERONAUTICS

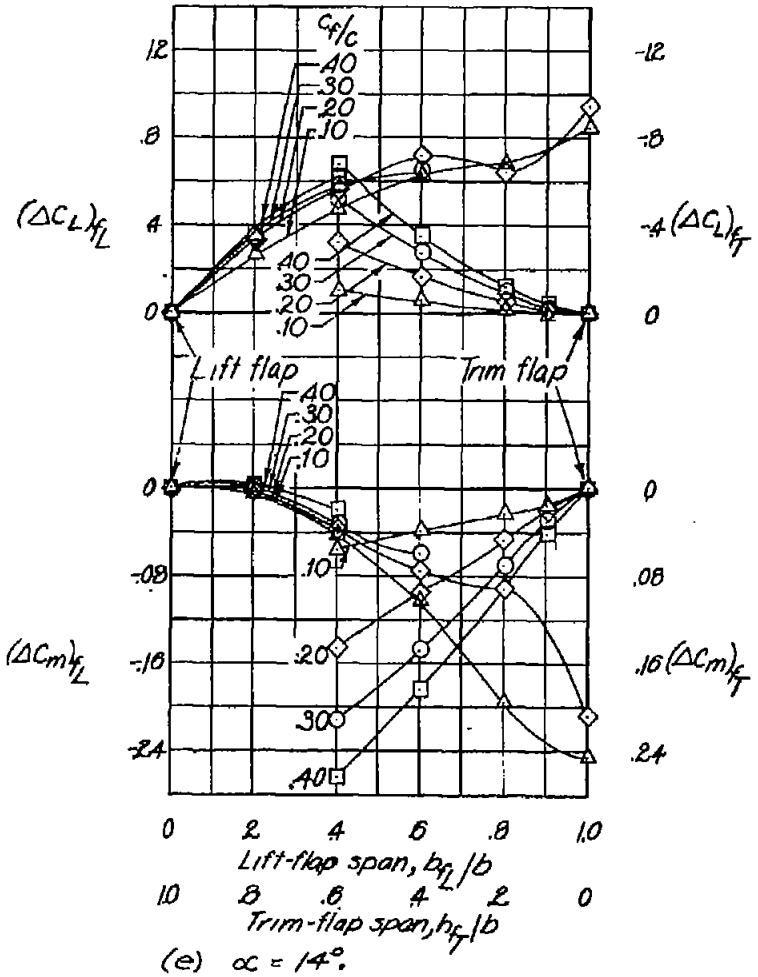

(e) $\alpha = 14°$.

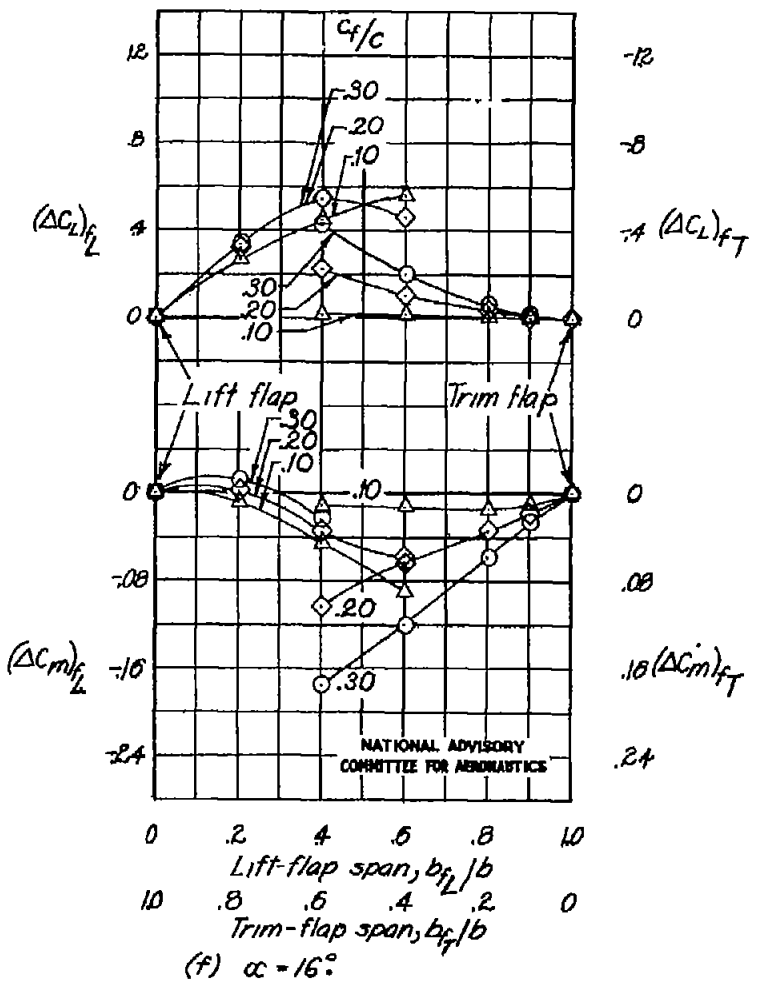

(f) $\alpha = 16°$.

Figure 22.- Concluded.

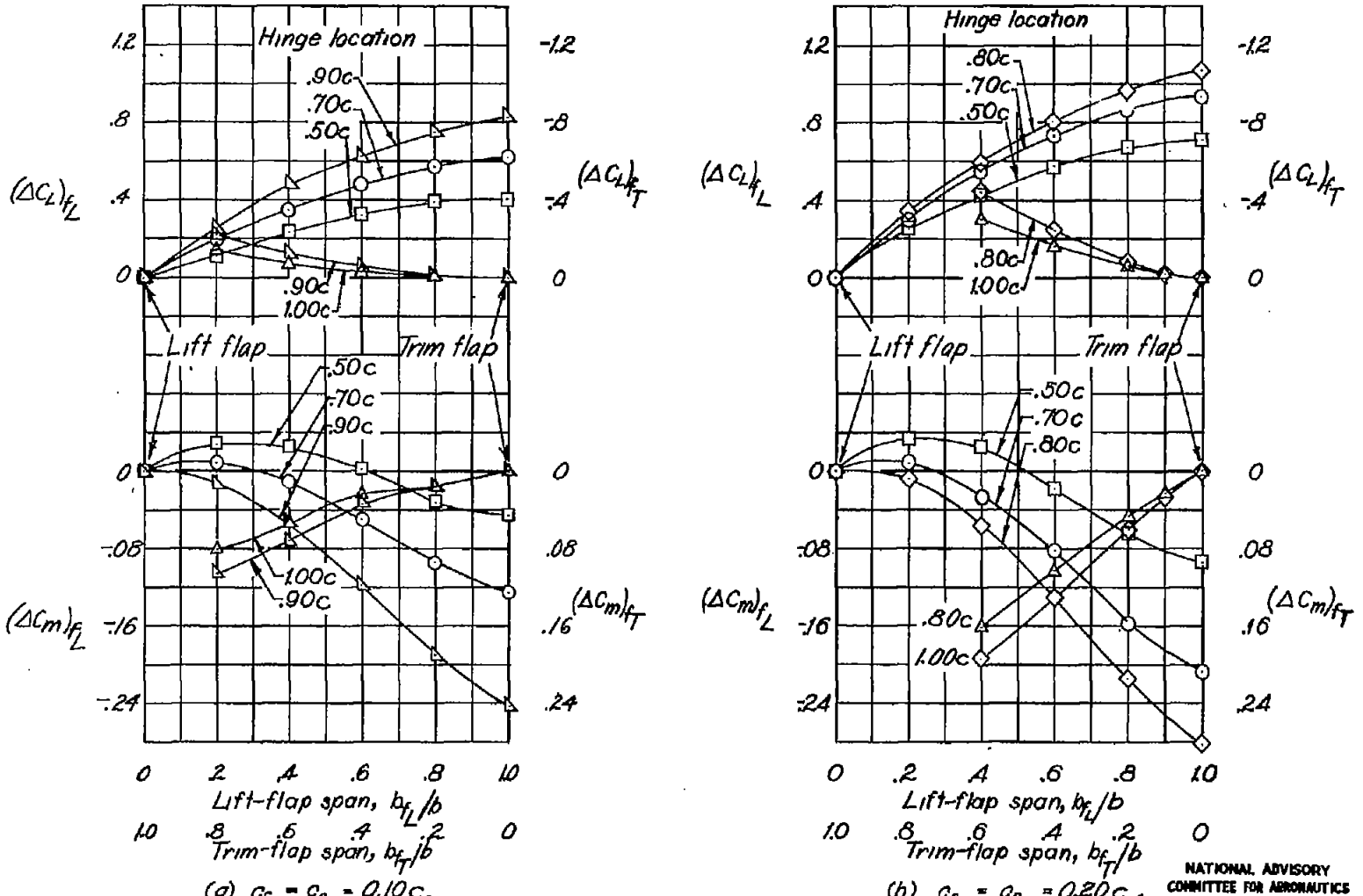

(a) $c_{f_L} = c_{f_T} = 0.10c$.

(b) $c_{f_L} = c_{f_T} = 0.20c$.

NATIONAL ADVISORY COMMITTEE FOR AERONAUTICS

Figure 23.—Effect of lift-flap span and trim-flap span on the increment of lift coefficient and increment of pitching-moment coefficient for various hinge locations of lift and trim flaps. $\alpha = 10°$; $\delta_{f_L} = \delta_{f_T} = 60°$.

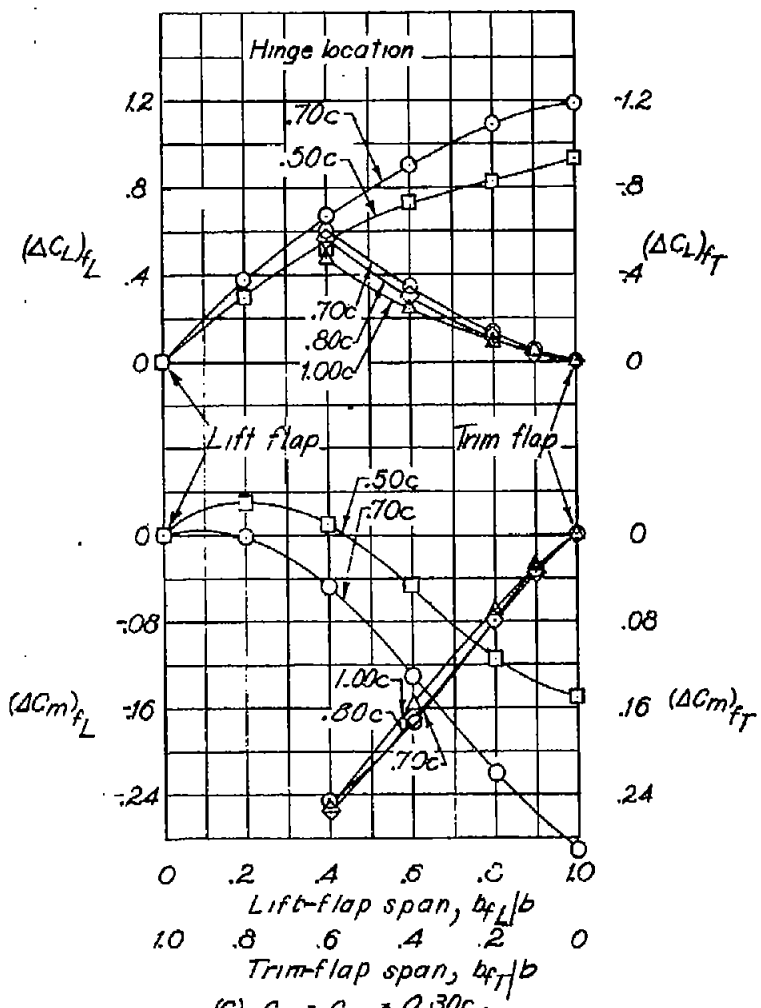

(c) $c_{f_L} = c_{f_T} = 0.30c$.

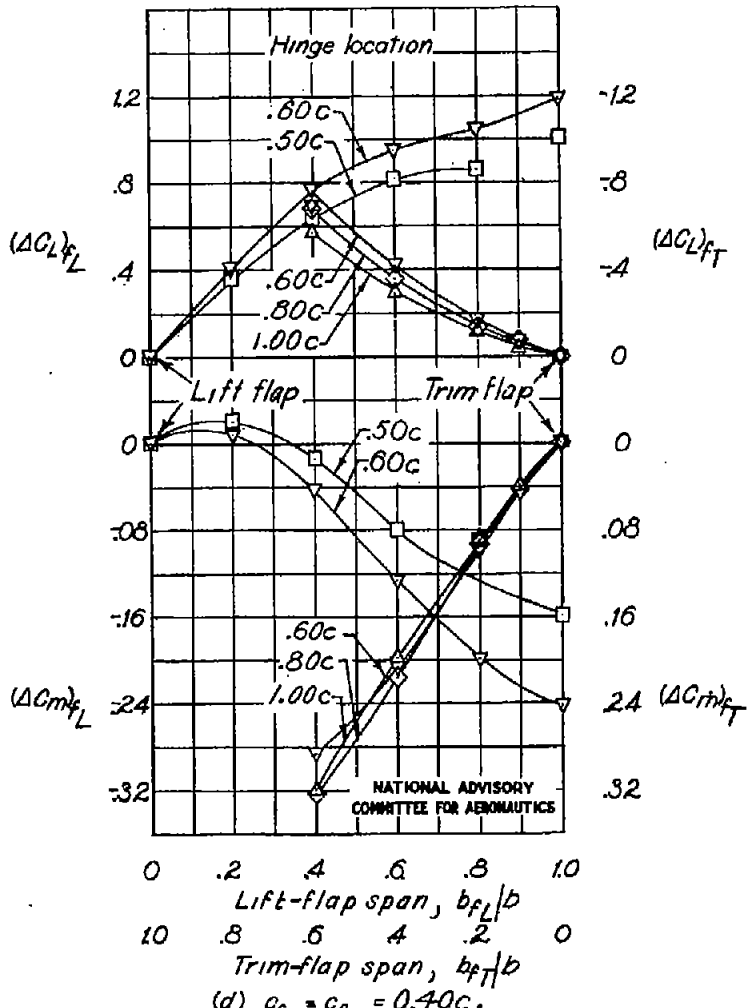

(d) $c_{f_L} = c_{f_T} = 0.40c$.

Figure 23. – Concluded.

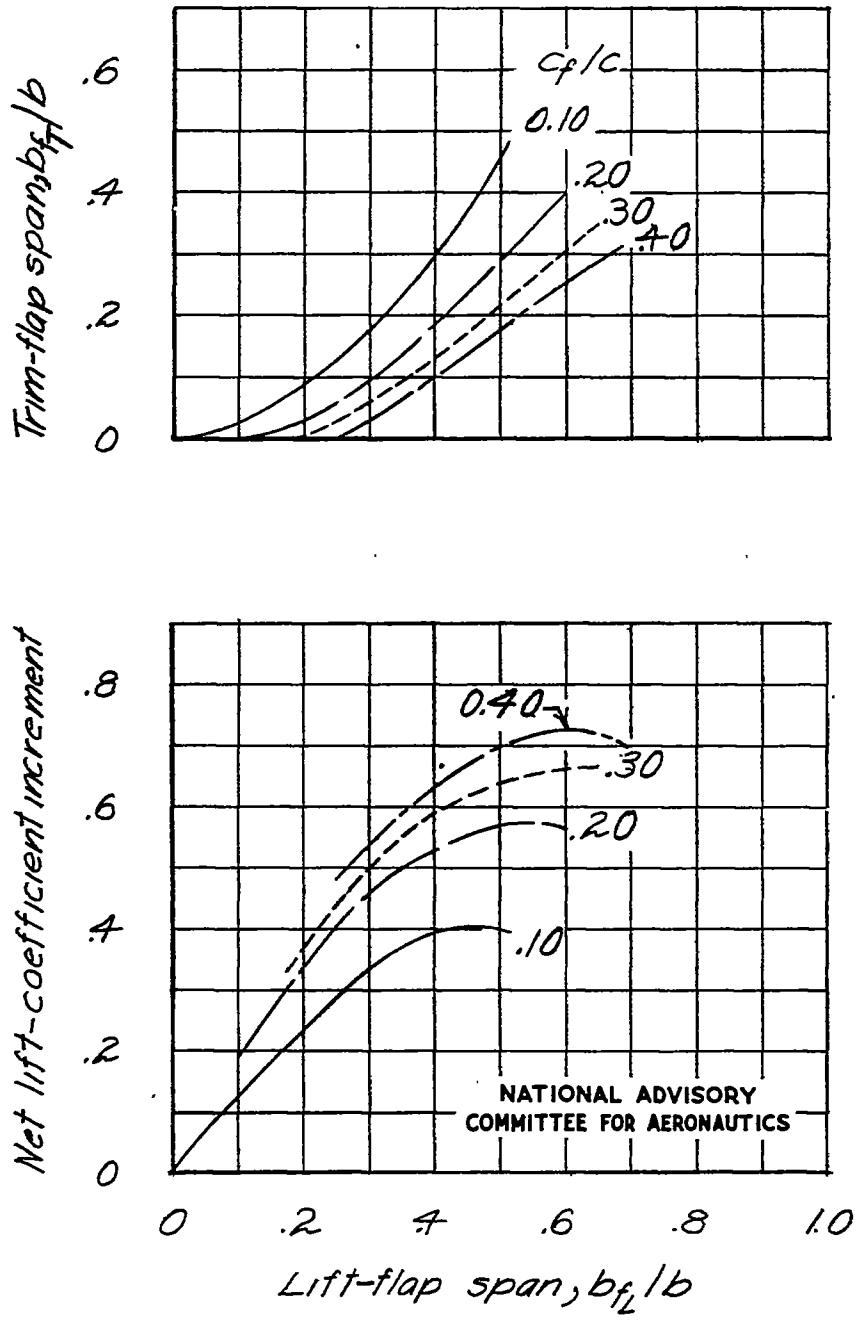

Figure 24.– Effect of lift-flap span on the net lift-coefficient increment and trim-flap span for various-chord lift and trim flaps. $\alpha = 10^\circ$; $\Delta C_m = 0$; $\delta_{f_L} = 60^\circ$; $\delta_{f_T} = 60^\circ$.

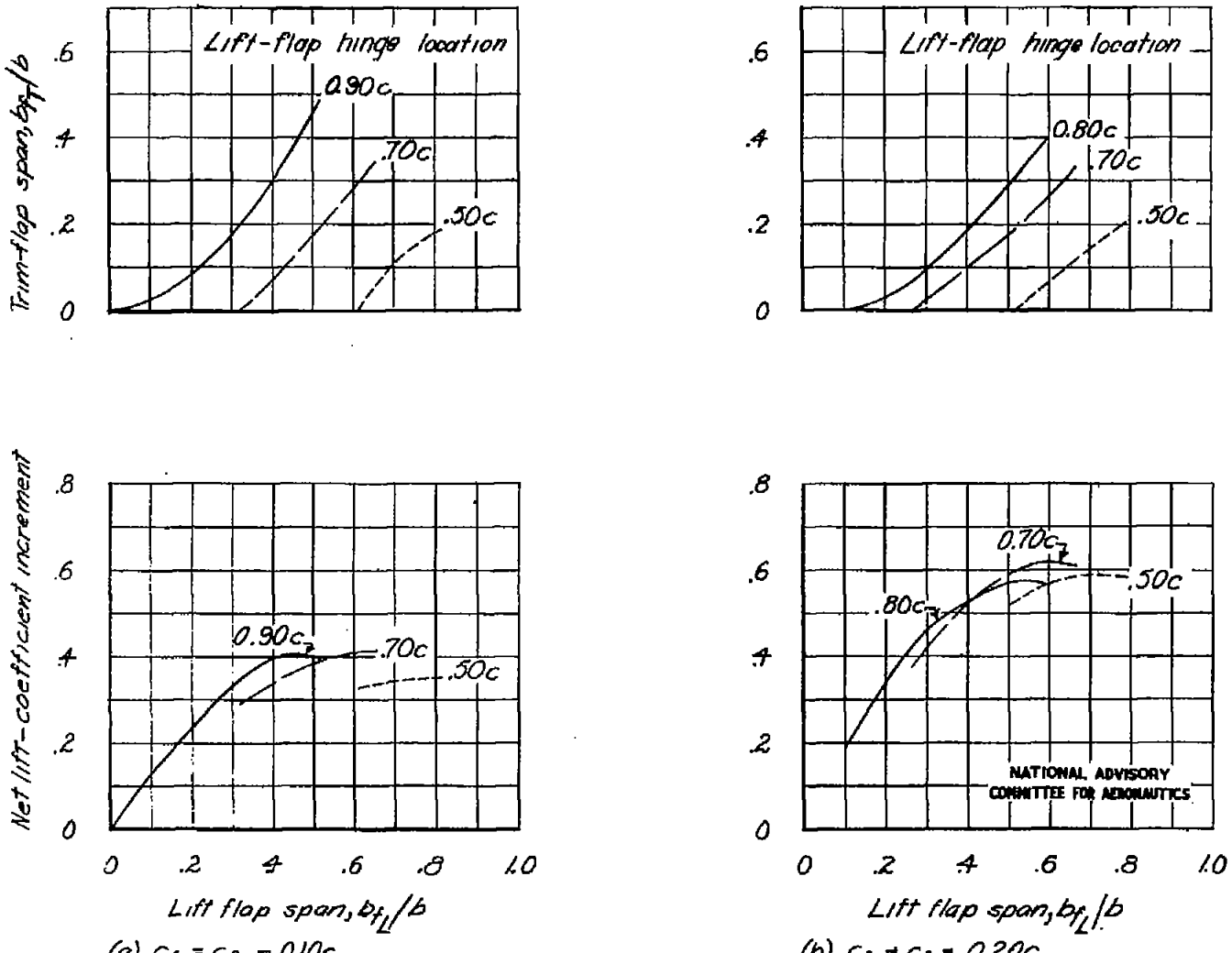

(a) $c_{f_L} = c_{f_T} = 0.10c$.

(b) $c_{f_L} = c_{f_T} = 0.20c$.

Figure 25.—Effect of lift-flap span on the net lift-coefficient increment and trim-flap span for various locations of the lift flap hinge. Trim flap hinged in normal location. $\Delta C_m = 0$; $\delta_{f_L} = 60°$; $\delta_{f_T} = 60°$; $\alpha = 10°$.

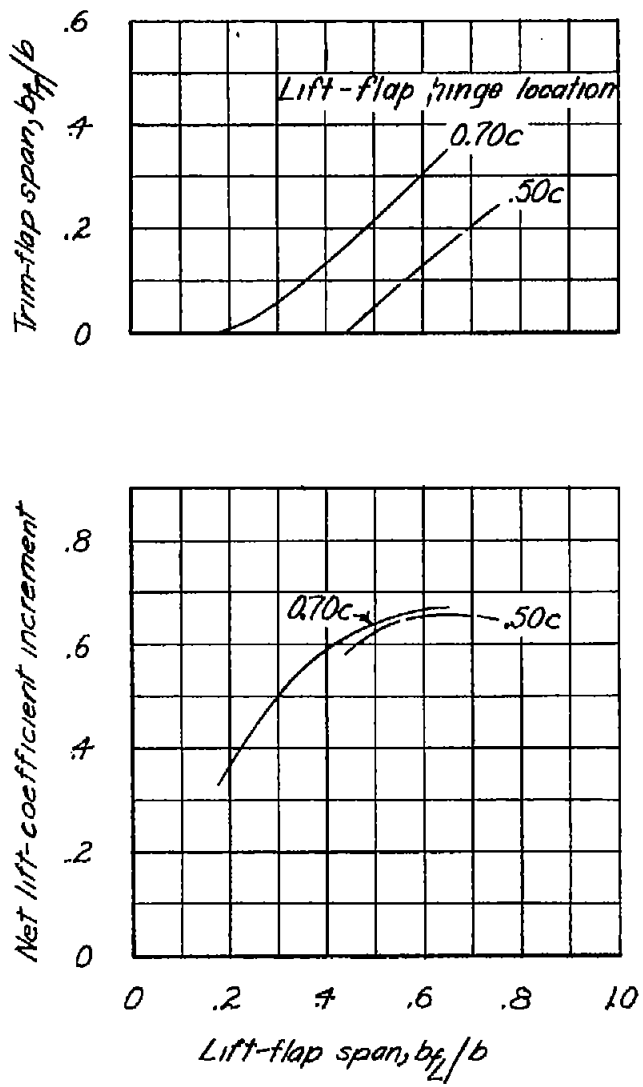

(c) $c_{f_L} = c_{f_T} = 0.30c$.

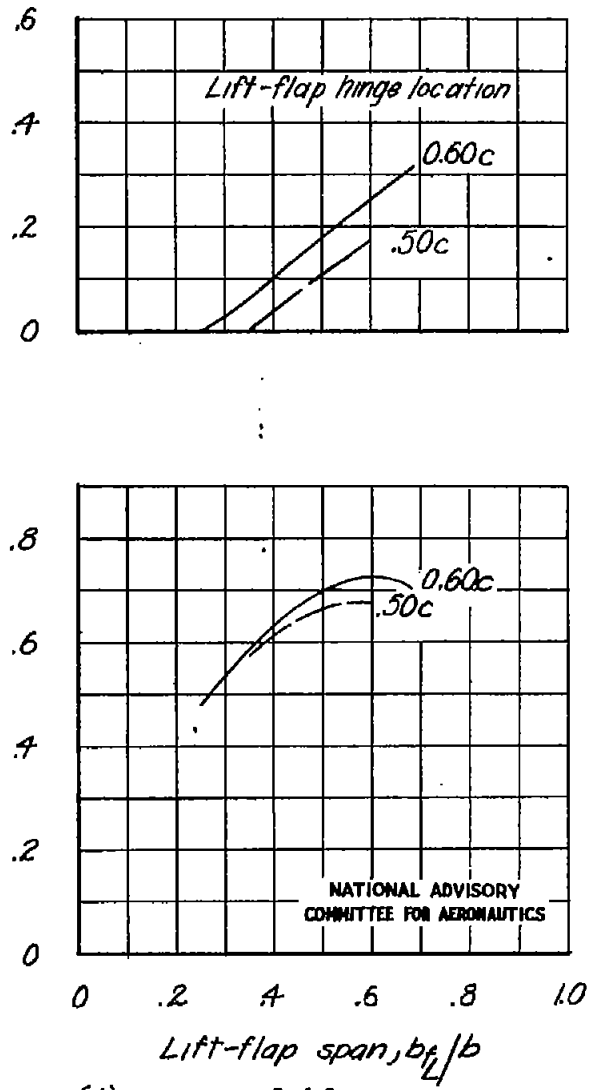

(d) $c_{f_L} = c_{f_T} = 0.40c$.

Figure 25.- Concluded.

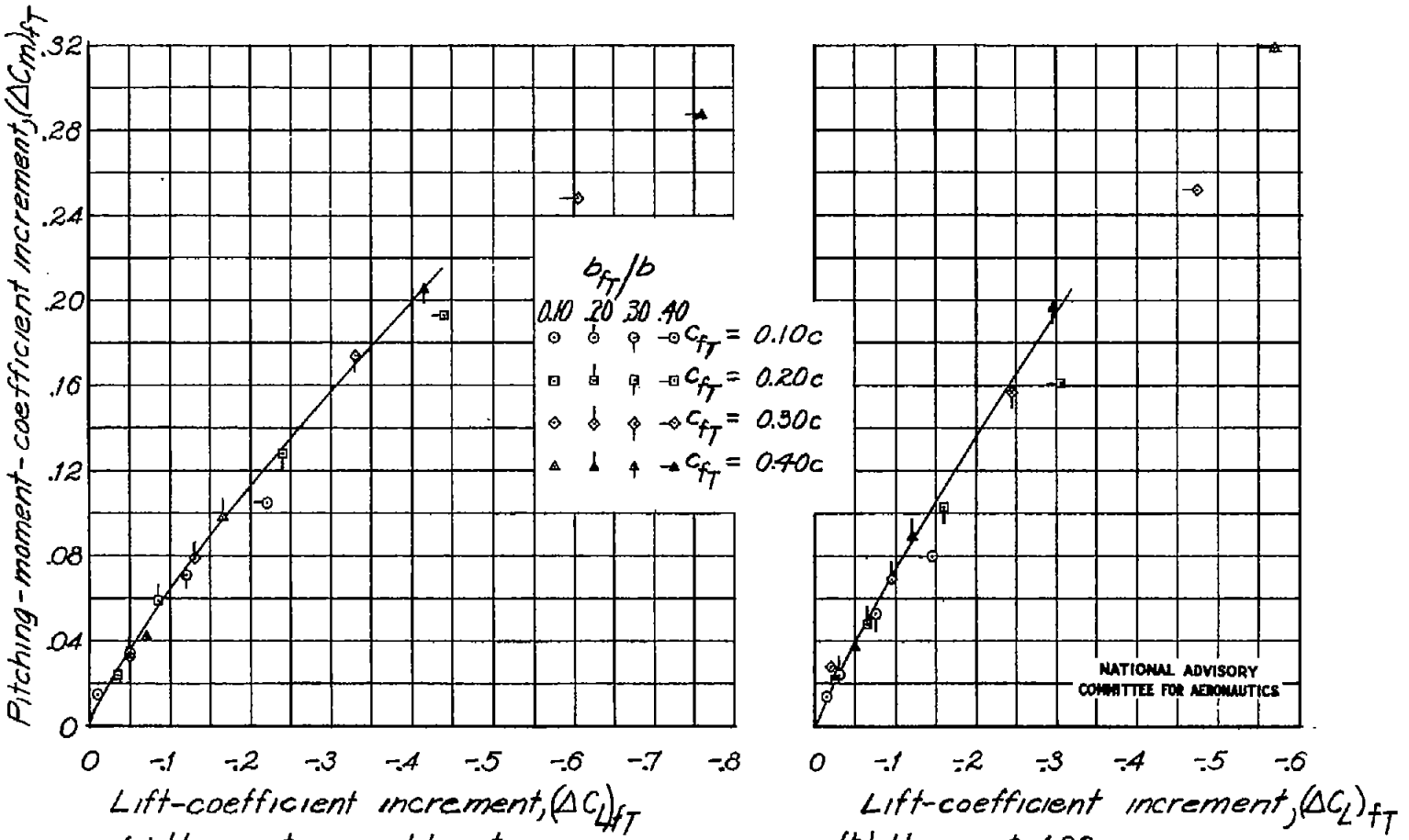

(a) Hinge at normal location. (b) Hinge at 1.00c.

Figure 26.-Variation of pitching-moment-coefficient increment with lift-coefficient increment of trim flaps. $\alpha = 10°$; $\delta_{f_T} = 60°$.

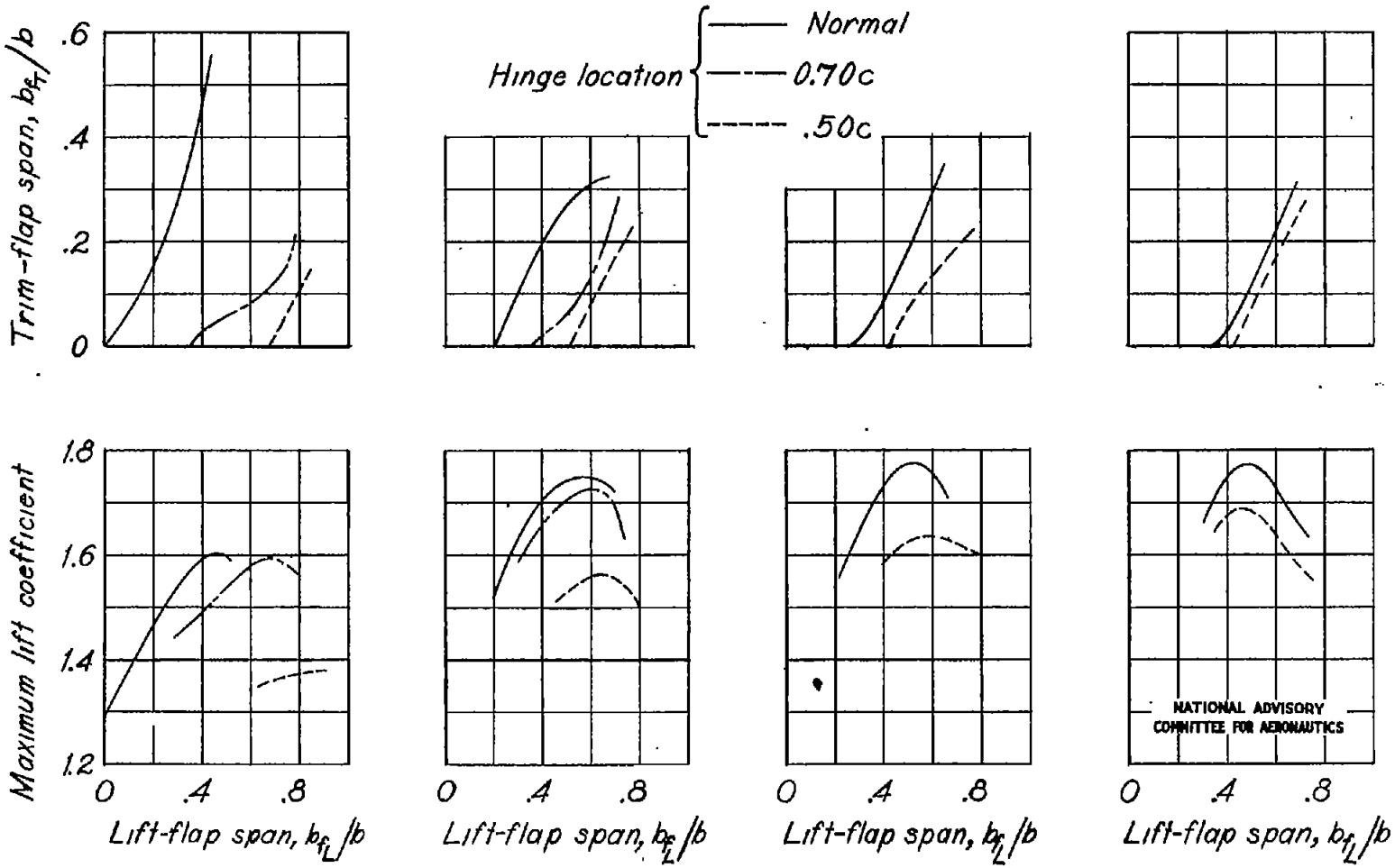

(a) $c_{f_L} = c_{f_T} = 0.10c$. (b) $c_{f_L} = c_{f_T} = 0.20c$. (c) $c_{f_L} = c_{f_T} = 0.30c$. (d) $c_{f_L} = c_{f_T} = 0.40c$.

Figure 27. – Variation of trimmed maximum lift coefficient and trim-flap span required with lift-flap span for various lift-flap hinge locations.

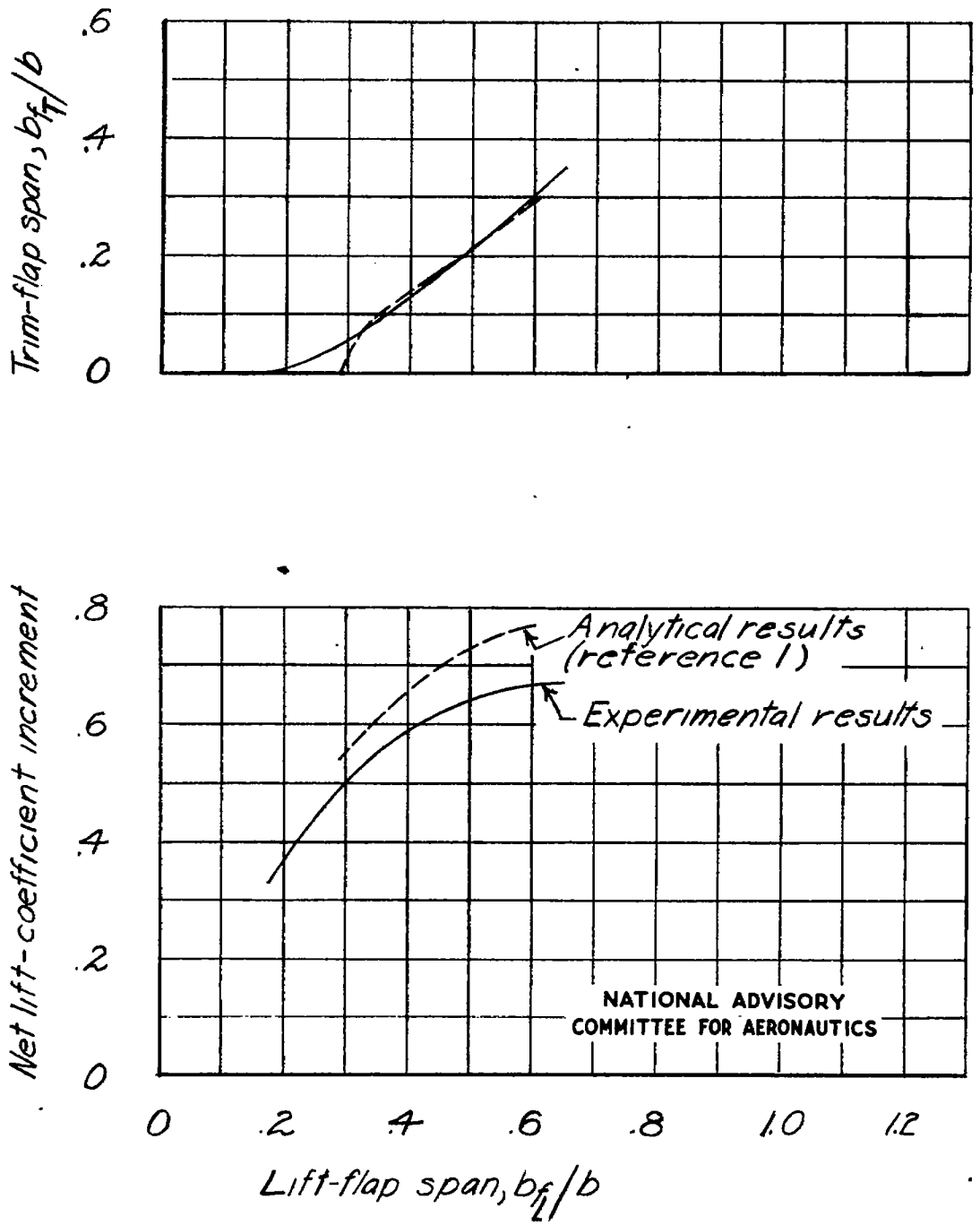

Figure 28.- Comparison of experimental results with results based on analytical methods of reference 1. Sweepback of quarter-chord line 23°; $c_{f_L} = c_{f_T} = 0.30c$.

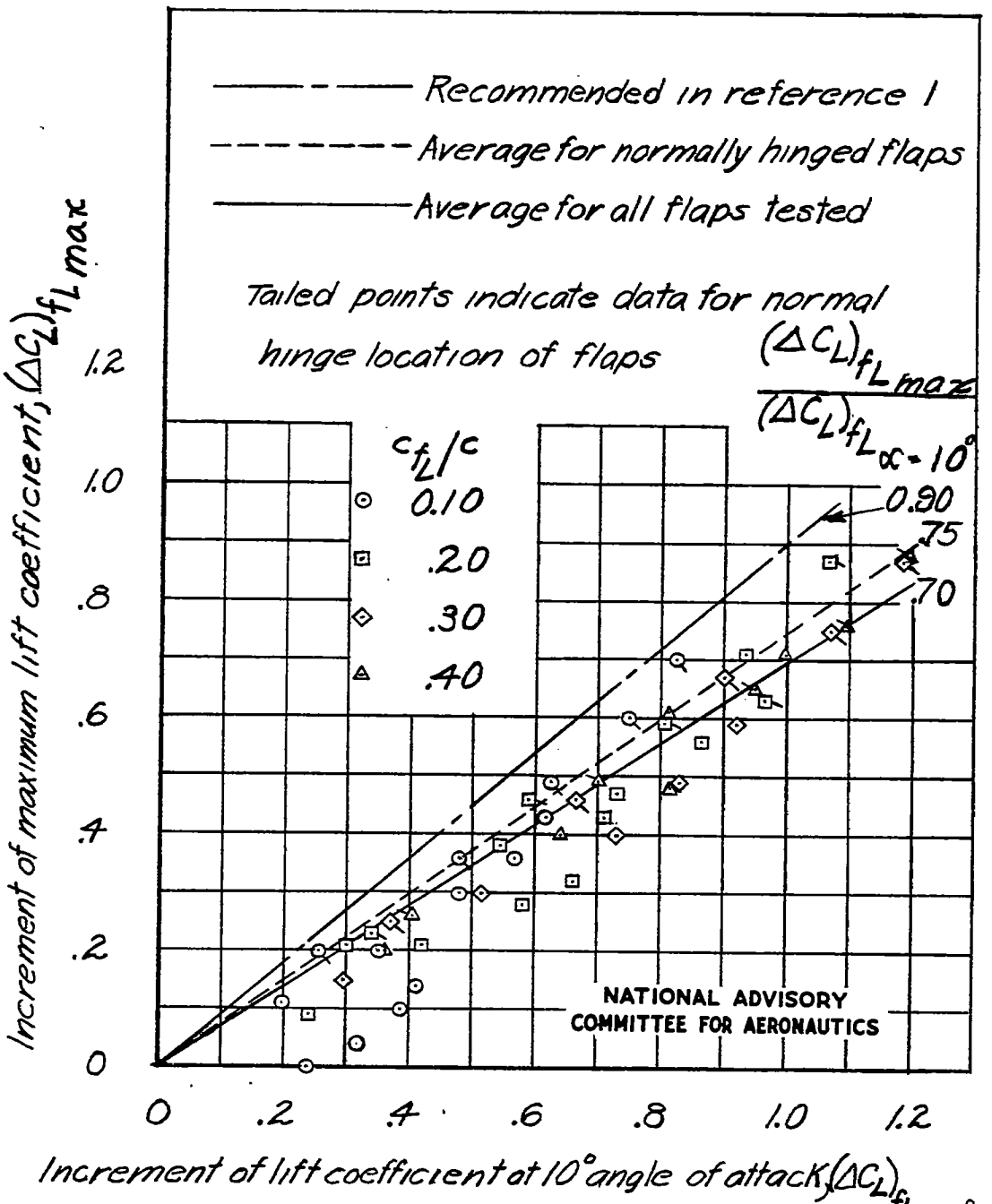

Figure 29.- Increment of maximum lift coefficient against increment of lift coefficient at 10° angle of attack for all flaps tested.